ACI 549.4R-13

Guide to Design and Construction of Externally Bonded Fabric-Reinforced Cementitious Matrix (FRCM) Systems for Repair and Strengthening Concrete and Masonry Structures

Reported by ACI Committee 549

American Concrete Institute®

American Concrete Institute®
Advancing concrete knowledge

First Printing
December 2013

Guide to Design and Construction of Externally Bonded FRCM Systems for Repair and Strengthening Concrete and Masonry Structures

The technical committees responsible for ACI committee reports and standards strive to avoid ambiguities, omissions, and errors in these documents. In spite of these efforts, the users of ACI documents occasionally find information or requirements that may be subject to more than one interpretation or may be incomplete or incorrect. Users who have suggestions for the improvement of ACI documents are requested to contact ACI via the errata website at www.concrete.org/committees/errata.asp. Proper use of this document includes periodically checking for errata for the most up-to-date revisions.

ACI committee documents are intended for the use of individuals who are competent to evaluate the significance and limitations of its content and recommendations and who will accept responsibility for the application of the material it contains. Individuals who use this publication in any way assume all risk and accept total responsibility for the application and use of this information.

All information in this publication is provided "as is" without warranty of any kind, either express or implied, including but not limited to, the implied warranties of merchantability, fitness for a particular purpose or non-infringement.

ACI and its members disclaim liability for damages of any kind, including any special, indirect, incidental, or consequential damages, including without limitation, lost revenues or lost profits, which may result from the use of this publication.

It is the responsibility of the user of this document to establish health and safety practices appropriate to the specific circumstances involved with its use. ACI does not make any representations with regard to health and safety issues and the use of this document. The user must determine the applicability of all regulatory limitations before applying the document and must comply with all applicable laws and regulations, including but not limited to, United States Occupational Safety and Health Administration (OSHA) health and safety standards.

Participation by governmental representatives in the work of the American Concrete Institute and in the development of Institute standards does not constitute governmental endorsement of ACI or the standards that it develops.

Order information: ACI documents are available in print, by download, on CD-ROM, through electronic subscription, or reprint and may be obtained by contacting ACI.

Most ACI standards and committee reports are gathered together in the annually revised *ACI Manual of Concrete Practice* (MCP).

American Concrete Institute
38800 Country Club Drive
Farmington Hills, MI 48331
U.S.A.
Phone: 248-848-3700
Fax: 248-848-3701

www.concrete.org

ISBN: 978-0-87031-852-8

ACI 549.4R-13

Guide to Design and Construction of Externally Bonded Fabric-Reinforced Cementitious Matrix (FRCM) Systems for Repair and Strengthening Concrete and Masonry Structures

Reported by ACI Committee 549

John Jones, Chair

Corina-Maria Aldea†

P. N. Balaguru
Hiram Price Ball Jr.
Nemkumar Banthia
Gordon B. Batson
Neeraj J. Buch
Cesar Chan
James I. Daniel
Antonio De Luca†
Ashish Dubey
Garth J. Fallis†
Graham T. Gilbert
Antonio J. Guerra
James R. McConaghy
Barzin Mobasher†
Antoine E. Naaman
Antonio Nanni*
Alva Peled
D. V. Reddy
Paul T. Sarnstrom
Scott Shafer
Surendra P. Shah
Yixin Shao
Robert C. Zellers

Consulting Members
Lloyd E. Hackman
Paul Nedwell
P. Paramasivam
Parviz Soroushian
Ronald F. Zollo

*Chair of the subcommittee that prepared this document.
†Members of the subcommittee that prepared this document,

The Committee thanks Associate Member J. Gustavo Tumialan for his contribution.

Fabric-reinforced cementitious matrix (FRCM) systems for repairing and strengthening concrete and masonry structures are an alternative to traditional techniques such as fiber-reinforced polymers (FRPs), steel plate bonding, section enlargement, and external post-tensioning. An FRCM is a composite material consisting of one or more layers of cement-based matrix reinforced with dry fibers in the form of open mesh or fabric. The cement-based matrixes are typically made of combinations of portland cement, silica fume, and fly ash as the binder. When adhered to concrete or masonry structural members, they form an FRCM system that acts as supplemental, externally bonded reinforcement. This guide addresses the history and use of FRCM system repair and strengthening; their unique material properties; and recommendations on their design, construction, and inspection. Guidelines are based on experimental research, analytical work, and field applications.

Keywords: bridges; buildings; cracking; cyclic loading; deflection; development length; earthquake-resistant; fabric-reinforced cementitious matrix; fatigue; fiber-reinforced polymer; flexure; lap splices; masonry; meshes; mortar matrix; shear; stress; structural analysis; structural design; substrate repair; surface preparation; unreinforced masonry.

CONTENTS

ACI 549.4R-13 was adopted and published December 2013.

CHAPTER 1—INTRODUCTION AND SCOPE

1.1—Introduction

Fabric-reinforced cementitious matrix (FRCM) composites have recently emerged as a viable technology for repairing and strengthening concrete and masonry structures. The repair, retrofit, and rehabilitation of existing concrete and masonry structures has traditionally been accomplished using new and conventional materials and construction techniques, including externally bonded fiber-reinforced polymer (FRP) systems, steel plates, reinforced concrete (RC) overlays, and post-tensioning.

The primary reasons for considering FRCM as a suitable strengthening material stems from the cementitious matrix that shows properties of:

a) Inherent heat resistance

b) Compatibility with the substrate (that is, allows vapor permeability and application on a wet surface)

c) Long-term durability

FRCM is a system where all constituents are developed and tested as a unique combination and should not be created by randomly selecting and mixing products available in the marketplace.

ICC Evaluation Services (ICC-ES) first addressed acceptance criteria for cement-based matrix fabric composite systems for reinforced and unreinforced masonry in 2003. In 2013, this document was expanded and superseded by AC434-13, which provides guidance for evaluation and characterization of FRCM systems. AC434-13 was developed in consultation with industry, academia, and other parties. For FRCM manufacturers, AC434-13 establishes guidelines for the necessary tests and calculations required to receive a product research report from ICC-ES. Once received, the evaluated system can be accepted by code officials under Section 104.11.1 of the International Building Code (IBC 2012). Section 104.11.1 allows research reports to be used as a source of information to show building code compliance of alternative materials.

1.2—Scope

This guide covers FRCM composite systems used to strengthen existing concrete and masonry structures, providing background information and field applications; FRCM material properties; axial, flexural, and shear capacities of the FRCM-strengthened structures; and structural design procedures.

CHAPTER 2—NOTATION AND DEFINITIONS

2.1—Notation

A_c = net cross-sectional area of compression member, in.^{2} (mm^2)
A_e = area of effectively confined concrete, in.^{2} (mm^2)
A_f = area of mesh reinforcement by unit width, in.^{2}/in. (mm^2/mm)
A_g = gross cross-sectional area of compression member, in.^{2} (mm^2)
A_s = area of longitudinal steel reinforcement, in.^{2} (mm^2)
b = short side dimension of compression member with rectangular cross section, in. (mm)
b_w = web width, in. (mm)
D = diameter of compression member, in. (mm)
d = distance from extreme compression fiber to centroid of tension reinforcement, in. (mm)
d_f = effective depth of the FRCM shear reinforcement, in. (mm)
E_2 = slope of linear portion of stress-strain model for FRCM-confined concrete, psi (MPa)
E_c = modulus of elasticity of concrete, psi (MPa)
E_f = tensile modulus of elasticity of cracked FRCM (Avg.), psi (MPa)
E_f^* = tensile modulus of elasticity of uncracked FRCM (Avg.), psi (MPa)
f_c = compressive stress in concrete, psi (MPa)
f_c' = specified compressive strength of concrete, psi (MPa)
f_{cc}' = maximum compressive strength of confined concrete, psi (MPa)
f_{fd} = design tensile strength ($E_f\varepsilon_{fd}$), psi (MPa)
f_{fe} = effective tensile stress level in FRCM attained at failure, psi (MPa)
f_{ft} = transition stress corresponding to transition point, psi (MPa)
f_{fu} = ultimate tensile strength of FRCM (Avg.), psi (MPa)
f_{fv} = design tensile strength of FRCM shear reinforcement, psi (MPa)
f_{fs} = tensile stress in FRCM reinforcement under service load, psi (MPa)
f_l = maximum confining pressure due to FRCM jacket, psi (MPa)
f_{ss} = tensile stress in the steel reinforcement under service load, psi (MPa)
f_y = steel tensile yield strength, psi (MPa)
H_w = height of masonry wall, in. (mm)
h = long side dimension of compression member with rectangular cross section, in. (mm)
L = length of wall in direction of applied shear force, in. (mm)
ℓ_{df} = critical length to develop bond capacity of FRCM, in. (mm)
M_{cr} = cracking moment of unstrengthened member, in.-lbf (N-mm)
M_f = contribution of FRCM to nominal flexural strength, in.-lbf (N-mm)
M_m = contribution of reinforced masonry to nominal flexural strength, in.-lbf (N-mm)
M_n = nominal flexural strength, in.-lbf (N-mm)
M_s = contribution of steel reinforcement to nominal flexural strength, in.-lbf (N-mm)
n = number of layers of mesh reinforcement
P_n = nominal axial strength, lbf (N)
r = radius of edges of a rectangular cross section confined with FRCM, in. (mm)
V_c = contribution of concrete to nominal shear strength, lbf (N)
V_f = contribution of FRCM to nominal shear strength, lbf (N)
V_m = contribution of (unreinforced or reinforced) masonry to nominal shear strength, lbf (N)
V_n = nominal shear strength, lbf (N)
V_s = contribution of steel reinforcement to nominal shear strength, lbf (N)
t = thickness of masonry wall in. (mm)
ε_c = compressive strain level in concrete, in./in. (mm/mm)
ε_c' = compressive strain of unconfined concrete corresponding to f_c', in./in. (mm/mm); may be taken as 0.002
ε_{ccu} = ultimate compressive strain of confined concrete corresponding to $0.85f_{cc}'$ in a lightly confined member (member confined to restore its concrete design compressive strength), or ultimate compressive strain of confined concrete corresponding to failure in a heavily confined member
ε_{fd} = design tensile strain of FRCM (ε_{fu} – 1STD), in./in. (mm/mm)
ε_{fe} = effective tensile strain level in FRCM composite material attained at failure, in./in. (mm/mm)

ε_{ft} = transition strain corresponding to the transition point, in./in. (mm/mm)
ε_{fv} = design tensile strain of FRCM shear reinforcement, in./in. (mm/mm)
ε_{fu} = ultimate tensile strain of FRCM (Avg.), in./in. (mm/mm)
ε_{sy} = steel tensile yield strain, in./in. (mm/mm)
ε_t = net tensile strain in extreme tension steel reinforcement at nominal strength, in./in. (mm/mm)
ε_t' = transition strain in the stress-strain curve of FRCM-confined concrete, in./in. (mm/mm)
ϕ_m = strength reduction factor for flexure
ϕ_v = strength reduction factor for shear
$\phi_{v,f}$ = strength reduction factor for shear in out-of-plane masonry
κ_a = efficiency factor for FRCM reinforcement in the determination of f_{cc}' (based on the geometry of cross section)
κ_b = efficiency factor for FRCM reinforcement in the determination of ε_{ccu} (based on the geometry of cross section)
ρ_g = ratio of the area of longitudinal steel reinforcement to the cross-sectional area of a compression member (A_s/bh).

2.2—Definitions

ACI provides a comprehensive list of definitions through an online resource, "ACI Concrete Terminology," at http://terminology.concrete.org. Definitions provided herein complement that source.

cement-based matrix—inorganic hydraulic and nonhydraulic cementitious binder (mortar) that holds in place the structural reinforcement meshes in fabric-reinforced cementitious matrix (FRCM) composite material. If the mortar is polymer-modified, the maximum content of organic compounds (dry polymers) in the matrix is limited to 5 percent by weight of cement.

coating—an organic compound applied to fabric after weaving to protect fibers, increasing the long-term durability and stability of the fabric, and allowing for ease of handling and installation.

engineered cementitious composite (ECC)—also called bendable concrete, is an easily molded mortar-based composite reinforced with specially selected short random fibers, usually polymer fibers.

fabric—manufactured planar textile structure made of fibers, yarns, or both, that is assembled by various means such as weaving, knitting, tufting, felting, braiding, or bonding of webs to give the structure sufficient strength and other properties required for its intended use.

fabric-reinforced cementitious matrix composite material—composite material consisting of a sequence of one or more layers of cement-based matrix reinforced with dry fibers in the form of open single or multiple meshes that, when adhered to concrete or masonry structural members, forms a FRCM system.

fabric-reinforced cementitious matrix composite material configuration—combination of all applicable parameters that affect the performance of FRCM, such as layers, thicknesses, components, and bonding agents.

greige fabric—unfinished fabric just off the loom or knitting machine.

mesh—fabric (two-dimensional structure) or textile (two- or three-dimensional-structure) with open structure; in an open structure, the yarns or strands do not come together, leaving interstices in the fabric or textile.

passive composite system—composite system that is not pre- or post-tensioned during installation.

sizing—organic compound applied to fibers during the fiber manufacturing process to provide enhanced fiber characteristics such as abrasion resistance.

strand—ordered assemblage of filaments of predetermined quantity based on the number of filaments per strand that have a high ratio of length to diameter, are normally used as a unit, and are bundled together to resist splitting or filamentation.

structural reinforcement mesh—open mesh of strands made of dry fibers, like alkali-resistant glass, aramid, basalt, carbon, and polyparaphenylene benzobisoxazole, consisting of primary-direction (PD) and secondary-direction (SD) strands connected perpendicularly; polymeric coatings are typically applied to fibers to increase long-term durability of the mesh and ease of handling and installation; the typical strand spacing of PD and SD strands is less than 0.75 in. (19 mm).

CHAPTER 3—BACKGROUND

3.1—FRCM systems advantages and disadvantages

FRCMs are systems based on inorganic (cementitious) matrixes. Unlike polymeric binders, cementitious matrixes cannot fully impregnate individual fibers. Therefore, the fiber sheets typically used in FRP that are installed by manual layup are replaced in FRCM with a structural reinforcing mesh (fabric). The strands of the FRCM reinforcing mesh are typically made of fibers that are individually coated, but are not bonded together by a polymeric resin. If a polymer is used to either cover or bond the strands, such polymer does not fully penetrate and impregnate the fibers as it would in FRP. For these reasons, the term "dry fiber" is used to characterize an FRCM mesh.

Fiber-reinforced polymers for reinforcement of concrete and masonry, in both new construction and repair, are addressed in other documents produced by ACI Committee 440 (ACI 440R-07; ACI 440.2R-08; ACI 440.7R-10). One example of an FRP material system for concrete reinforcement, in the form of a closely-spaced grid, is an epoxy-impregnated carbon fiber grid successfully used in precast and prestressed concrete products (Grimes 2009).

FRCM systems have several advantageous features (RILEM Technical Committee (TC) 201 2006; Peled 2007c; Fallis 2009):

a) Compatibility with chemical, physical, and mechanical properties of the concrete or masonry substrate

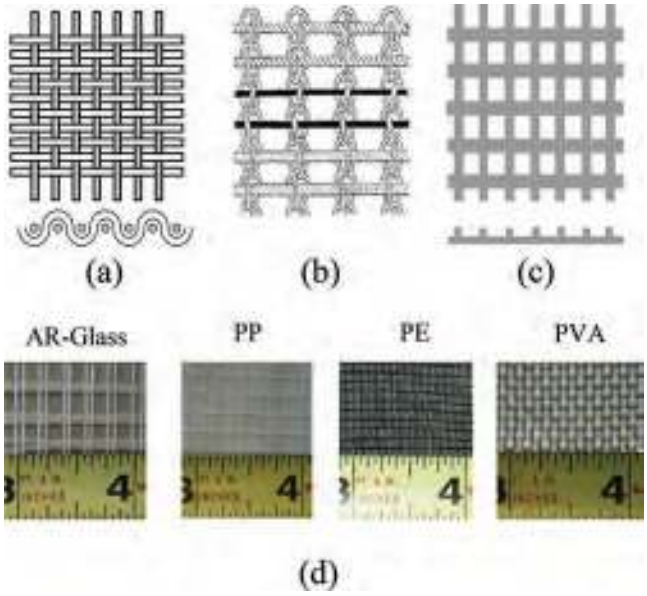

Fig. 3.2—Different fabrics: (a) woven; (b) knitted; (c) bonded; and (d) four commercially available fabrics: AR-glass, polypropylene (PP), polyethylene (PE), and polyvinyl alcohol (PVA).

b) Ease of installation as traditional plastering or trowel trades can be used

c) Porous matrix structure that allows air and moisture transport both into and out of the substrate

d) Good performance at elevated temperatures in addition to partial fire resistance

e) Ease of reversibility (that is, the ability to undo the repair without harming the original structure)

3.2—Historical development

Fabric-reinforced cementitious matrix composite systems evolved from ferrocement where the metallic reinforcement is replaced by fabrics of dry fibers (Fig. 3.2). Recent advances in textile engineering have added significant knowledge to this area where reinforcement options have been extended to two-dimensional fabrics and three-dimensional textiles made from carbon, alkali-resistant (AR) glass, polymeric fibers, or hybrid systems using a variety of configurations. Figures 3.2(b) and (c) present fabrics with open constructions or meshes.

Textile-reinforced concrete (TRC) has been used in Europe for new construction such as cladding applications or industrially-manufactured products (Aldea 2007, 2008; Dubey 2008). In particular, the emphasis on textile has been to signify continuous dry fibers (that is, not resin-impregnated) arranged in the direction of the tensile stresses rather than randomly distributed short fibers. Development work has been conducted since the late 1990s on topics including advanced processing, bonding, interface characteristics, and strengthening of concrete (Brückner et al. 2006; Hartig et al. 2008; Zastrau et al. 2008; Banholzer 2004; Banholzer et al. 2006; Peled et al. 1994, 1997, 1998a, 1999; Peled and Bentur 1998).

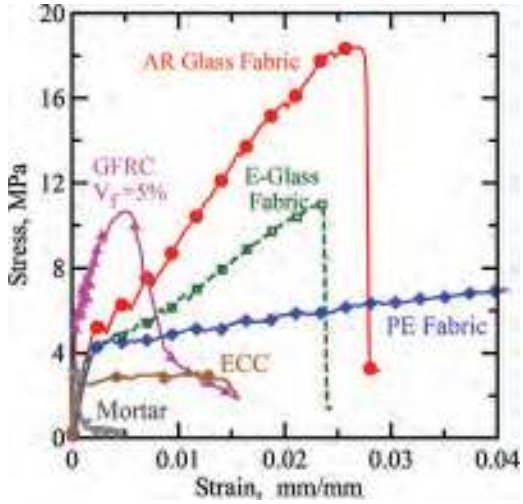

Fig. 3.2.1a—Tensile stress-strain behavior of FRCM with AR glass, E-glass, and polyethylene meshes compared with GFRC and ECC.

RILEM Technical Committee (TC) 201 (2006) includes information about applications of TRC and strengthening systems for unreinforced masonry. In addition to TRC, FRCM has also been identified in the technical literature as textile-reinforced mortar (TRM) (Triantafillou et al. 2006; Triantafillou and Papanicolaou 2006), mineral-based composites (MBC) (Blanksvärd et al. 2009), and fiber-reinforced cement (Wu and Sun 2005).

The following sections report on published technical literature covering topics from material systems to structural performance of strengthened members.

3.2.1 *FRCM mechanical properties*—The mechanical properties of FRCM materials have been addressed in a series of publications by various researchers. Detailed analysis of the tensile mechanical response of these composites revealed that microcracking and crack distribution are two main internal parameters that result in pseudo-ductility. Three distinct measures of damage under tensile loading include quantitative crack spacing, stiffness degradation, and microstructural evaluation (Peled and Mobasher 2007; Mobasher et al. 2004). Using an automated method to determine crack density, crack spacing, and damage accumulation, statistical measures of the evolution of a distributed cracking system as a function of applied strain were correlated with tensile response and stiffness degradation (Mobasher et al. 2004). Similarly, microstructural evaluation refers to a broad range of tools that were used to better understand FRCM modes of failure. These included microscopic evaluation; thin sectioning microscopy; microcrack freezing by means of vacuum impregnation of tested samples using fluorescent epoxy; and thin sectioning to evaluate the interaction of yarns with matrix in crack opening, bifurcation, crack bridging, fiber debonding, and fiber fracture.

Figure 3.2.1a shows the tensile stress-strain behavior of specimens with various fiber meshes compared with the performance of glass fiber-reinforced concrete (GFRC) and engineered cementitious composite (ECC). Figure 3.2.1b shows the formation of distributed crack spacing throughout

Table 3.2.1—PBO- and carbon-FRCM tensile coupons tested according to AC434

FRCM property	Symbol	PBO-FRCM		Carbon-FRCM	
		Mean	STD	Mean	STD
Modulus of elasticity of the uncracked specimen, msi (GPa)	E_f^*	261 (1805)	65 (452)	74 (512)	19 (130)
Modulus of elasticity of the cracked specimen, msi (GPa)	E_f	18 (128)	2 (15)	12 (80)	3 (18)
Tensile stress corresponding to the transition point, ksi (MPa)	f_{ft}	54 (375)	12 (82)	66 (458)	7 (48)
Tensile strain corresponding to the transition point, %	ε_{ft}	0.0172	0.0044	0.1020	0.0449
Ultimate tensile strength, ksi (MPa)	f_{fu}	241 (1664)	11 (77)	150 (1031)	8 (54)
Ultimate tensile strain, %	ε_{fu}	1.7565	0.1338	1.0000	0.1405

Note: Coupon tested with 6 in. (150 mm) long tabs.

Fig. 3.2.1b—Distributed cracking in AR glass-FRCM (width = 1 in. [25 mm]).

Fig. 3.2.1c—Tensile test with clevis-type grips.

an AR glass FRCM specimen (Peled and Mobasher 2006). Different fibers and mesh configurations have varying characteristic responses that correlate to crack spacing and composite stiffness (Mobasher et al. 2006).

Contamine et al. (2011) developed a direct tensile test for design purpose that is reliable, efficient, and relatively easy to implement. Results were based on a large series of experiments using a laminating technique and field measurements known as photogrammetry measurements. Protocol limitations were identified, including the poorly reproducible nature of the initial zone and the impact of implementation defects. As FRCM presents significant defects (for example, warping and reinforcement asymmetry), behavior prior to the onset of the first through-crack is not exploitable. However, the states that follow are representative of the FRCM composite's overall behavior. Although the number and the spacing of cracks is the same on the two sides in the case of warping specimens, this is not the case for specimens with asymmetrical reinforcement. Therefore, it is important to be cautious when considering the spacing and the crack opening as intrinsic properties of the FRCM composite.

Arboleda et al. (2012) performed experiments with the objective of investigating the mechanical properties of two FRCM systems, where carbon fibers and polyparaphenylene benzobisoxazole (PBO) fibers were used. They determined the values of the tensile modulus of elasticity of the cracked and uncracked coupons, transition point of the bilinear behavior, and ultimate point (Table 3.2.1). The strain properties show the most variation because displacement measurement did not cover the entire coupon length (Fig. 3.2.1c). The main failure mode was by slippage of fibers—an indicator of the importance of bond strength in the performance of these materials.

In addition to tensile characterization under quasi-static conditions, research work has been undertaken in tension under high-speed impact and flexure (Peled et al. 1994, 1999; Zhu et al. 2010a,b, 2011; Haim and Peled 2011; Butnariu et al. 2006; Peled 2007b).

3.2.1.1 *Fabric geometry and fiber type*—Existing literature indicates that the mechanical properties of FRCM are greatly influenced by: a) textile/yarn/fiber geometry, including three-dimensional structures (Peled et al. 1998a, 2008a, 2011b; Peled and Bentur 2000, 2003; Peled 2007a); and b) fiber type, including hybrid combinations (Peled et al. 2009, 2011a).

3.2.1.2 *Modification of cement matrix*—Penetration of cement paste between the openings of the mesh and fibers in the strands is a controlling factor in improving the mechanical properties of FRCM. Penetration is dependent on fiber, strand size, mesh opening, and viscosity of the matrix (Peled et al. 2006). Research has focused on optimizing mixture viscosity during the manufacturing process and optimal mechanical performance.

3.2.1.3 *Shrinkage and time-dependent behavior*—Researchers have studied the effects of fibers on plastic

shrinkage cracking behavior in FRCM (Mechtcherine 2012; Mechtcherine and Lieboldt 2011). A general observation is that fiber fineness is effective in reducing the width of plastic shrinkage cracks (Qi and Weiss 2003; Banthia and Gupta 2006). The effectiveness of fiber meshes in improving the shrinkage resistance of concrete materials has also been studied (Poursaee et al. 2010, 2011). Fine microfibers with a high specific fiber surface area are particularly effective in reducing plastic shrinkage cracking. Test methods to address creep behavior of fiber reinforcements for FRCM have been developed (Seidel et al. 2009).

3.2.1.4 *Glass fiber durability*—Alkali-resistant glass fibers have been widely and successfully used with cementitious matrixes (MNL128-01). Their change in properties with time has been studied for more than 35 years. A design methodology based on durability has been established that considers the long-term properties of glass fibers (MNL128-01). There have been no demonstrated product failures due to durability issues in AR glass fibers. Design procedures can be based on the empirical relationships between accelerated aging regimens using a range of temperatures between 41 and 176°F (5 and 80°C) along with real weathering acceleration factors (Aindow et al. 1984; Litherland 1986; Proctor et al. 1982). Tables that include the relationship between time in accelerated aging at varying temperatures to the exposure to real weather have been proposed (Proctor et al. 1982).

Matrix modifications to improve long-term durability that are aimed at reducing portlandite produced during hydration include the addition of certain ingredients, additives, or both. They include ground-granulated blast furnace slag, silica fume (Kumar and Roy 1986), fly ash (Leonard and Bentur 1984), finely ground E-glass fiber (Jones et al. 2008), or the use of other hydraulic cement matrixes—in particular, calcium aluminate or sulpho-aluminate cements (Litherland and Proctor 1986). The use of fly ash in the matrix modifies rheology and improves the bond between the mesh and cement paste (Peled and Mobasher 2007), in addition to improving the durability of glass and natural fibers (Mobasher et al. 2004). ACI 544.5R presents details of various degradation mechanisms and options to improve long-term durability of AR glass fiber systems.

Recent work has been successfully undertaken to improve durability of glass fibers by filling the spaces between yarns with polymers and nano silica particles (Cohen and Peled 2010, 2012; Bentur et al. 2008).

3.2.2 *Concrete strengthening*—FRCM systems have been developed to strengthen existing concrete structures. The following sections present an overview of research used to verify bond behavior and flexural, shear, and axial strengthening of existing structures.

3.2.2.1 *Bond behavior*—Bond development within a woven mesh composite system contributes to crack-bridging mechanisms (Peled et al. 2006). The woven strands stretch and straighten to continue carrying the load across the matrix crack. This process is repeated as FRCM is loaded beyond the multiple-cracking region. Ultimate strength of the composite is determined by the strength of the fiber mesh or the interface fiber-matrix as delamination and fiber debonding occurs.

The bond between a PBO FRCM-strengthening material and the concrete was experimentally analyzed by means of double shear tests (D'Ambrisi et al. 2013) to evaluate an effective anchorage length of 9.8 to 11.8 in. (250 to 300 mm) and a maximum debonding fiber strain of 0.00825. A calibration of a local bond-slip relation based on experimental results published a year later (D'Ambrisi et al. 2013) is reported in D'Ambrisi et al. (2012).

3.2.2.2 *Flexural strengthening*—Triantafillou (2007) reports on a feasibility study to investigate the effectiveness of carbon FRCM as flexural strengthening materials of RC beams subjected to four-point bending. One control beam was tested without strengthening and the second one strengthened with four-layer mesh FRCM. The FRCM-strengthened beam displayed a failure mechanism governed by inter-laminar shear and showed pseudo-ductility.

In another study, Papanicolaou et al. (2009) carried out experimental and analytical investigations on the use of carbon and glass FRCM to strengthen 6.6 x 6.6 ft (2 x 2 m) two-way slabs subjected to concentrated forces. The load-carrying capacity of the FRCM-strengthened slabs using one carbon, two carbon, and three glass fabric layers increased by more than 25, 50, and 20 percent, respectively, over the control specimen with experimental results in good agreement with analytical predictions.

Gencoglu and Mobasher (2007) strengthened plain concrete flexural members with glass FRCM. Results indicated an increase in load-carrying and deformation capacities, and also pseudo-ductility by using multiple layers of AR glass mesh. A design procedure based on composite laminate theory was proposed (Mobasher 2012) to address the contribution of FRCM, where an algorithm produces a moment-curvature relationship for the section, which in turn can be used to calculate the load-deflection response of a structural member (Soranakom and Mobasher 2010b). Flexural performance of concrete members strengthened with FRCM under impact rather than from quasi-static loads has also been reported (Katz et al. 2011).

Experimental results of RC beams strengthened in flexure with various types of FRCM materials are discussed in D'Ambrisi and Focacci (2011). Carbon and PBO meshes and two types of cementitious matrixes were tested. The failure of FRCM-strengthened beams was caused by loss of strengthening action as a result of fiber debonding; three different debonding modes were identified. In most cases, the fiber debonding involved the fiber/matrix interface instead of the concrete substrate. PBO FRCM performed better than carbon FRCM. The fiber strain at beam failure was estimated at 0.8 to 0.9 percent in carbon FRCM and 1.3 to 1.5 percent for PBO FRCM. The performance of FRCM materials is strongly dependent on the matrix design and constituents as they affect the fibers/matrix bond.

3.2.2.3 *Shear strengthening*—Triantafillou and Papanicolaou (2006) investigated the use of FRCM to increase the shear resistance of RC members with rectangular cross sections under monotonic or cyclic loading. They concluded

that FRCM jacketing provides substantial gain in shear resistance. This gain increases as the number of mesh layers do and, depending on the number of layers, could transform the shear-type failure into flexural failure.

Al-Salloum et al. (2012) investigated the use of basalt FRCM as a means of increasing the shear resistance of RC beams using two mortar types—cementitious and polymer-modified cementitious—as binder. The studied parameters also included the number of reinforcement layers and their orientation. The experimental program comprised of testing two control beams that were intentionally designed to be deficient in shear, in addition to testing eight strengthened beams. It was concluded that FRCM provides substantial gain in shear resistance and this gain is higher as the number of reinforcement layers increases. With a higher number of layers, 45-degree orientation and polymer-modified cementitious mortar provides the highest shear strength enhancement.

3.2.2.4 *Axial strengthening*—Confinement with FRCM systems has been investigated for damaged and undamaged RC members (Peled 2007c).

Triantafillou et al. (2006) used cylindrical and prismatic plain concrete specimens. The investigation with cylindrical specimens studied the effects and strength of two inorganic mortars and a number of reinforcement layers (two and three). Jacketing of all cylinders was accomplished with the use of a single mesh in a spiral configuration until the desired number of layers was achieved. Testing on rectangular prisms aimed at investigating the number of reinforcement layers (two and four) and effectiveness of bonded versus unbonded confinement. Considering all results, it was concluded that:

a) Fabric-reinforced cementitious matrix-confining jackets provide substantial gain in compressive strength and deformation capacity. In the case of ultimate capacity, for example, the increase over the unconfined specimen varies between 25 and 75 percent based on mortar type, number of reinforcement layers, and specimen cross section type.

b) This gain increases as the number of mesh layers increases and is dependent on the tensile strength of the mortar, which determines whether failure of the jacket occurs due to fiber fracture or debonding.

c) Failure of FRCM jackets is due to the slowly progressing fracture of individual fiber strands.

De Caso y Basalo et al. (2009, 2012) reported on a feasibility study to develop a reversible and potentially fire-resistant FRCM system for concrete confinement applications. A candidate system was selected from different fiber and cementitious matrix combinations on the basis of: a) constructibility; b) confined concrete cylinders enhancement of strength and deformability; c) quality of the concrete FRCM interface; and d) level of fiber impregnation monitored with scanning electron microscope images. The selected FRCM system was further assessed using different reinforcement ratios and by introducing a bond breaker between concrete and jacket to facilitate reversibility. Substantial increases in strength and deformability with respect to unconfined cylinders were attained. For example, in the case of bonded jackets, the increase in ultimate capacity over the unconfined specimen varied between 21 and 121 percent when the number of reinforcement layers varied from one to four. The predominant failure mode was fiber-matrix separation, which emphasized the need of improving fiber impregnation.

Di Ludovico et al. (2010) appraised the performance of basalt FRCM as a strengthening material for the confinement of RC members. Effectiveness of the technique was assessed by comparing different confinement schemes on concrete cylinders. Based on experimental results, the basalt FRCM technique showed an increase of peak stress between 27 and 45 percent over the unconfined member when the number of reinforcement layers varied from one to two.

Abegaz et al. (2012) tested a total of 27 approximately 1/4-scale RC columns wrapped with FRCM to investigate and quantify the enhancement in strength and ductility for different cross-sectional shapes. Rectangular, square, and circular specimens with equal cross-sectional area and slenderness ratio were considered to properly isolate the effect of shape on the confinement effectiveness. In addition to cross-sectional shape, columns with one and four layers of FRCM wrapping were tested to investigate the effect of the number of plies. Results indicated that FRCM wrapping can significantly enhance the load-bearing capacity (up to 71 percent) and ductility (exceeding 200 percent) of RC columns subjected to a monotonic axial compressive load, with the highest improvement obtained for circular cross sections.

3.2.2.5 *Seismic retrofitting*—Bournas et al. (2007) investigated the effectiveness of FRCM jackets as a means of confining RC columns. Tests were carried out on short prisms under concentric compression and on nearly full-scale, nonseismically detailed RC columns subjected to cyclic uniaxial flexure under constant axial load. Compression tests on prisms indicated that FRCM jackets provide substantial gain in compressive strength and deformation capacity by delaying buckling of the longitudinal bars; this gain increases with the volumetric ratio of the jacket. Tests on nearly full-scale columns show that FRCM jacketing is effective as a means of increasing the cyclic deformation capacity and energy dissipation of RC columns with poor steel detailing by delaying bar buckling. Further experimental and analytical investigations on bar buckling at the plastic hinge of old-type RC columns confined with FRCM jackets are reported in Bournas and Triantafillou (2011).

Bournas et al. (2009, 2011) investigated the effectiveness of FRCM as a means of confining old-type RC columns with limited capacity due to bond failure at lap splice regions and made comparisons with equal stiffness and strength FRP jackets. Tests on nearly full-scale columns subjected to cyclic uniaxial flexure under constant axial load indicated that FRCM jacketing is effective as a means of increasing the cyclic deformation capacity by preventing splitting bond failures in columns with lap-spliced bars. Compared with their FRP counterparts, the FRCM jackets used in these studies were found to be equally effective in terms of increasing strength and deformation capacity of the retrofitted columns. As a result of the experimental investigation

of RC members confined with FRCM, simple equations were proposed for calculating the bond strength of lap splices.

3.2.2.6 *Beam-column connections*—The performance and behavior of RC exterior beam-column joints rehabilitated using FRCM was studied (Mobasher 2012). The strengthening was applied to seismically deficient beam-column joints subjected to cyclic loads that simulate seismic excitation. Six 1/2-scale exterior beam-column joints were prepared. One specimen was designed in accordance with ACI 318 and the others insufficiently reinforced to study the shear, anchorage, and ductility aspects of the beam-column connection. Two beam-column joints used an AR glass FRCM as the basis for the retrofit. By shifting failure location and failure mode of the exterior beam-column hinges that form during reverse cyclic loads, FRCM strengthening showed better results than the ACI 318-detailed specimen in terms of ductility; total absorbed, dissipated, and recovery energy; ultimate displacement; and load-carrying capacity.

Al-Salloum et al. (2011) studied efficiency and effectiveness of FRCM on upgrading the shear strength and ductility of seismically-deficient exterior beam-column joints compared with that of carbon fiber-reinforced polymer (CFRP) and GFRP systems. Joints were constructed with deficient design and encompassing the majority of existing beam-column connections. Two specimens were used as a baseline and the third was strengthened with FRCM. All sub-assemblages were subjected to quasi-static cyclic lateral load histories to provide the equivalent of severe earthquake damage. The results demonstrated that FRCM can effectively improve the shear strength and deformation capacity of seismically deficient beam-column joints. In particular, the peak load increased 10 percent and the ultimate displacement (measured after a 20 percent drop in peak load) increased 28 percent.

3.2.3 *Strengthening of masonry*—Extensive experimental results indicate that FRCM systems represent a viable solution for structural strengthening of masonry structures. Results in the literature are available for FRCM systems using coated AR glass, bitumen-coated E-glass, basalt, bitumen-coated polyester, polypropylene, and greige carbon meshes to strengthen walls made of concrete masonry units (CMUs), fired clay bricks, tuff blocks, and stone blocks.

3.2.3.1 *CMU walls and piers*—Marshall (2002), Mobasher et al. (2007), and Aldea et al. (2007) used a coated AR glass FRCM and reported in-plane shear concrete masonry full-scale pier (lightly reinforced single-wythe masonry walls) tests to simulate seismic action. The FRCM system was compared with a number of commercially available FRP systems using E-glass meshes applied in various reinforcement configurations (Fig. 3.2.3.1a) as part of a broad experimental program with goals to: a) add strength and assess the effectiveness of novel systems on improving masonry seismic performance; and b) improve wall performance by increasing deflection limits of the wall, as required by acceptance criteria for new or nonstandard materials for earthquake design. The FRCM system was applied full coverage only on one side of the wall (refer to Walls 1, 2, and 3 in Fig. 3.2.3.1b):

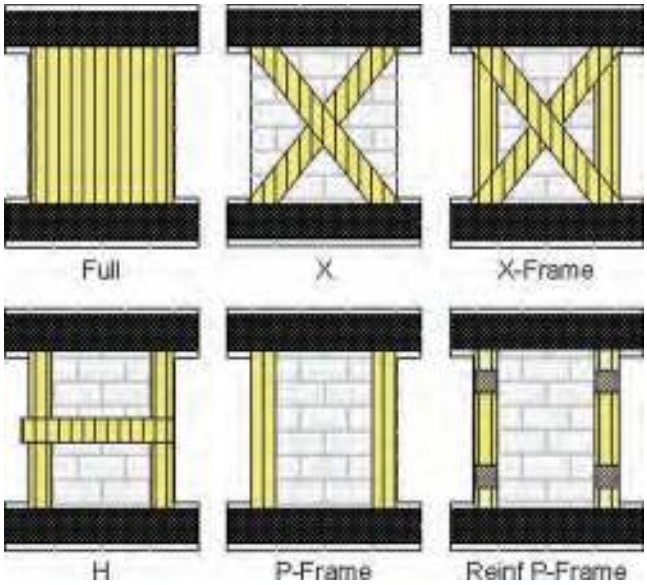

Fig. 3.2.3.1a—Reinforcement configuration for walls (Aldea et al. 2007).

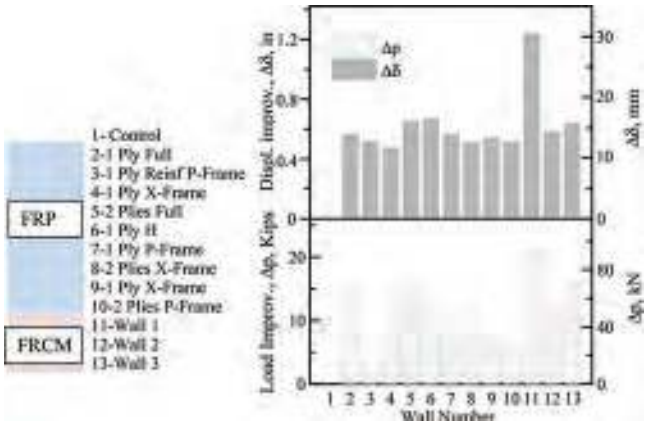

Fig. 3.2.3.1b—Load and displacement improvements for walls strengthened with FRCM and FRP under in-plane shear (Aldea et al. 2007).

a) Wall 1—Two plies 0 to 90 degrees (that is, fiber strands in both the vertical and horizontal directions relative to the wall)

b) Wall 2—Two plies 0 to 90 degrees and one ±45 degrees (that is, fiber strands in both the diagonal directions relative to the wall)

c) Wall 3— Three plies 0 to 90 degrees and two ±45 degrees

Figure 3.2.3.1b compares the load and horizontal displacement improvements provided by the FRP and FRCM systems. The FRCM system added 38 to 57 percent to the shear strength and 29 to 44 percent to horizontal displacement for the wall specimens tested in in-plane shear. In the FRCM strengthened walls, failures were due to shear between the front and rear faces of the blocks, with no delamination of the inorganic system from the CMU walls while holding the masonry pier together at failure.

3.2.3.2 *Clay brick walls and piers*—Papanicolaou et al. (2007, 2008) studied the effectiveness of carbon FRCM

for out-of-plane and in-plane strengthening of unreinforced masonry (URM) walls made of fired clay bricks. Medium-scale masonry walls were subjected to out-of-plane bending (Papanicolaou et al. 2008) and in-plane cyclic loading, where three types of specimens were used: shear walls, beam-columns, and beams (Papanicolaou et al. 2007).

The effect of matrix type, number of reinforcement layers, and the compressive stress level applied to the shear walls and beam columns were also investigated (Papanicolaou et al. 2008). In conclusion, it was found that FRCM jacketing provides substantial increase and effectiveness in terms of strength and deformation capacities for both out-of-plane and in-plane cyclic loads.

3.2.3.3 *Tuff walls and piers*—Tuff is a rock consisting of consolidated volcanic ash. Tuff masonry structures are common in the Mediterranean region. In the past decade, interest in strengthening historical tuff masonry buildings has led to the development of specific and noninvasive architectural and engineering strategies. Faella et al. (2004) and Prota et al. (2006) used carbon and coated AR-glass FRCM applied to tuff masonry walls in one and two plies, on one and two sides. Walls were tested in diagonal compression to measure their in-plane deformation and strength properties, and to assess performance in a seismic event.

The increase in shear strength provided by FRCM compared with as-built ranged between 20 percent (one ply, 0 to 90 degrees, one side of the wall) and 250 percent (two plies, 0 to 90 degrees and ±45 degrees, both sides of the wall) for the system using greige carbon mesh, and between 67 percent (one ply, 0 to 90 degrees, both sides) and 143 percent (two plies, 0 to 90 degrees, both sides) for the system using coated AR glass mesh.

The carbon FRCM failed due to loss of bond resulting in complete separation at the FRCM-masonry interface rather than a fiber rupture, regardless of the system installation on one or both sides (Faella et al. 2004). This failure mode suggested that the weak link lies in the FRCM masonry interface. In conclusion, it was found that the reinforcement was over-designed, as the strength capacity of the mesh was not fully used.

The coated AR glass FRCM showed no delamination of the system from the substrate at failure. Its failure mode was dependent on the number of plies and configuration, and varied from sliding along the mortar joints to splitting (Prota et al. 2006). The results suggest that, overall, AR glass provides a more efficient reinforcement than carbon does due to its considerably smaller stiffness and strain to failure.

The FRCM system assessed by Prota et al. (2006) by means of diagonal compression tests on tuff panels was also validated on a two-story building subjected to dynamic tests on a shake table (Langone et al. 2006).

Balsamo et al. (2010) investigated the effectiveness of FRCM made of coated AR glass and basalt meshes with a premixed high-ductility hydraulic lime and pozzolan-based mortar by means of diagonal compression tests on five tuff masonry panels. The strengthening system was specifically conceived to develop sustainable and reversible strengthening strategies. A mortar with mechanical properties and porosity similar to mortars used in the existing historical buildings was formulated and tested with basalt fabric. Experiments showed that a higher shear strength increase was achieved on specimens reinforced with AR-glass FRCM and a better post-peak response was attained with the basalt FRCM. Experimental results confirmed the effectiveness of FRCM technique to increase the tuff panel shear strength (up to 3.4 times that of the control panel with splitting failure) and validated the use of a mortar specifically formulated for compatibility with tuff material and historical grouting.

Augenti et al. (2011) applied a coated AR-glass FRCM to a full-scale tuff masonry wall with an opening, which was tested under cyclic in-plane lateral loading up to near collapse. The unstrengthened wall was first tested under monotonically increasing lateral displacements until diagonal shear cracking occurred in the spandrel panel, which is the masonry panel above the opening connecting the piers. The pre-damaged wall was then cyclically tested up to approximately the same lateral drift reached during monotonic loading, and diagonal cracking was again observed in the spandrel. Cracks were filled with mortar and the specimen was upgraded by applying FRCM to both sides of the spandrel. Finally, the FRCM-upgraded wall was cyclically tested to assess the increase in the energy dissipation capacity of the spandrel, which is a critical design parameter for strengthening existing masonry buildings. The failure mode of the FRCM-upgraded spandrel panel changed from brittle diagonal shear cracking to ductile horizontal uniform cracking, producing a 17 percent increase in the lateral load-bearing capacity of the wall. Nonlinear finite element analysis and a simplified analytical model developed by Parisi et al. (2011) confirmed that the change in failure mode of the spandrel panel and increase in the load-bearing capacity of the wall were due to the FRCM-strengthening system. Furthermore, analysis of the experimental force-displacement response of the FRCM-upgraded wall demonstrated that strength degradation did not exceed 15 percent at a lateral drift approximately equal to 2.5 percent in correspondence with a lateral displacement of approximately 3 in. (75 mm), which was more than twice that of the as-built and predamaged tests. Bilinear idealizations of the experimental force-displacement curve related to the FRCM-upgraded wall evidenced displacement ductility ratios, global overstrength ratios, and strength-reduction factors significantly higher than those currently required by seismic codes. Improvement in the lateral response of the wall was substantiated by the following:

a) FRCM bridged existing cracks of the predamaged wall without debonding at the matrix substrate interface

b) Failure mode of the spandrel panel changed from brittle diagonal shear cracking to ductile horizontal uniform cracking

c) Cyclic behavior of the composite system was stable

d) The FRCM system did not induce any modification in the stiffness of the spandrel panel and, sequentially, in the spandrel-piers interaction

Full reversibility of the FRCM system is emphasized because it ensures structural upgrading in compliance with

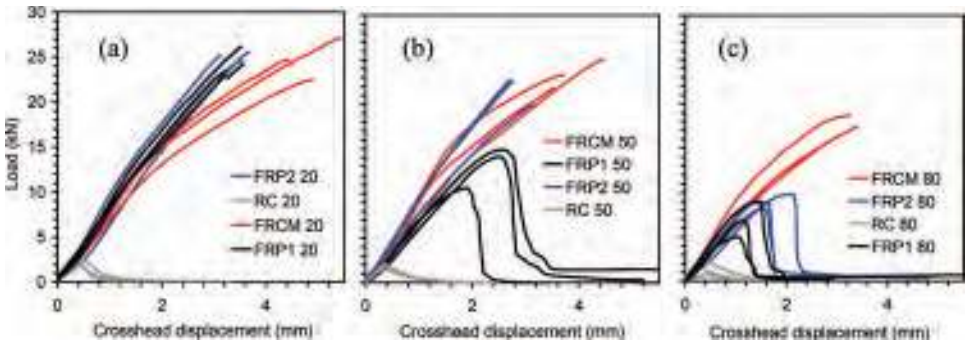

Fig. 3.2.4—Load-deflection response for FRCM-strengthened concrete prisms tested at: (a) 68°F (20°C); (b) 122°F (50°C); and (c) 176°F (80°C).

generally accepted restoration principles for cultural heritage construction.

3.2.3.4 *Stone walls and piers*—Papanicolaou et al. (2011) investigated the effectiveness of externally bonded FRCM as a means of increasing the load-carrying and deformation capacity of unreinforced stone masonry walls subjected to cyclic loading. Beam-type specimens were subjected to out-of-plane flexure parallel to the bed joints according to five configurations, four of them symmetrically strengthened with a different layer of mesh:

1) Symmetrically-strengthened with one mesh layer of bitumen-coated E-glass

2) Symmetrically-strengthened with one mesh layer of E-glass

3) Symmetrically-strengthened with one mesh layer of bitumen-coated polyester, polypropylene, and basalt in a fiber-reinforced mortar

4) Single-layered basalt mesh in a low-strength mortar

Shear walls were also subjected to in-plane shear under compressive loading equal to 3 percent of the wall compressive strength. Two specimens were tested, each symmetrically strengthened with one layer of basalt-FRCM. The first specimen incorporated a fiber-reinforced mortar and the second a low-strength mortar. It was concluded that even the weakest FRCM configuration, when adequately anchored, results in more than a 400 percent increase in strength and a 130 percent increase in deformation capacity.

3.2.4 *Elevated temperature performance*—Performance of FRCM exposed to elevated temperatures in tension and bending was studied (Kulas et al. 2011; Antons et al. 2012; Colombo et al. 2011).

An important consideration in applying any strengthening system in an existing building is its performance during fire. Fire severity, flame spread, smoke generation, and toxicity cannot be ignored as they impact the tenability conditions in a building during the early stages of a fire. Fabric-reinforced cementitious matrix systems are inherently noncombustible and can be used unprotected.

Research aimed at comparing the performance of members strengthened with an FRCM system against FRP systems was performed (Bisby et al. 2009, 2011) to investigate the idea that FRCM can provide retention of mechanical and bond properties at elevated temperatures. Steady-state flexural tests were performed on commercially available FRCM-strengthened RC beams and unreinforced concrete prisms at elevated temperatures. The test data showed good performance of the FRCM system (Fig. 3.2.4). Combined with FRCM-inherent noncombustibility, nontoxic, and nonflaming characteristics, FRCM-strengthening systems are an attractive option for fire-safe structural strengthening, and also in warm climates or industrial environments. Additional testing is needed to clearly define upper service temperature limits for FRCM.

3.3—Commercially available FRCM systems

A number of commercially available FRCM systems for strengthening of concrete and masonry structural members are available. Appendix A shows a representative sample of constituent properties of available systems as provided by the manufacturers.

CHAPTER 4—FIELD APPLICATION EXAMPLES

Examples of commercial projects provide evidence of the potential uses for FRCM technology for repairing and strengthening concrete and masonry structures.

4.1—Concrete repair applications

4.1.1 *Strengthening roof openings for high-temperature ducts*—FRCM was used to strengthen a roof slab to allow an opening to be cut for the passage of air ducts. These ducts were to be operated at temperatures considered too high for conventional FRP repair systems. As per design requirements, strengthening was completed before slab cutting (Fig. 4.1.1). For ease of access and installation, the application was performed on the top side of the roof slab. First, the insulation and roof deck membrane were removed, followed by preparation of the concrete surface by means of grinding. After the first layer of mortar matrix was applied, fiber mesh was installed by pressing it into the mortar layer, which was followed immediately by installing the top mortar layer. Once the FRCM had reached the required strength, openings were cut in the slab and new insulation and roof membrane were placed.

4.1.2 *Unreinforced concrete vault strengthening*—FRCM was used to strengthen a railroad bridge along the Roma-Formia line in Italy (Berardi et al. 2011). The superstruc-

Fig. 4.1.1—Installation of FRCM on roof slab around area where slab opening will be cut for duct passage.

ture consists of six semicircular vaults made of unreinforced concrete with approximately the same span, resting on masonry abutments made of blocks of tuff (Fig. 4.1.2a(a)). The deck is 34.4 ft (10.5 m) wide with a vault thickness that varies between 27.5 in. (0.7 m) at the crown to 39.4 in. (1.0 m) at the skewback. The project was preceded by a field investigation for characterization of the geometry and evaluation of the material mechanical properties. FRCM was adhered to the soffit of each vault to prevent formation of hinges at the exterior surface. This repair method that can be implemented without disrupting traffic modifies the vault ultimate behavior without affecting behavior of the structure under service loads. Safety of the structure was assessed by the limit state analysis considering all possible mechanisms of collapse with formation of hinges.

Final design called for the soffit of each vault to be strengthened by application of a two-ply mesh FRCM. To begin, the concrete surface was thoroughly cleaned and portions of deteriorated concrete removed and reconstructed. A first layer of cementitious matrix, approximately 0.12 to 0.20 in. (3 to 5 mm) thick, was applied on the concrete surface, followed by application of the first fiber mesh (Fig. 4.1.2a(b)). A second, thinner layer of cementitious matrix and the second fiber mesh were added. Figure 4.1.2b shows the fiber mesh rolls freely hanging from the vault as the scaffolding is moved to the next location. Strengthening concludes with application of a final top layer of the same matrix.

4.1.3 *Strengthening of reinforced concrete (RC) tunnel lining*—The RC lining of a vehicular tunnel along the Egnatia Odos Motorway in Greece was strengthened with FRCM to correct a structural deficiency (Nanni 2012). The original lining was 25.6 in. (650 mm) thick with clear cover of 2 in. (50 mm) and was reinforced with top and bottom steel bar mats. According to a structural analysis, the ultimate flexural capacity in the transverse direction of the tunnel lining was increased 14 percent (top portion) and 4 percent (side portions) by adding a single fiber mesh. Additionally, a flexural strength increment of 100 percent (which would exceed the usable limit imposed by this guide) was

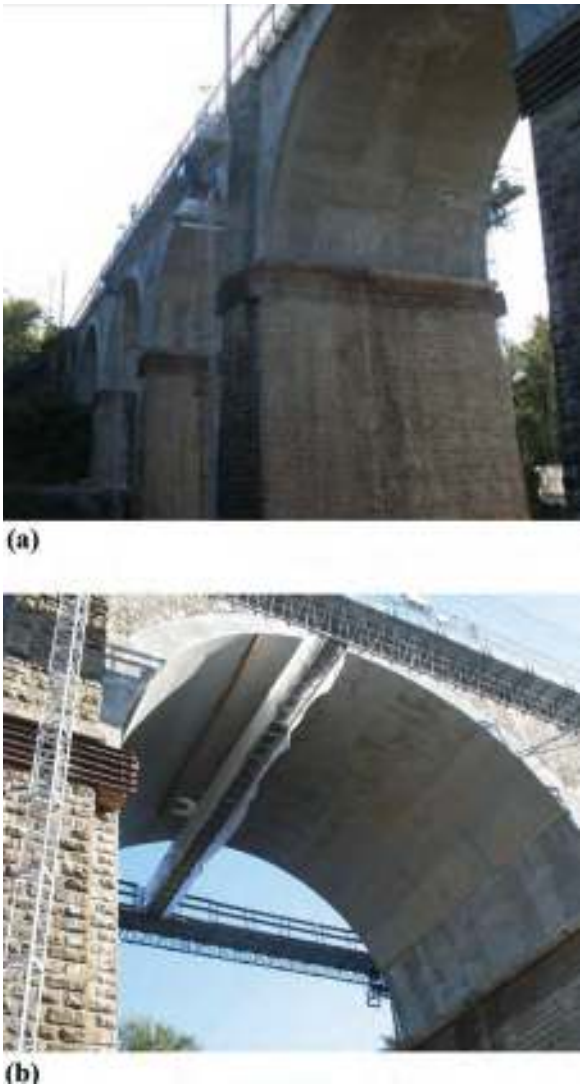

Fig. 4.1.2a—(a) Bridge structure with view of scaffolding; and (b) installation of FRCM.

Fig. 4.1.2b—Details of work in progress (second fiber mesh).

attained in the longitudinal direction in the top portion of the tunnel lining using two fiber meshes. The concrete surface was scarified using hydrojetting (Fig. 4.1.3(a)) followed by FRCM installation and finishing (Fig. 4.1.3(b)).

(a)

(b)

Fig. 4.1.3—(a) Surface preparation by hydrojetting; and (b) application of reinforcement mesh at top portion of tunnel lining.

4.1.4 *Trestle bridge base confinement*—FRCM was chosen to provide confinement to the concrete support base for the trestle of a railway bridge in New York (Nanni 2012) because a breathable strengthening material was required. The base had cracked and the concrete deteriorated over time (Fig. 4.1.4a). Although cracking and deterioration did not necessarily affect performance of the support base, long-term durability of the concrete base was a concern that had to be addressed. The first step was to remove and replace the deteriorated concrete by chipping it out and replacing it with an engineered fast-set concrete repair material. The concrete surface was prepared by grinding to provide a good bonding surface. The FRCM matrix was applied and the fiber mesh pressed into the substrate (Fig. 4.1.4b). Last, the crew installed the top mortar layer and a curing compound.

4.1.5 *Equipment base confinement in high ambient temperature*—FRCM was chosen to confine the concrete support base of a piece of equipment in an industrial plant in the Midwestern United States because the ambient temperature of the concrete was approximately 180°F (82°C), which is considered too high for conventional FRP repair systems. The concrete substrate was first prepared by means of grinding to provide a good bonding surface. Because the concrete temperature during the installation was at approximately 140°F (60°C), its surface was constantly wetted to have it in a saturated surface-dry condition at the application of FRCM. A crew then applied the first matrix layer to the surface and immediately after, because of high temperature, a second crew installed the mesh by pressing it into the initial layer of mortar (Fig. 4.1.5). A third crew followed with the

Fig. 4.1.4a—Trestle of the railway bridge before repair.

Fig. 4.1.4b—Installation of FRCM system.

Fig. 4.1.5—Installation of reinforcement mesh on equipment base.

top mortar layer. Upon completion, a polymer coating and wet burlap were installed to provide proper curing.

4.1.6 *Strengthening of reinforced concrete bridge pier*—The RC bridge piers of a structure located in Novosibirsk, Russia were strengthened with FRCM (Nanni 2012). The piers of this bridge were reconstructed in 1958 by increasing their height to 32.4 ft (9.87 m) and their width at the top to 34.8 ft (10.6 m). Significant temperature and shrinkage stresses following reconstruction caused the formation of cracks along the construction joints and new corbels. Although the cracks were epoxy-injected in 1991, they reappeared 6 years later with widths ranging from 0.08 to 0.20 in. (2 to 5 mm). Given the lack of success with the previous repair techniques, the owner elected to repair and strengthen the structure with FRCM. The project, which was completed in 2007, was made up of the following:

1) Sandblasting the concrete surface
2) Rounding corners to a radius of 1.2 in. (30 mm)
3) Repairing cracks and resurfacing with single-component polymer-modified cementitious mortar
4) Strengthening with FRCM
5) Surface sealing with a two-component, polymer-modified, cementitious waterproofing and protective slurry

Given the cold weather conditions of this region, curing tents warmed from within by construction-grade heaters kept a constant air temperature in the enclosure at approximately 59 to 64°F (15 to 18°C). The heaters remained until 7 days after project completion.

Fig. 4.2.1a—Chimney with scaffolding during repair.

4.2—Masonry repair applications

4.2.1 *Strengthening of unreinforced masonry chimney*—FRCM was used to strengthen the masonry chimney part of the now-closed sawmill François Cuny complex located in the municipality of Gerardmer, France (Nanni 2012). This chimney, a symbol of industrial heritage, was to be preserved and restored. The chimney has a height of approximately 124.7 ft (38 m) with a diameter ranging from 11.8 ft (3.60 m) at the base to 5.6 ft (1.70 m) at the top (Fig. 4.2.1a). Today, the structure is used to support several telephone antennas and their cabling.

The technical challenge of the high capillary absorption of the clay bricks, including their sand-lime joints (Fig. 4.2.1b(a)), was addressed by using a cementitious repair mortar to rectify the existing surface without any surface pretreatment such as sandblasting. The chimney was analyzed as a cantilever beam with wind being the primary load condition. The analysis indicated that it was necessary to strengthen the structure with 0.47 in. (10 mm) thick FRCM reinforced by a single fiber mesh (Fig. 4.2.1b(b)).

4.2.2 *School building strengthening*—FRCM was selected to strengthen a school building in Karystos, Greece (Triantafillou 2007). This involved both flexural strengthening of RC slabs with heavily corroded reinforcement and shear strengthening of unreinforced stone masonry walls. Strengthening was completed using fiber meshes combined with cementitious mortar (Fig. 4.2.2).

4.2.3 *Masonry dome strengthening*—A clay brick masonry cylindrical dome in the old church of Panaghia Crina in the

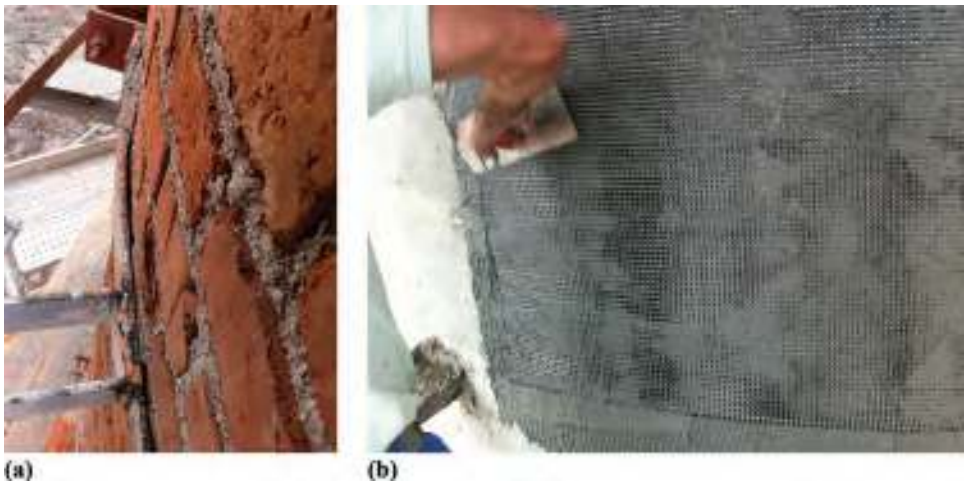

Fig. 4.2.1b—Chimney masonry surface: (a) before strengthening; and (b) during strengthening.

Fig. 4.2.2—School building strengthening of: (a) concrete slabs; and (b) stone masonry walls.

Fig. 4.2.3—Strengthening of clay brick masonry dome.

island of Chios, Greece, was strengthened with two layers of fiber mesh combined with a hydraulic lime-based mortar applied to the exterior surface (Fig. 4.2.3) (Triantafillou 2007).

CHAPTER 5—FRCM CONSTITUENT MATERIALS AND SYSTEM QUALIFICATIONS

5.1—Constituent materials

The two principal components of FRCM are the cementitious matrix and the structural reinforcement mesh. The former is typically a grout system based on portland cement and a low dosage of dry polymers at less than 5 percent by weight of cement. The organic polymer compounds are sometimes used to ensure proper workability, setting time, and mechanical properties. Nonhydraulic mortars, such as lime-based mortars, may be used for masonry strengthening, particularly in the case of historical structures. The mechanical effectiveness of FRCM is strongly influenced by: a) capacity of the cementitious matrix to impregnate the dry fiber strands (Peled and Bentur 1998; Banholzer 2004; Wiberg 2003; Peled et al. 2008a); b) effective fiber/matrix interface bond properties (Peled et al. 1997, 1998a,b, 2006, 2008b; Bentur et al. 1997; Hartig et al. 2008; Soranakom and Mobasher 2009; Sueki et al. 2007; Cohen and Peled 2012); and c) bond between the cementitious matrix and the concrete or masonry substrate (Ortlepp et al. 2004, 2006; Mobasher et al. 2007).

There are a variety of fiber meshes available in the marketplace that could be potentially used as constituents of FRCM systems. In these meshes, the typical spacing of primary-direction (PD) and secondary-direction (SD) strands is less than 1 in. (25.4 mm), and the total coverage area of the fiber mesh is less than 2/3 of total area (that is, there is at least 33.3 percent of open area among strands). With reference to fiber types in particular, extensive descriptions of various physical and mechanical properties exists in the literature (ACI 440R-07; ACI 440.2R-08; ACI 440.7R-10; ACI 544.1R-96; RILEM Technical Committee (TC) 201 [2006]). Although a significant amount of research was carried out on the use of greige (uncoated) alkali-resistant (AR) glass fibers, the results, although interesting, appear to be of limited practical application. This is because AR glass meshes for the applications discussed in this guide are typically coated to improve their long-term durability in a cementitious matrix and for ease of handling and installation.

While many interesting and promising field applications have been undertaken, and FRCM technology has been proven reliable, experimental and theoretical research continues to fully characterize FRCM and quantify its mechanical effectiveness based on parameters such as type and arrangement of fibers, type of cementitious matrix, and conditions of the substrate (D'Ambrisi and Focacci 2011). Several analytical approaches are available that allow for measurement of the contribution of different reinforcement meshes and matrix systems using mechanics-based approaches (Mobasher 2012; Soranakom and Mobasher 2010a,b).

Appendix A in this guide presents the constituent material properties of some commercially available FRCM systems as provided by the respective manufacturers. While these parameters must be disclosed by manufacturers, they cannot be directly used to infer the values of the parameters to be used in design, nor to assess the durability of an FRCM system. Based on the provisions of AC434, 5.2 to 5.4 of this guide describe the test protocols required to qualify an

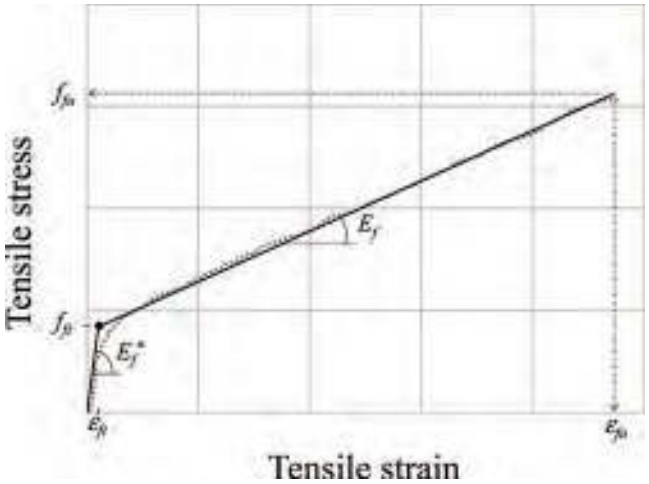

Fig. 5.3.2a—Idealized tensile stress-versus-strain curve of an FRCM coupon specimen.

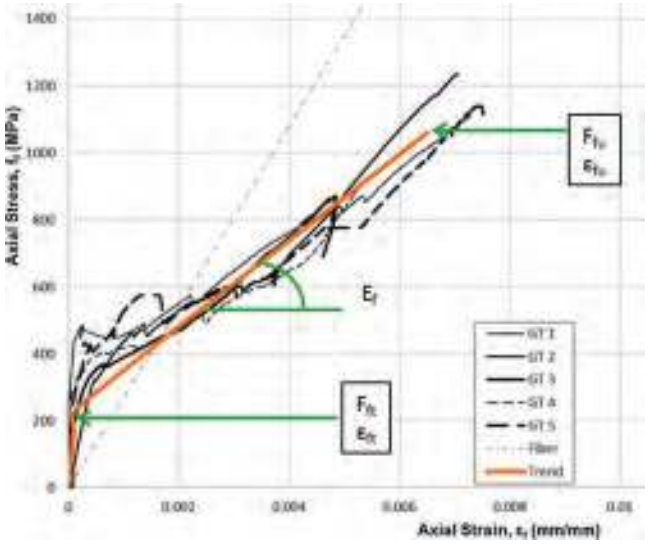

Fig. 5.3.2b—Experimental tensile stress-versu-strain curve of FRCM coupons as per Annex A of AC434.

FRCM system and how to obtain the design values used in Chapters 10 through 13.

5.2—Fabric-reinforced cementitious matrix system qualification

Each FRCM system should be qualified for use in a project based on the independent laboratory test data of the FRCM constituent materials and coupons made with them, structural test data for the type of application being considered, and durability data representative of the anticipated environment. Test data provided by the FRCM system manufacturer demonstrating that the proposed FRCM system meets all mechanical and physical design requirements including tensile strength, durability, and bond to substrate should be considered, but not used as the sole basis for qualification. The specified material-qualification programs should require laboratory testing to measure repeatability and reliability of critical properties. Untested FRCM systems should not be considered for use.

5.2.1 *Qualification test plan according to AC434*—A qualification test plan should be undertaken following the requirements of AC434 with the intent of verifying the design properties to be used in FRCM systems. This testing would provide data on material properties, force, and deformation limit states, including failure modes of FRCM to support a rational analysis, and design procedure. Specimens should be constructed under conditions specified by AC434 and be prepared to verify the range of FRCM configurations, including layers, thickness, components, and bonding agents recommended by the manufacturer. Tests should simulate the anticipated range of loading conditions, load levels, deflections, and ductility.

In 5.3 and 5.4, a list of physical, mechanical, and durability properties that should be determined to characterize each FRCM system according to AC434 is presented.

5.3—Physical and mechanical properties

5.3.1 *Drying shrinkage and void content*—For each FRCM system, drying shrinkage and void content of the cementitious matrix should be determined. Drying shrinkage tests should be conducted in accordance with the general procedures outlined in ASTM C157/C157M and void content tests conducted in accordance with ASTM C138/C138M.

5.3.2 *Tensile properties*—Quantities considered to characterize the tensile behavior of each FRCM system are:

a) Tensile modulus of elasticity of the uncracked specimen, E_f^*

b) Tensile modulus of elasticity of the cracked specimen, E_f

c) Ultimate tensile strain ε_{fu}

d) Tensile strain corresponding to the transition point, ε_{ft}

e) Ultimate tensile strength f_{fu}

f) Tensile stress corresponding to the transition point, f_{ft}

g) Lap tensile strength

The idealized tensile stress-strain curve of an FRCM coupon specimen is initially linear until cracking of the cementitious matrix occurs, deviates from linearity, and becomes linear again until failure by slippage, as illustrated in Fig. 5.3.2a. The plot can be reduced to a simple bilinear curve with a bend-over point (transition point as defined in AC434) corresponding to the intersection point obtained by continuing the initial and secondary linear segments of the response curve. The initial linear segment of the curve corresponds to the FRCM uncracked linear behavior and it is characterized by the uncracked tensile modulus of elasticity E_f^*. The second linear segment, which corresponds to the FRCM cracked linear behavior, is characterized by the cracked tensile modulus of elasticity E_f.

FRCM tensile properties should be determined according to the test procedure specified in Annex A of AC434. Figure 5.3.2b shows five experimental curves obtained with tests conducted according to Annex A of AC434 using the clevis-type grips prescribed in its provisions (Fig. 3.2.1c). In particular, Fig. 5.3.2b shows the tensile modulus of elasticity and the ultimate tensile strain as computed based on AC434. That is, on the segment of the response curve corresponding to cracked behavior after the transition point, two points are selected on the experimental curve at a stress level equal to

$0.90f_{fu}$ and $0.60f_{fu}$. The slope of the line that connects these two points represents the tensile modulus of elasticity at that region

$$E_f = \Delta f/\Delta\varepsilon = (0.90f_{fu} - 0.60f_{fu})/(\varepsilon_{f@0.90ffu} - \varepsilon_{f@0.60ffu})$$

Ultimate tensile strain ε_{fu} is the y-intercept of the line used to compute E_f (that is, $y_{intercept} = 0.60f_{fu} - E_f\varepsilon_{f@0.60ffu}$) and the following equation

$$\varepsilon_{fu} = (f_{fu} - y_{intercept})/E_f$$

5.3.3 *Bond and inter-laminar shear strength*—The bond strength of FRCM to the concrete and masonry substrates and the composite inter-laminar shear strength between the fiber mesh and the cementitious matrix should be evaluated for each FRCM system according to the procedures indicated in ASTM C1583/C1583M and ASTM D2344/D2344M, respectively. AC434 offers interpretation and limits for three possible modes of failure:

a) Cohesive when failure occurs in the substrate material

b) Adhesive when failure occurs at the interface FRCM and substrate material

c) Adhesive when failure is at the interface between the reinforcement mesh and matrix within the FRCM

5.3.4 *Properties of matrix*—For each FRCM system, normal compressive strength of the cementitious matrix compliant with ASTM C387/387M should be evaluated at 7 and 28 days according to ASTM C109/C109M.

5.4—Durability

5.4.1 *Aging*—For each FRCM system, the tensile properties, bond, and composite inter-laminar shear strengths should be evaluated on FRCM specimens after being subjected to each of the conditioning regimens (AC434):

a) Ambient

b) Aging in water vapor (100 percent humidity, 100°F [37.7°C]) for 1000 and 3000 hours

c) Aging in saltwater (immersion, 73°F [22°C]) for 1000 and 3000 hours

d) Aging in alkaline environment (immersion, pH ≥ 9.5, 73°F [22°C]) for 1000 and 3000 hours

5.4.2 *Freezing and thawing*—For each FRCM system, the tensile properties and composite inter-laminar shear strength should be evaluated on specimens after being subjected to freezing-and-thawing cycles, with each cycle consisting of a minimum of 4 hours at 0°F (–18°C), followed by 12 hours in a humidity chamber (100 percent humidity, 100°F [37.7°C]).

5.4.3 *Fuel resistance*—For each FRCM system, the tensile properties should be determined on FRCM specimens after being exposed to diesel fuel reagent for a minimum of 4 hours.

CHAPTER 6—SHIPPING, STORAGE, AND HANDLING

6.1—Shipping

The user of FRCM constituent materials is advised to observe federal and state packaging and shipping regulations. Packaging, labeling, and shipping for construction materials are controlled by the Code of Federal Regulations. The Code of Federal Regulations (CFR) annual edition is the codification of the general and permanent rules published in the Federal Register by the departments and agencies of the Federal Government and is electronically available at: http://www.gpo.gov/fdsys/browse/collectionCfr.action?collectionCode=CFR.

6.2—Storage

6.2.1 *Storage conditions*—To preserve the properties of and maintain safety in FRCM system constituents, materials should be stored in accordance with the manufacturer's recommendations. In particular, for the fabric reinforcement before encapsulation in the matrix, consider exposure to ultraviolet light (UV), extreme temperatures, moisture, and other environmental conditions that can be deleterious to synthetic fibers such as aramid and polyparaphenylene benzobisoxazole (PBO) (Chin et al. 1997). Certain constituent materials have safety-related requirements and should be stored as recommended by the manufacturer and Occupational Safety and Health Administration (OSHA).

6.2.2 *Shelf life*—The manufacturer sets a recommended shelf life within which the properties of materials should continue to meet or exceed stated performance criteria. Any component material that has exceeded its shelf life, deteriorated, or been contaminated should not be used. FRCM materials deemed unusable should be disposed of as specified by the manufacturer and in a manner acceptable to state and federal environmental control regulations.

6.3—Handling

6.3.1 *Material Safety Data Sheet (MSDS)*—For all FRCM constituent materials and components, an MSDS should be obtained from the manufacturer and be accessible at the job site.

6.3.2 *Information sources*—Detailed information on the handling and potential hazards of FRCM constituent materials can be found in information sources, such as ACI and International Concrete Repair Institute (ICRI) reports, manufacturer literature and guides, and OSHA guidelines.

6.3.3 *Personnel safe handling and clothing*—Gloves and safety glasses or goggles are suitable for handling FRCM materials.

6.3.4 *Workplace safe handling*—Each FRCM system constituent material may have handling and storage requirements to prevent damage. Consult with the material system manufacturer for guidance. Consult the system manufacturer's literature for proper mixing procedures and MSDSs for specific handling hazards.

6.3.5 *Clean-up and disposal*—All waste materials should be contained and disposed of as prescribed by the prevailing environmental authority.

CHAPTER 7—INSTALLATION

7.1—Contractor qualifications

The FRCM system installation contractor should demonstrate competency for surface preparation and application of

the FRCM system to be installed. Contractor competency can be demonstrated by providing evidence of training and documentation of related work previously completed by the contractor; for example, surface preparation and installation of the FRCM system on portions or mockups of the structure. The FRCM system manufacturer or its authorized agent should train the contractor's application personnel in the installation procedures of its system.

7.2—Environmental considerations

Temperature at the time of installation can affect performance of the FRCM system: temperatures in the range of 95 to 120°F (35 to 50°C) may reduce the workability of the mortar, while temperatures in the range of 39 to 43°F (4 to 6°C) may slow down setting considerably. Conditions observed and documented before and during installation include surface temperature of the substrate, air temperature, relative humidity, and wind speed.

When the surface temperature of the substrate falls below a minimum level as specified by the FRCM system manufacturer, improper installation can occur, compromising the integrity of the FRCM system. Auxiliary heat sources can be used to raise the ambient and surface temperature during installation. Heat sources should not contaminate the substrate surface or the uncured FRCM system.

When the surface temperature of the substrate is higher than an ambient level as specified by the FRCM system manufacturer, improper installation can occur, compromising the integrity of the FRCM system. At higher temperatures within the limits provided by the manufacturer, it is important that the surface be maintained at a saturated surface-dry condition until immediately prior to the FRCM installation.

When FRCM is applied in a wet environment, it is important that the surface be dried to a saturated surface-dry condition immediately prior to the FRCM installation.

FRCM systems can typically be applied to substrate surfaces subjected to moisture vapor transmission. The transmission of moisture vapor from a substrate surface does not typically compromise the bond between the FRCM system and substrate.

7.3—Equipment

As different FRCM systems are used in the field, equipment requirements are specific to the selected system. In general, the advantage of FRCM-strengthening is associated with light weight, ease, and speed of application; therefore, special equipment requirements are limited. Equipment may include grinding and grooving tools. All equipment should be maintained, clean, and in good operating condition.

The contractor should have personnel trained in equipment operation. Personal protective gear, such as gloves, eye guards, and coveralls, should be worn as required by manufacturer's specifications.

Equipment and material supplies in sufficient quantities should be available to allow continuity in installation and quality control tasks. Safe and convenient access to those surfaces being strengthened will help ensure proper FRCM application.

7.4—Substrate repair and surface preparation

The behavior of members strengthened or retrofitted with FRCM systems is highly dependent on substrate and proper preparation and profiling of the substrate surface. An improperly prepared surface can result in debonding or delamination of the FRCM system before achieving the design load transfer. General guidelines presented herein should be applicable to all bonded FRCM systems. Specific guidelines for a particular FRCM system should be obtained from its manufacturer.

7.4.1 *Substrate repair*—Problems associated with the condition of the original member and its substrate that can compromise the integrity of the FRCM system should be addressed before surface preparation begins. The FRCM system manufacturer should be consulted to verify the compatibility of materials used for repairing the substrate with the FRCM system.

7.4.2 *Surface preparation*—Surface preparation requirements depend on the FRCM system used. Specific guidelines regarding procedures for surface preparation for each FRCM system should be obtained from the system manufacturer.

Surface preparation might involve:

a) Sandblasting, roughening, grinding, or hydrojetting to abrade the surface

b) Grinding form lines in concrete and excess mortar in the joints in masonry

c) Application of primers and putty or mortar fillers as per manufacturer's recommendations

Particular care should be taken to ensure that the surface is clean from dust and laitance, and to avoid unintentional damage to the substrate by using excessive force.

7.5—Mixing of mortar matrix

Mixing of the mortar matrix should be done in accordance with the FRCM system manufacturer's recommended procedure. The manufacturer should provide recommended batch sizes and mixture ratios, methods, and times.

Mixing equipment can include small mortar mixers, specialty units, or by hand stirring, if allowed by the manufacturer. Batching should be in sufficiently small quantities to ensure that the mortar can be used within its plastic state. Batches that exceed their plastic life should not be used because the increased viscosity will adversely affect the ability of the mortar to penetrate the reinforcement mesh.

7.6—Application of FRCM systems

7.6.1 *Mortar matrix*—If required, matrix material could also be used to smooth surface discontinuities smaller than approximately 1/16 in. (2 mm) before the application of the layer necessary for embedding the reinforcement mesh. The mortar matrix is considered an inorganic glue and not a repair material. Special putty fillers or mortars can be used to fill voids and repair the substrate, as per manufacturer's recommendations, with typical thicknesses up to approximately 0.5 in. (12 mm).

7.6.2 *FRCM systems*—FRCM systems are typically installed by hand using a cementitious matrix with dry fiber mesh and installed per the manufacturer's recommendations. The procedure consists of applying the matrix and the mesh directly to the member being strengthened. The matrix is first applied uniformly to all prepared surfaces where the system is placed. Reinforcing mesh is gently pressed into the matrix in a manner recommended by the FRCM system manufacturer. Successive layers of matrix and mesh are placed before the complete cure of the previous layer of matrix.

7.6.3 *Protective coatings*—Coatings should be compatible with the FRCM system and applied in accordance with the manufacturer's recommendations. Coatings should be periodically inspected and maintenance provided to ensure their effectiveness. Inspections should be performed periodically in conjunction with other regular inspections of the structure or at a frequency that is based on the exposure conditions and facility use.

7.7—Alignment of FRCM reinforcement

The FRCM reinforcement mesh orientation and mesh stacking sequence should be specified by the licensed design professional (LDP). Fiber orientation for both the primary direction (PD) and secondary direction (SD) may vary depending on the purpose of strengthening, such as for flexure or shear, and is of critical importance when unbalanced (that is, PD different from SD) meshes are used.

Small variations in angle as little as ±5 degrees from the intended direction of fiber alignment can cause a substantial reduction in strengthening performance. Deviations in mesh orientation should only be made if approved by the LDP.

Reinforcement meshes should be handled in a manner to maintain the fiber straightness and orientation. Kinks, folds, or other forms of severe waviness in the fiber reinforcement layer should be reported to the LDP.

7.8—Multiple meshes and lap splices

Multiple meshes can be used, provided all meshes are fully impregnated with the matrix system, the matrix shear strength is sufficient to transfer the shearing load between meshes, and the bond strength between substrate and FRCM system is sufficient to transfer design forces. Lap splices should be staggered and without overlap so that at any cross section through the FRCM, only one fabric is spliced. Lap splice details, including lap length, should be based on the results of tests performed in accordance with AC434. Multiple meshes and lap splices may not always be possible, depending on the characteristics of the specific FRCM system.

7.9—Curing of mortar matrix

The matrix should be cured according to the system manufacturer's recommendation. Field modification of the matrix chemistry should not be permitted without consulting the system manufacturer.

When required as a result of hot and windy conditions, curing compounds may be applied on the fresh FRCM immediately following installation to prevent evaporation of water necessary for hydration of the mortar.

7.10—Temporary protection

Adverse temperatures and direct contact by rain, dust, dirt, or vandalism can damage an FRCM system during installation and cause improper curing of the matrix. Temporary protection such as tents and plastic screens could be required during installation and until the matrix has cured. If temporary shoring is required, the FRCM system should be fully cured before removing the shoring and allowing the structural member to carry the design loads. In the event of suspected damage to the FRCM system during installation, the LDP should be notified and the FRCM system manufacturer consulted.

CHAPTER 8—INSPECTION, EVALUATION, AND ACCEPTANCE

8.1—Inspection

FRCM systems and all associated work should be inspected as required by the applicable local codes. In the absence of such requirements, inspection should be conducted by or under the supervision of a licensed design professional (LDP) or qualified inspector. Inspectors should be knowledgeable of and trained in the installation of FRCM systems. The qualified inspector should require compliance with design drawings and project specifications. During installation of the FRCM system, the scope of the inspection should include:

a) Date and time of installation

b) Ambient temperature, relative humidity, and general weather observations

c) Surface temperature of substrate

d) Surface preparation methods and resulting profile

e) Qualitative description of surface cleanliness

f) Type of auxiliary heat source, if applicable, the start/stop times for the heaters

g) Reinforcement batch number(s) and approximate location in structure

h) Batch numbers, mixture ratios, mixing times, and qualitative descriptions of the appearance of all mixed matrix and additional materials such as primers, putties, and coatings mixed for the day

i) Conformance with installation procedures

j) Compression test results of mortar cubes of the matrix material, if required

k) Pull-off test results according to ASTM C1583/C1583M completed or supervised by an LDP or owner's independent testing agency, if required

l) FRCM properties from tests of field sample panels or witness panels, if required

m) Location and size of any defects

n) General progress of work

The inspector should provide the LDP or owner's representative with inspection records and witness test panels when required. The installation contractor should retain

sample mortar cubes or cylinders and maintain a record of the placement of each batch.

8.2—Evaluation and acceptance

FRCM systems should be evaluated based on conformance with the design drawings and specifications and the manufacturer's installation recommendations. Nonconformance of the FRCM system should be reported to the LDP for further evaluation. The FRCM system material properties, installation within specified placement tolerances, presence of defects, cure of matrix, and adhesion to substrate should be evaluated. The evaluation should also consider mesh orientation and lap splice lengths of the installed FRCM system.

Witness test panel and pull-off tests can be used to evaluate the installed FRCM system. In-place load testing can also be used where applicable to confirm the installed behavior of the FRCM-strengthened member.

8.2.1 *Materials*—Before starting the project, the FRCM system manufacturer should submit certification of specified material properties and identification of all materials to be used. Additional material testing can be conducted if deemed necessary based on the project's complexity. Evaluation of delivered FRCM materials can include tests for tensile and compressive strength of constituents. These tests are usually performed on material samples sent to a laboratory, according to the quality-control test plan. Materials that do not meet minimum requirements as specified by the LDP should be rejected.

Witness panels can be used to evaluate the tensile strength and modulus, and lap splice strength of the FRCM system installed and cured on-site using installation procedures similar to those used to install and cure the FRCM system. During installation, flat panels of the specified dimensions and thickness can be fabricated on-site according to a predetermined sampling plan. After curing on-site, the panels can then be sent to a laboratory for testing. Witness panels can be retained or submitted to an approved laboratory for testing of tensile strength. Strength and elastic modulus of the FRCM system is determined in accordance with the requirements of AC434. Properties to be evaluated by testing should be specified by the LDP, which may waive or alter the testing frequency.

8.2.2 *Mesh orientation*—Mesh orientation should be evaluated by inspection using a level or a straightedge. Mesh misalignment of more than ±5 degrees from that specified on the design drawings (approximately 1 in./ft [80 mm/m]) should be reported to the LDP for evaluation, who should calculate the capacity of the system considering this misalignment to determine if the design criteria are still satisfied. If the design criteria cannot be satisfied, remedial actions such as the use of a reduction factor to calculate effective strength may be warranted.

8.2.3 *Defects*—The cured FRCM system should be evaluated for defects between multiple layers or between the FRCM system and substrate surface. In addition to coring, nondestructive test methods such as acoustic sounding—for example, hammer sounding, impact-echo, impulse response, ultrasonic, and infrared thermography—can be used to detect delaminations. Delaminations should be evaluated and repaired in accordance with the LDP's direction. Upon completion of repairs, the FRCM should be re-inspected to verify the repair was properly installed.

8.2.4 *Cure of matrix*—The relative cure of FRCM systems can be evaluated by laboratory testing of matrix samples. The FRCM system manufacturer should be consulted to determine specific matrix-cure verification requirements.

8.2.5 *Adhesion strength*—Tension adhesion testing of cored samples should be conducted using ASTM C1583/C1583M. Sampling frequency should be specified. When the mode of failure is cohesive (substrate material) or if it is adhesive (interface FRCM and substrate material), strength should be at least 200 psi (1.38 MPa). When failure is at the interface fiber mesh-matrix within the FRCM, strength computed on the net matrix area should be at least 400 psi (2.76 MPa). The net matrix area is the total area under the disk minus the area covered by fiber mesh.

8.2.6 *Cured thickness*—Small core samples may be taken to visually determine the cured FRCM thickness or number of meshes at locations approved by the LDP. Cored samples required for adhesion testing also can be used to determine the FRCM thickness or number of meshes. The sampling frequency should be specified by the LDP. Taking samples from high-stress or splice areas should be avoided. For aesthetic reasons, the cored hole can be filled and smoothed with a repair mortar or the FRCM system matrix.

CHAPTER 9—MAINTENANCE AND REPAIR

9.1—General

As with any repair system (ACI 562), the owner or owner's representative should periodically inspect and assess the performance of the FRCM system used for strengthening. Inspections should be performed periodically in conjunction with other regular inspections of the structure or at a frequency that is determined based on the exposure conditions and facility use. The causes of any damage or deficiencies detected during routine inspections should be identified and addressed before performing any repairs or maintenance.

9.2—Inspection and assessment

9.2.1 *General inspection*—A visual inspection should be performed to observe any debonding, cracking, deflections, changes in color, and other anomalies. In addition, ultrasonic, acoustic sounding (hammer tap) or thermography tests may reveal signs of progressive debonding and delamination.

9.2.2 *Assessment*—Test data and observations are used to assess any damage and the structural integrity of the strengthening system. The assessment should include repair recommendations and suggestions for reducing the incidence of future damage.

9.3—Repair of strengthening system

The repair method for an FRCM strengthening system depends on causes of the damage, the type of material, the form of degradation, and the level and extent of damage.

Before repairing the FRCM system, causes of the damage should be identified. Consult the system manufacturer for repair methods and materials.

9.4—Repair of surface coating

If the surface protective coating requires replacement, the FRCM should be inspected for structural damage or deterioration. Consult the system manufacturer for surface coating repair.

CHAPTER 10—GENERAL DESIGN CONSIDERATIONS FOR REINFORCED CONCRETE STRENGTHENED WITH FRCM

10.1—Design philosophy

These design recommendations are based on limit-state design principles and are consistent with the provisions of AC434. This approach sets acceptable levels of safety for the occurrence of serviceability limit states such as excessive deflections and cracking, and ultimate limit states such as failure, stress rupture, and fatigue. When evaluating the serviceability of a member, linear elastic material properties may be assumed so that modular ratios and transformed sections can be used to calculate service stresses and deformations. In assessing the nominal strength of a member, the possible failure modes and subsequent strains and stresses in each material should be assessed.

Design procedures should be in accordance with ACI 318 and ACI 562, as applicable. Specific guidance on FRCM system design is presented in Chapter 11. Load and strength reduction factors for FRCM design should be obtained from ACI 318 and 562, as appropriate.

10.2—Strengthening limits

Careful consideration should be given to determine reasonable strengthening limits. These limits are imposed to guard against collapse of the structure should bond or other failure of the FRCM system occur due to damage, vandalism, or other causes. The required strength of a structure without repair should be as specified in ACI 562-13, Section 5.5.

For flexural strengthening applications, primary direction (PD) fiber strands should be oriented parallel to the major axes of the member and should be installed so that the strands are no more than ±5 degrees from the design orientation. Similarly, for shear strengthening applications, PD fiber strands are typically oriented perpendicular to the axis of the member and should not be misaligned more than ±5 degrees. For a combined contribution to shear strength of parallel and perpendicular fiber strands, however, it is allowable to orient PD fiber strands in a parallel direction to the member axis, provided that continuity of the mesh is maintained.

Appendix B provides a summary for relevant design limits for all types of strengthening methods.

10.3—Selection of FRCM system

Given the anticipated service conditions, the LDP should select an FRCM system based on the known behavior of that system as available in an ICC-ES Evaluation Report. Such reports can be obtained from the FRCM system manufacturer.

10.4—Design properties

FRCM properties to be used for design as described herein are obtained from tests performed in accordance to AC434 and recommended in Chapter 5. As per AC434-13, Section 8.0, the values of strength and strain used in the design equations herein (f_{fd}, ε_{fd}) are defined as the average value minus one standard deviation, and the elastic modulus (E_f) is the average value.

CHAPTER 11—STRENGTHENING OF REINFORCED CONCRETE MEMBERS WITH FRCM

11.1—FRCM contribution to flexural strength

The FRCM composite material bonded to surfaces of reinforced concrete (RC) members may be used to enhance the design flexural strength of sections by acting as external tension reinforcement. In such cases, section analysis is based on the following assumptions:

a) plane sections remain plane after loading

b) the bond between the FRCM and substrate remains effective

c) the maximum usable compressive strain in concrete is 0.003

d) FRCM has a bilinear behavior to failure where only the second linear part of the curve is used in analysis and design

This section does not apply to FRCM systems used to enhance the flexural strength of members in the expected plastic hinge regions of ductile moment frames resisting seismic loads.

The flexural strength of an RC section depends on the controlling failure mode. Failure modes for an FRCM-strengthened section include:

a) Crushing of the concrete in compression before yielding of the reinforcing steel

b) Yielding of the steel in tension followed by concrete crushing

c) Shear/tension delamination of the concrete cover or cover delamination

d) Debonding of the FRCM from the concrete substrate (FRCM debonding)

e) Interlaminar debonding

f) Slippage of fiber mesh within the cementitious matrix

Effective tensile strain level in the FRCM reinforcement attained at failure, ε_{fe}, should be limited to the design tensile strain of the FRCM composite material, ε_{fd}, defined in Eq. (11.1a)

$$\varepsilon_{fe} = \varepsilon_{fd} \le 0.012 \quad (11.1a)$$

The effective tensile stress level in the FRCM reinforcement attained at failure, f_{fe}, in the FRCM reinforcement is calculated in accordance with Eq. (11.1b)

$$f_{fe} = E_f \varepsilon_{fe} \text{ where } \varepsilon_{fe} \le \varepsilon_{fd} \quad (11.1b)$$

Table 11.1.3—Creep rupture and fatigue stress limits for reinforcement based on fiber type

	Fiber type				
	AR glass	Aramid	Basalt	Carbon	PBO
Creep rupture and fatigue	$0.20f_{fd}$	$0.30f_{fd}$	$0.20f_{fd}$	$0.55f_{fd}$	$0.30f_{fd}$

The design flexural strength is calculated in accordance with Eq. (11.1c)

$$\phi_m M_n = \phi_m(M_s + M_f) \quad (11.1c)$$

where M_n is the nominal flexural strength, and M_s and M_f are the contribution of steel reinforcement and FRCM composite material to the nominal flexural strength, respectively. The strength reduction factor ϕ_m is given by Eq. (11.1d), as defined in ACI 318 and ACI 562

$$\phi_m = \begin{cases} 0.90 \text{ for } \varepsilon_t \geq 0.005 \\ 0.65 + \dfrac{0.25(\varepsilon_t - \varepsilon_{sy})}{0.005 - \varepsilon_{sy}} \text{ for } \varepsilon_{sy} < \varepsilon_t < 0.005 \\ 0.65 \text{ for } \varepsilon_t < \varepsilon_{sy} \end{cases} \quad (11.1d)$$

where ε_t is the net tensile strain in extreme tension steel reinforcement at nominal strength, and ε_{sy} is the steel tensile yield strain.

11.1.1 *Design limitations*—To limit the total force per unit width transferred to the concrete, the increase in flexural strength provided by the FRCM reinforcement should not exceed 50 percent of the existing flexural capacity of the structure without strengthening. This increase should be checked before applying the strength reduction factor and cannot exceed the limit for strengthening established in ACI 562.

11.1.2 *Serviceability*—The tensile stress in the steel reinforcement under service load, f_{ss}, should be limited to 80 percent of the steel yield strength, f_y, as indicated in Eq. (11.1.2).

$$f_{ss} \leq 0.80 f_y \quad (11.1.2)$$

11.1.3 *Creep-rupture and fatigue stress limits*—The tensile stress levels in the FRCM reinforcement under service load, f_{fs}, should be limited to the values shown in Table 11.1.3.

11.2—Shear strengthening

This section presents guidance on the calculation of added shear strength resulting from the addition of FRCM shear reinforcement to reinforced concrete (RC) beams or columns. The additional shear strength that can be provided by the FRCM system is based on many factors, including geometry of the beam or column, wrapping scheme, and existing concrete strength.

11.2.1 *FRCM contribution to shear strength*—The FRCM composite material bonded to surfaces of an RC member can be used to enhance the design shear strength by acting as external shear reinforcement. Shear strengthening using external FRCM can be provided at locations of expected plastic hinges or stress reversal and for enhancing post-yield flexural behavior of members in moment frames resisting seismic loads only by completely wrapping the section. Only continuous FRCM U-wraps (beams) or continuous complete wraps (beams and columns) should be considered.

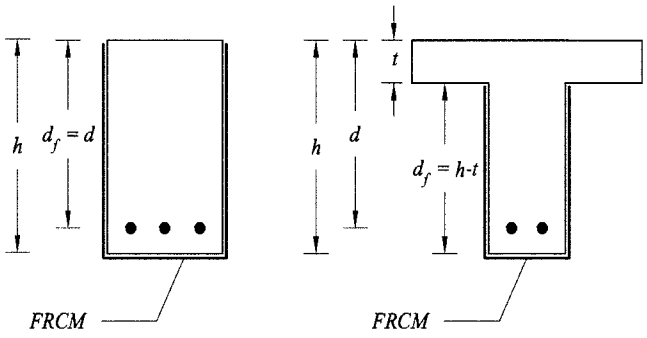

Fig. 11.2.1—d_f *values for rectangular and T-sections.*

The design tensile strain in the FRCM shear reinforcement, ε_{fv}, is calculated by Eq. (11.2.1a)

$$\varepsilon_{fv} = \varepsilon_{fu} \leq 0.004 \quad (11.2.1a)$$

The design tensile strength of the FRCM shear reinforcement, f_{fv}, is calculated in accordance with Eq. (11.2.1b)

$$f_{fv} = E_f \varepsilon_{fv} \quad (11.2.1b)$$

where E_f is the tensile modulus of elasticity of the cracked FRCM composite material.

The design shear strength is calculated in accordance with Eq. (11.2.1c).

$$\phi_v V_n = \phi_v(V_c + V_s + V_f) \quad (11.2.1c)$$

where V_n is the nominal shear strength, and V_c, V_s, and V_f are the contribution of concrete, existing steel reinforcement, and FRCM composite material to the nominal shear strength, respectively. The strength reduction factor ϕ_v should be equal to 0.75 as per ACI 318 and ACI 562. V_c and V_s are calculated according to ACI 318. The shear contribution of FRCM shear reinforcement, V_f, is given by Eq. (11.2.1d)

$$V_f = nA_f f_{fv} d_f \quad (11.2.1d)$$

where n is the number of layers of mesh reinforcement; A_f is the area of mesh reinforcement by unit width effective in shear; and d_f is the effective depth of the FRCM shear reinforcement (Fig. 11.2.1). Where PD and SD fiber strands are used to reinforce the same portion of a member, V_f is computed as the sum of the values computed for the two shear reinforcement directions. At least 50 percent of the reinforcement shall be provided by the fiber strands perpendicular to the member axis. The total shear strength provided by FRCM and steel reinforcement should be limited to the following

$$V_s + V_f \le 8\sqrt{f_c'}\, b_w d \qquad (11.2.1e)$$

$$V_s + V_f \le 0.66\sqrt{f_c'}\, b_w d \quad \text{(SI units)} \qquad (11.2.1f)$$

where b_w is the web width. For rectangular sections with shear enhancement provided by transverse FRCM composite material, section corners must be rounded to a radius not less than 3/4 in. (20 mm) before placement of the FRCM material.

11.2.1.1 *Design limitations*—To limit the total force per unit width transferred to the concrete, the increase in shear strength provided by the FRCM reinforcement should not exceed 50 percent of the existing shear strength capacity. This increase cannot exceed the limit for strengthening established in ACI 562-13.

11.3—Strengthening for axial force

Confinement of RC columns by means of FRCM jackets can be used to enhance existing column strength and ductility. The increase in capacity is an immediate outcome typically expressed in terms of improved peak load resistance. Overall ductility enhancement requires more complex calculations to determine the ability of a member to sustain rotation and drift without a substantial loss in strength. Therefore, this section applies only to flexural ductility enhancement resulting from increasing the effective ultimate compression strain.

11.3.1 *Axial load capacity enhancement*—The FRCM composite material may be applied to external surfaces of circular and rectangular RC compression members to enhance the axial load capacity (Bournas et al. 2007; Abegaz et al. 2012; De Caso y Basalo et al. 2012).

The stress-strain for FRCM-confined concrete is illustrated in Fig. 11.3.1 and is determined using the following expressions

$$f_c = \begin{cases} E_c\varepsilon_c - \dfrac{(E_c - E_2)^2}{4f_c'}(\varepsilon_c)^2 & 0 \le \varepsilon_c \le \varepsilon_t' \\ f_c' + E_2\varepsilon_c & \varepsilon_t' \le \varepsilon_c \le \varepsilon_{ccu} \end{cases} \qquad (11.3.1a)$$

$$\varepsilon_t' = \frac{2f_c'}{E_c - E_2} \qquad (11.3.1b)$$

$$E_2 = \frac{f_{cc}' - f_c'}{\varepsilon_{ccu}} \qquad (11.3.1c)$$

where E_c is the modulus of elasticity of concrete; E_2 is the slope of linear portion of stress-strain model for FRCM-confined concrete; f_c is the compressive stress in concrete; f_c' is the specified compressive strength of concrete; f_{cc}' is the maximum compressive strength of confined concrete;

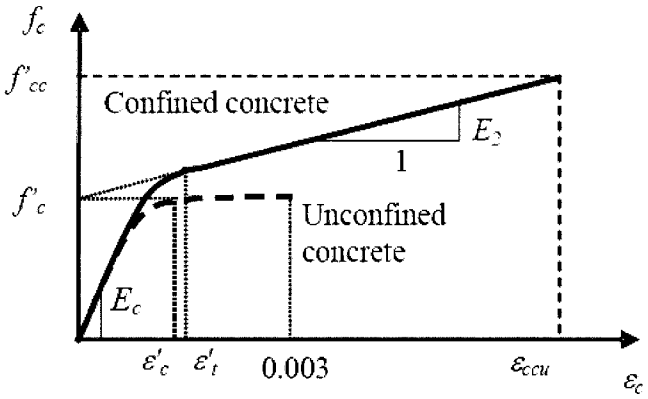

Fig. 11.3.1—Idealized stress-strain diagram for FRCM-confined concrete.

ε_c is the compressive strain level in the concrete; ε_{ccu} is the ultimate axial compressive strain of confined concrete that corresponds to f_{cc}'; and ε_t' is the transition strain in the stress-strain curve of FRCM-confined concrete.

The maximum confined concrete compressive strength, f_{cc}', and the maximum confinement pressure, f_l, is calculated using Eq. (11.3.1d), (11.3.1e), and (11.3.1f)

$$f_{cc}' = f_c' + 3.1\kappa_a f_l \qquad (11.3.1d)$$

$$f_l = (2nA_f E_f \varepsilon_{fe})/D \quad \text{for circular cross section} \qquad (11.3.1e)$$

$$f_l = (2nA_f E_f \varepsilon_{fe})/(b^2 + h^2)^{1/2} \quad \text{for rectangular cross section} \qquad (11.3.1f)$$

where A_f is the area of mesh reinforcement by unit width; n is the number of layers of mesh reinforcement; D is the diameter of the compression member with circular cross section; and b and h are the short and the long side dimensions of the compression member with rectangular cross section, respectively. The efficiency factor κ_a is a function of the cross section shape and is calculated as given in 11.3.1.1 and 11.3.1.2 of this guide, respectively. The effective tensile strain level in the FRCM, ε_{fe}, is given by

$$\varepsilon_{fe} = \varepsilon_{fd} \le 0.012 \qquad (11.3.1g)$$

The contribution of mortar matrix to compressive strength of the FRCM-confined compression member should be neglected.

The ultimate axial compressive strain of confined concrete, ε_{ccu}, should not exceed 0.01 to prevent excessive cracking and the resulting loss of concrete integrity. ε_{ccu} is calculated using the following stress-strain relationship

$$\varepsilon_{ccu} = \varepsilon_c'\left(1.5 + 12\kappa_b \frac{f_l}{f_c'}\left(\frac{\varepsilon_{fe}}{\varepsilon_c'}\right)^{0.45}\right) \le 0.01 \qquad (11.3.1h)$$

where ε_c' is the compressive strain of unconfined concrete corresponding to f_c'. The efficiency factor κ_b is calculated as given in 11.3.1.1 and 11.3.1.2, respectively.

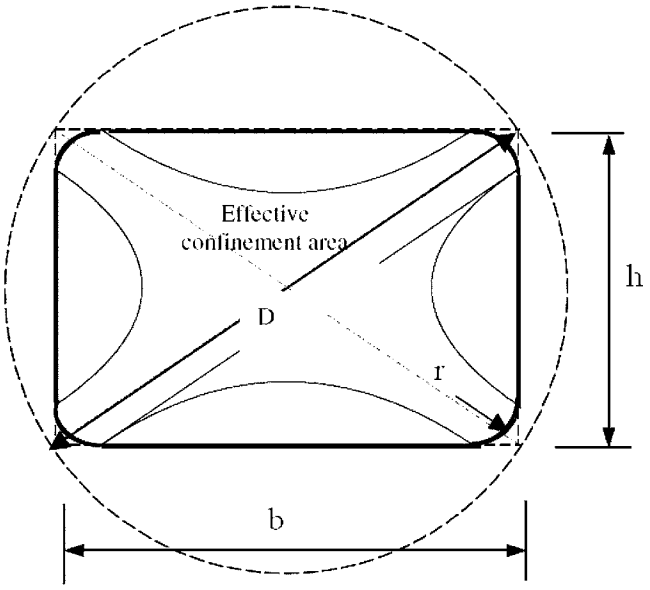

Fig. 11.3.1.2—Equivalent circular cross section.

Based on the limitation set by Eq. (11.3.1h), f_{cc}' should not exceed the value of the stress corresponding to ε_{ccu} equal to 0.01.

11.3.1.1 *Circular sections*—For circular cross sections, the shape factors κ_a and κ_b in Eq. (11.3.1d) and (11.3.1h), respectively, should be taken as 1.0.

11.3.1.2 *Rectangular sections*—Rectangular sections where the ratio of longer to shorter section side dimension is not greater than 2.0 may have axial compression capacity enhanced by the confining effect of FRCM material placed with fiber strands running essentially perpendicular to the member axis. For rectangular cross sections, the shape factors κ_a in Eq. (11.3.1d) and κ_b in Eq. (11.3.1h) is calculated using Eq. (11.3.1.2a) and (11.3.1.2b), respectively (Fig. 11.3.1.2).

$$\kappa_a = \frac{A_e}{A_c}\left(\frac{b}{h}\right)^2 \qquad (11.3.1.2a)$$

$$\kappa_b = \frac{A_e}{A_c}\left(\frac{h}{b}\right)^2 \qquad (11.3.1.2b)$$

where

$$\frac{A_e}{A_c} = \frac{1 - \dfrac{\left[\left(\dfrac{b}{h}\right)(h-2r_c)^2 + \left(\dfrac{h}{b}\right)(b-2r_c)^2\right]}{3A_g} - \rho_g}{1-\rho_g} \qquad (11.3.1.2c)$$

In Eq. (11.3.1.2c), A_c is the net cross-sectional area of the compression member; A_e is the area of the effectively confined concrete; A_g is the gross cross-sectional area of the compression member; and ρ_g is the ratio of the area of longitudinal steel reinforcement, A_s, to the gross cross-sectional area of the compression member.

For rectangular sections within aspect ratio $h/b > 2.0$, the effectiveness of the confinement should be subject to special analysis confirmed by test results.

11.3.1.3 *Design limitations*—The increase in axial strength provided by the FRCM reinforcement shall not exceed 20 percent of the existing capacity of the column without strengthening. This increase cannot exceed the limit for strengthening established in ACI 562.

When the intent of the design is to restore the existing compressive strength (for example, lightly confined member), ε_{ccu} should be limited to the value corresponding to $0.85f_{cc}'$.

Unless confirmed by experimental evidence, the strengthening of existing columns should be limited to elements having a cross section with a maximum dimension of 24 in. (610 mm) for the long side (rectangular) or diameter (circular). This limit is based on half-scale tests (Bournas et al. 2007).

11.3.1.4 *Flexural ductility enhancement*—The FRCM composite material with PD strands oriented essentially perpendicular to the member axis may be used to enhance flexural ductility capacity of circular and rectangular sections where the ratio of longer to shorter section dimension does not exceed 2.0. The enhancement is provided by increasing the effective ultimate compression strain of the section as computed in Eq. (11.3.1h).

11.4—Design axial strength

The design axial strength $\phi_m P_n$ of a compression member should be computed according to the provisions of ACI 318 and ACI 562. For the calculation of $\phi_m P_n$, consideration should be given to the presence of steel tie or spiral reinforcement in the existing RC member and the limit based on the axial strength at zero eccentricity. The expression for ϕ_m given in Eq. (11.1d) is for members without spiral reinforcement. For members with spiral reinforcement, ϕ_m becomes 0.75 when the tensile strain at failure is less or equal to ε_y.

Members subject to compressive axial load should be designed for the maximum moment that can accompany the axial load.

CHAPTER 12—GENERAL DESIGN CONSIDERATIONS FOR MASONRY STRENGTHENED WITH FRCM

12.1—Design philosophy

The design philosophy is based on limit-state design principles to provide acceptable safety levels and is consistent with AC434. To evaluate the nominal strength of FRCM-strengthened masonry, all possible failure modes with associated strains and stresses in each material should be assessed.

Material properties such as compressive and tensile strength, elastic modulus in compression, and shear strength of existing masonry, should preferably be determined by in-place tests or laboratory tests of extracted samples. If

these are unavailable, default material properties of existing masonry may be obtained from available guidelines, including ASCE 41 and MSJC. Dimensions of the masonry elements should be obtained from the existing drawings, field measurements, or both. If there are uncertainties regarding existing material strengths or substrate conditions, the LDP may wish to incorporate more conservative strength-reduction factors than those discussed in this guide.

This guide can be used to design the FRCM strengthening system for existing individual masonry walls subject to in-plane and out-of-plane loads resulting from wind and earthquakes (ASCE 7). The LDP designing the FRCM strengthening system for individual walls should evaluate the effect wall strengthening has on the overall structure. If appropriate, a global analysis of the overall structure should be performed (ASCE 41). In strengthening of masonry members, the relationship between each element and the entire structure is of particular relevance. Specifically, the in-plane rigidity of floor diaphragms and the effectiveness of the connections between the floor diaphragms and the walls as well as among intersecting walls themselves can be critical to the global behavior of the building.

12.2—Strengthening limits

The licensed design professional (LDP) should consider strengthening limits. FRCM-strengthened masonry may be subjected to extraordinary loading events (such as fire, impact, and blast). These loads are rare and typically not sustained but need to be considered when computing the required strength of a structure without repair as specified in ACI 562-13, Section 5.5.

Wind and earthquake forces are not considered extraordinary events, as they are unlikely to cause damage to the unprotected external reinforcing systems; therefore, a strengthening limit for these applications is unnecessary.

For out-of-plane loading, primary-direction (PD) fiber strands should be oriented perpendicular to the direction of the applied bending moment and should be installed so that the strands are no more than ±5 degrees from the design orientation. Similarly, for in-plane loading, FRCM should be applied with PD fiber strands oriented perpendicular to the applied shear force and the fiber strands should not have a misalignment of more than ±5 degrees.

Appendix B provides a summary for relevant design limits for various strengthening methods.

12.3—Design properties

FRCM properties to be used for design as described in this guide are obtained from tests performed in accordance to AC434 and as reported in Chapter 5 of this guide. As per AC434, the values of strength and strain (f_{fd}, ε_{fd}) to be used in the design equations of this guide are defined as the average value minus one standard deviation, whereas the elastic modulus (E_f) is simply the average value.

CHAPTER 13—STRENGTHENING OF MASONRY WALLS WITH FRCM

13.1—Out-of-plane loads

13.1.1 *Nominal flexural strength*—The FRCM composite material bonded to surfaces of masonry may be used to enhance the design flexural strength out of the plane of the wall by acting as additional tension reinforcement. In such cases, the section analysis is based on the following assumptions:

a) Strain compatibility between masonry, steel reinforcement (if any), and FRCM composite material

b) Plane sections remain plane after loading

c) The maximum usable compressive strain in the masonry is per MSJC-11 or from field tests as per 13.1

d) FRCM has a bilinear behavior to failure where FRCM contribution prior to cracking is neglected. The out-of-plane flexural strength of a (reinforced or unreinforced) masonry wall depends on the controlling failure mode. Failure modes for an FRCM-strengthened wall include:

i. Crushing of the masonry in compression (before steel yielding, if present)

ii. Debonding of the FRCM from the masonry substrate (FRCM debonding)

iii. Slippage of the fiber mesh within the cementitious matrix

iv. Tensile yielding of the steel reinforcement (if present)

The effective tensile strain level in the FRCM composite material attained at failure, ε_{fe}, should be limited to the design tensile strain of the FRCM composite material, ε_{fd}, defined in Eq. (13.1.1a)

$$\varepsilon_{fe} = \varepsilon_{fd} \le 0.012 \qquad (13.1.1a)$$

The effective tensile stress level in the FRCM reinforcement attained at failure, f_{fe}, is calculated in accordance with Eq. (13.1.1b)

$$f_{fe} = E_f \varepsilon_{fe} \text{ where } \varepsilon_{fe} \le \varepsilon_{fd} \qquad (13.1.1b)$$

where E_f is the tensile modulus of elasticity of the cracked FRCM composite material.

The design flexural strength is calculated in accordance with Eq. (13.1.1c)

$$\phi_m M_n = \phi_m (M_m + M_f) \qquad (13.1.1c)$$

where M_n is the nominal flexural strength, and M_m and M_f are the contribution of reinforced masonry and FRCM composite material to the nominal flexural strength, respectively. In the case of unreinforced masonry (URM) not subjected to axial load, only the term M_f is considered. The strength reduction factor for flexure, ϕ_m, is equal to 0.6 for reinforced and unreinforced masonry. Similarly, the corresponding strength reduction factor for shear, $\phi_{v,f}$, is equal to 0.8.

For the computation of M_n, when the FRCM composite material is applied on both sides of the wall, the contribution of FRCM in the compression side is neglected.

FRCM application does not contribute to the enhancement of the nominal out-of-plane shear strength of the masonry wall that is calculated according to MSJC-11.

13.1.1.1 *Design limitations*—In the case of URM, when subjected to out-of-plane loading, the wall behaves as a simply supported element or very nearly so, and the influence of wall arching mechanisms can be neglected. An arching mechanism can potentially develop in a wall with a height-to-thickness ratio (H/t) of less than 8 when the wall is built between stiff supports. The influence of arching in the out-of-plane behavior decreases for walls with H/t greater than 14. As a reference, Tables 7-5 and 7-10 of ASCE 41-06 provide H/t where a URM wall does not need to be analyzed for out-of-plane seismic forces and, therefore, does not require strengthening.

For URM out-of-plane strengthening, the maximum force transferred by the FRCM to the masonry substrate should not be larger than 6000 lbf/ft (87.6 kN/m). For conventionally reinforced masonry walls, to limit the total force per unit width transferred to the masonry, the increment in flexural strength provided by the FRCM reinforcement should not exceed 50 percent of the existing capacity of the structure without strengthening.

13.2—In-plane loads

13.2.1 *Nominal shear strength*—The FRCM composite material bonded to surfaces of masonry may be used to enhance the design shear strength in the plane of the wall by acting as shear reinforcement.

The design tensile strain in the FRCM shear reinforcement, ε_{fv}, is calculated by Eq. (13.2.1a)

$$\varepsilon_{fv} \le 0.004 \qquad (13.2.1a)$$

The design tensile strength in the FRCM shear reinforcement, f_{fv}, is calculated in accordance with Eq. (13.2.1b)

$$f_{fv} = E_f \varepsilon_{fv} \qquad (13.2.1b)$$

FRCM is preferably applied on both sides of the wall for reasons of symmetry and effectiveness. When applied only on one side, the LDP should consider the effects of eccentricity.

The design shear strength is calculated in accordance with Eq. (13.2.1c)

$$\phi_v V_n = \phi_v (V_m + V_f) \qquad (13.2.1c)$$

where V_n is the nominal shear strength, and V_m and V_f are the contribution of (unreinforced or reinforced) masonry and FRCM composite material to the nominal shear strength, respectively. V_m is calculated in accordance with MSJC-11 and V_f is calculated as defined in Eq. (13.2.1d)

$$V_f = 2nA_f L f_{fv} \qquad (13.2.1d)$$

where A_f *is* the area of the mesh reinforcement by unit width effective in shear; n is the number of layers of mesh reinforcement, and L is the length of wall in the direction of applied shear force. The strength reduction factor for shear, ϕ_v, is equal to 0.75.

13.2.1.1 *Design limitations*—To limit the total force per unit width transferred to the masonry, the increment in shear strength provided by the FRCM reinforcement should not exceed 50 percent of the capacity of the structure without strengthening for unreinforced and conventionally reinforced masonry walls. In addition, the summation of the URM and FRCM shear contributions before the strength reduction factors are applied (Eq. (13.2.1c)) should be checked against the substrate toe crushing capacity computed in accordance with the provisions of ASCE 41. Strengthening is limited to a maximum wall thickness of 12 in. (305 mm).

CHAPTER 14—FRCM REINFORCEMENT DETAILS

This chapter offers guidance for detailing externally bonded FRCM. Detailing typically depends on the geometry of the structure, the soundness and quality of the substrate, and the levels of load that are to be sustained by the FRCM system. Bond-related failures may be avoided by following these general guidelines for detailing:

a) Do not turn inside corners such as at the intersection of beams and joists with the underside of slabs. If this is unavoidable, proper anchorage is to be provided.

b) The cross section corners must be rounded to a radius r not less than 3/4 in. (20 mm), before placing FRCM material.

c) Provide adequate development length (minimum of 6 in. [152 mm]).

d) Provide sufficient overlap when splicing fiber meshes as determined according to test methods specified in AC434.

14.1—Bond and delamination

14.1.1 *FRCM bond strength*—The bond strength of an FRCM system is determined according to test methods specified in AC434. Mechanical anchorages can be effective in increasing stress transfer, although their efficacy results from their ability to resist the tensile normal stresses rather than in enhancing the interfacial shear capacity. The performance of any anchorage system should be substantiated through testing and approved by the licensed design professional (LDP).

14.1.2 *Development length*—The bond capacity of FRCM is developed over a critical length ℓ_{df}. To develop the effective FRCM stress at a section, the available anchorage length of FRCM should exceed the minimum development length of 6 in. (152 mm) for any type of substrate material. Longer values of ℓ_{df} may be necessary for multi-layer FRCM application.

The LDP should also consider the concrete cover delamination that can result from the normal stresses developed at the ends of externally bonded FRCM. With this type of delamination, the existing internal reinforcing steel essentially acts as a bond breaker in a horizontal plane, and the concrete cover pulls away from the rest of the element. The following general guidelines for the location of cutoff points for FRCM can be used to avoid concrete cover delamination failure mode:

a) For simply supported beams, FRCM reinforcement should be terminated at least a distance equal to ℓ_{df} past the point along the span corresponding to the cracking moment M_{cr}.

b) For continuous beams, FRCM reinforcement should be terminated at $d/2$ or ℓ_{df}, whichever is larger, beyond the inflection point (point of zero moment resulting from factored loads).

14.1.3 *Detailing of laps and splices*—Splices of FRCM reinforcement should be provided only as permitted on drawings, specifications, or as authorized by the LDP and as recommended by the system manufacturer.

The fiber mesh should be continuous and oriented in the direction of the largest tensile forces. Fiber continuity can be maintained with a lap splice. For FRCM systems, a lap splice should be made by overlapping the two fiber meshes along their length. The required overlap, or lap-splice length, depends on the tensile strength and thickness of the FRCM material system and on the bond strength between adjacent layers of FRCM reinforcement. Sufficient overlap should be provided to promote the failure of the FRCM reinforcement before debonding of the overlapped FRCM reinforcement. The required overlap for an FRCM system should be provided by the material manufacturer and substantiated through testing that is independent of the manufacturer.

Jacket-type FRCM systems used for column members should provide appropriate development area at splices, joints, and termination points to ensure failure through the FRCM jacket thickness rather than failure of the spliced sections.

Unless otherwise specified, lap splices are not required in the transverse direction of the fiber mesh. FRCM reinforcement consisting of multiple meshes oriented in more than one direction or multidirectional meshes require lap splices in more than one direction to maintain the continuity of the fibers and the overall strength of the FRCM reinforcement.

To determine the relative tensile strength at the mesh overlap area, lap tensile strength testing is required as per AC434. This test method is particularly useful if the joint configuration closely simulates the actual joint in material field application. It is understood that in application of multilayer FRCM composite materials, the laps should be staggered from the laps in the nearby layer. Laps in one layer should start with a minimum distance equivalent to the development length of fiber strands in the matrix established by the FRCM manufacturer, or larger.

CHAPTER 15—DRAWINGS, SPECIFICATIONS, AND SUBMITTALS

15.1—Engineering requirements

Although federal, state, and local codes for the design of externally bonded FRCM systems do not exist, other applicable code requirements may influence the selection, design, and installation of the FRCM system. All design work should be performed under the guidance of a licensed design professional (LDP) familiar with the properties and applications of FRCM strengthening systems.

15.2—Drawings and specifications

The LDP should document calculations summarizing the assumptions and parameters used to design the FRCM strengthening system and should prepare design drawings and project specifications. The drawings and specifications should show, at a minimum, the following information specific to externally applied FRCM systems:

a) FRCM system to be used

b) Location of the FRCM system relative to the existing structure

c) Dimensions and orientation of each fiber mesh

d) Number of reinforcement meshes and the sequence of installation

e) Location of splices and lap length

f) General notes listing design loads and allowable strains in the FRCM reinforcement

g) Design properties of the FRCM and concrete substrate

h) Concrete surface preparation requirements, including corner preparation and maximum irregularity limitations

i) Installation procedures, including surface temperature and application time limits between successive layers

j) Curing procedures for FRCM system

k) Protective coatings and sealants, if required

l) Shipping, storage, handling, and shelf-life guidelines

m) Quality control and inspection procedures, including acceptance criteria

n) In-place load testing of strengthened FRCM structure, if necessary

15.3—Submittals

Specifications should require the FRCM system manufacturer, installation contractor, inspection agency (if required), and all those involved with the project to submit product information and evidence of their qualifications and experience to the LDP for review.

15.3.1 *FRCM system manufacturer*—Submittals required of the FRCM system manufacturer should include:

a) Product data sheets indicating the physical, mechanical, and chemical characteristics of all constituent materials

b) Mechanical properties of the FRCM system, including the method of reporting properties, test methods used, and the statistical basis used for determining the properties as per AC434-13

c) Installation instructions, maintenance instructions, and general recommendations regarding each material to be used. Installation procedures should include surface preparation requirements

d) Manufacturer's Material Safety Data Sheets (MSDSs) for all materials to be used

e) Quality control procedure for tracking FRCM materials and material certifications

f) Durability test data for the FRCM system as per AC434 and for the types of environments expected, if necessary

g) Structural test reports pertinent to the proposed application

h) Reference projects

15.3.2 *FRCM system installation contractor*—Submittals required of the FRCM system installation contractor should include:

a) Documentation from the FRCM system manufacturer of having been trained to install the proposed FRCM system

b) Project references, including installations similar to the proposed installation

c) Evidence of competency in surface preparation techniques

d) Quality-control testing procedures including voids and delaminations, FRCM bond to concrete, and FRCM tensile properties

e) Daily log or inspection forms used by the contractor

15.3.3 *FRCM system inspection agency*—If an independent inspection agency is used, submittals required of that agency should include:

a) The inspector must meet minimum qualifications required by local codes

b) A list of inspectors to be used on the project and their qualifications

c) Sample inspection forms

d) A list of previous projects inspected by the inspector

Chapter 16—Design examples

The design examples that make up this chapter were developed using Mathcad™ software. As such, some symbols are unique to this computational software and should not mislead the reader (e.g., ":=" for "="; "Φ" for "Φ_m or Φ_v"; and "lbf" for "lb.").

The material properties shown in the examples were selected for illustration purposes and should not be used in design without verification.

16.1-Flexural strengthening of interior RC slab

A one-way multi-span continuous concrete slab reinforced with a top and bottom steel wire mat of No. 3@12 in. (71 mm² @ 304 mm) is subjected to a 70 percent increase in its live-load carrying requirements. An analysis of the existing slab indicates that the slab still has sufficient shear strength to resist the additional load and meets the deflection and crack-control serviceability requirements. Flexural strength at the interior supports (negative moment), however, is inadequate to carry the increased live load. Summarized in the following sections are the information about the existing slab, the existing and new loading conditions, and associated negative moments for the slab. The existing RC slab is strengthened with FRCM, whose mechanical properties are reported below.

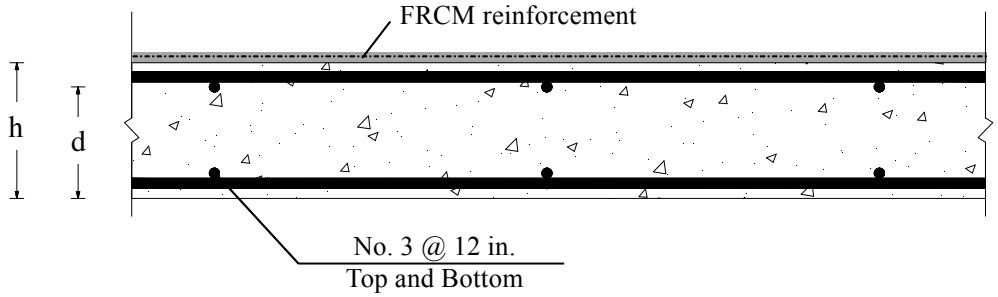

Slab cross-section

Information about the existing slab

Geometrical properties

Length of the span	$l_{span} := 10ft = 3m$
Width of the strip	$b := 12in = 305 \cdot mm$
Effective depth of steel reinforcement	$d := 4.06in = 103 \cdot mm$
Thickness of the slab	$h := 5.0in = 127 \cdot mm$

Concrete mechanical properties

Nominal compressive strength	$f'_c := 4000psi = 28 \cdot MPa$
Compressive ultimate strain	$\varepsilon_{cu} := 0.003$

Steel reinforcement geometrical and mechanical properties

Area of steel bars	$A_s := 0.11 \frac{in^2}{ft} = 0.233 \cdot \frac{mm^2}{mm}$
Bar spacing	$s_{bar} := 12in = 305 \cdot mm$
Yield strength	$f_y := 60ksi = 414 \cdot MPa$
Steel modulus of elasticity	$E_s := 29000ksi = 200 \cdot GPa$

Flexural strength without fabric-reinforced cementitious matrix

Existing nominal flexural strength	$M_n := 1990 \cdot \frac{lbf \cdot ft}{ft} = 8.85 \cdot \frac{kN \cdot m}{m}$
Existing design flexural strength	$\phi M_n := 1790 \cdot \frac{lbf \cdot ft}{ft} = 7.96 \cdot \frac{kN \cdot m}{m}$
Strength-reduction factor	$\phi := 0.9$

Loading information

Existing conditions

Dead-load negative bending moment $M_{DL} := 750 \cdot \frac{lbf \cdot ft}{ft} = 3.34 \cdot \frac{kN \cdot m}{m}$

Live-load negative bending moment $M_{LL} := 500 \cdot \frac{lbf \cdot ft}{ft} = 2.22 \cdot \frac{kN \cdot m}{m}$

Service-load negative bending moment $M_S := M_{DL} + M_{LL} = 1250 \cdot \frac{lbf \cdot ft}{ft} \quad (5.56 \frac{kN \cdot m}{m})$

Factored negative bending moment $M_u := 1.2M_{DL} + 1.6M_{LL} = 1700 \cdot \frac{lbf \cdot ft}{ft} \quad (7.56 \frac{kN \cdot m}{m})$

Anticipated conditions

Dead-load negative bending moment $M_{DL'} := 750 \cdot \frac{lbf \cdot ft}{ft} = 3.34 \cdot \frac{kN \cdot m}{m}$

Live-load negative bending moment $M_{LL'} := 850 \cdot \frac{lbf \cdot ft}{ft} = 3.78 \cdot \frac{kN \cdot m}{m}$

Service-load negative bending moment $M_{S'} := M_{DL'} + M_{LL'} = 1600 \cdot \frac{lbf \cdot ft}{ft} \quad (7.12 \frac{kN \cdot m}{m})$

Factored negative bending moment $M_{u'} := 1.2M_{DL'} + 1.6M_{LL'} = 2260 \cdot \frac{lbf \cdot ft}{ft} \quad (10.1 \frac{kN \cdot m}{m})$

Factored shear force $V_{u'} := 960 \frac{lbf}{ft} = 14 \cdot \frac{kN}{m}$

Mesh reinforcement properties

The FRCM material system to be used should be ICC-ES approved, and its geometrical and mechanical properties should be the ones reported in the relative ICC-ES Research Report.

It must be noted that the properties reported below are valid for the sole purpose of this design example.

Area of mesh reinforcement by unit width $A_f := 0.0018 \cdot \frac{in^2}{in} = 0.0457 \cdot \frac{mm^2}{mm}$

Tensile modulus of elasticity (Ave.) $E_f := 18000ksi = 124 \cdot GPa$

Ultimate tensile strength ($\varepsilon_{fc} E_f$) $f_{fd} := 130ksi = 896 \cdot MPa$

Ultimate tensile strain (ε_{fu} - 1 STD) $\varepsilon_{fd} := 0.0072$

Compute the new flexural capacity

Step 1 - Preliminary calculations

Concrete modulus of elasticity (ACI 318) $E_c := 57000 \cdot \sqrt{f'_c} \cdot \sqrt{psi} = 3605 \cdot ksi \quad (24.8GPa)$

Steel yield strain $\varepsilon_y := \frac{f_y}{E_s} = 0.00207$

Steel reinforcement ratio: $\rho_s := \frac{A_s \cdot b}{d \cdot b} = 0.00226$

Effective depth of the FRCM reinforcement $d_f := h = 5.0 \cdot in$ (127mm)

Step 2 - Determine the existing state of strain of the top of the member

The existing state of strain is calculated assuming the slab is cracked and the only load acting on the slab at the time of the FRCM installation is the self-weight of the slab. A cracked section analysis is presented as follows.

Existing negative bending moment at the time of the installation of FRCM $M_{SL} := 625 \cdot \frac{lbf \cdot ft}{ft} = 2.78 \cdot \frac{kN \cdot m}{m}$

This value of the bending moment takes into account the reduced superimposed dead load acting at the time of the installation of FRCM.

Neutral axis depth of the cracked section (ACI 318) $c_{cr} := d \cdot \left[\sqrt{\left(\rho_s \cdot \frac{E_s}{E_c} \right)^2 + 2 \cdot \left(\rho_s \cdot \frac{E_s}{E_c} \right)} - \rho_s \cdot \frac{E_s}{E_c} \right]$

$c_{cr} = 0.704 \cdot in$ (17.9mm)

Cracked moment of inertia $I_{cr} := \frac{b \cdot c_{cr}^3}{3} + \frac{E_s}{E_c} \cdot A_s \cdot b \cdot \left(d - c_{cr} \right)^2$

$I_{cr} = 11.36 \cdot in^4$ ($4728389\ mm^4$)

Existing state of tensile strain on top of the slab $\varepsilon_{bi} := \frac{M_{SL} \cdot b \cdot \left(h - c_{cr} \right)}{I_{cr} \cdot E_c} = 0.000787$

Step 3 - Calculate the FRCM design tensile strain

The FRCM design tensile strain is computed according to Eq. (11.1a):

Design ultimate strain $\varepsilon_{fe} := \min\left(\varepsilon_{fd}, 0.012 \right) = 0.00720$

Step 4 - Select the number of FRCM plies and the width of the FRCM strip

The number of plies of FRCM should not exceed the maximum number of plies to be used for flexural strengthening as specified in the relative ICC-ES Research Report.

Number of FRCM plies $n := 1$

The width of the FRCM strip should be in agreement with the relative ICC-ES Research Report. In this example, a width of 12 in. (305 mm) is considered.

Width of the FRCM strip $w_f := 12in = 305 \cdot mm$

Step 5 - Calculate the new nominal flexural strength

The effective tensile strain level in the FRCM reinforcement attained at failure can be calculated as follows as a function of the neutral axis depth:

$$\varepsilon_{fe1}(c_u) := \begin{cases} \left[0.003\cdot\left(\frac{h - c_u}{c_u}\right) - \varepsilon_{bi}\right] & \text{if } 0.003\cdot\left(\frac{h - c_u}{c_u}\right) - \varepsilon_{bi} \le \varepsilon_{fe} \\ \varepsilon_{fe} & \text{otherwise} \end{cases}$$

The effective stress level in the FRCM reinforcement attained at failure can be expressed as a function of the neutral axis depth and is calculated according to Eq. (11.1b):

$$f_{fe}(c_u) := E_f\cdot\varepsilon_{fe1}(c_u)$$

The concrete compressive strain level at failure can be expressed as a function of the neutral axis depth and computed as follows:

$$\varepsilon_c(c_u) := \left(\varepsilon_{fe} + \varepsilon_{bi}\right)\cdot\left(\frac{c_u}{h - c_u}\right)$$

The steel tensile strain and stress level at failure can be expressed as a function of the neutral axis depth and computed as follows:

$$\varepsilon_s(c_u) := \left(\varepsilon_{fe} + \varepsilon_{bi}\right)\cdot\left(\frac{d - c_u}{h - c_u}\right)$$

$$f_s(c_u) := \begin{cases} \left(\varepsilon_s(c_u)\cdot E_s\right) & \text{if } \varepsilon_s(c_u)\cdot E_s \le f_y \\ f_y & \text{otherwise} \end{cases}$$

The concrete stress block factors can be expressed as a function of the neutral axis depth and computed as follows according to ACI 318:

$$\varepsilon'_c := \frac{1.7\cdot f'_c}{E_c} = 0.00189$$

$$\beta_1(c_u) := \frac{4\cdot\varepsilon'_c - \varepsilon_c(c_u)}{6\cdot\varepsilon'_c - 2\cdot\varepsilon_c(c_u)} \qquad \alpha_1(c_u) := \frac{3\cdot\varepsilon'_c\cdot\varepsilon_c(c_u) - \left(\varepsilon_c(c_u)\right)^2}{3\cdot\beta_1(c_u)\cdot{\varepsilon'_c}^2}$$

A reasonable initial estimate of the neutral axis depth at failure must be considered.

Initial estimate of neutral axis depth $c_{u1} := 0.2\cdot d = 0.812\cdot in$ (20.6mm)

FRCM effective tensile strain $\varepsilon_{fe1}(c_{u1}) = 0.00720$

FRCM effective tensile stress $f_{fe}(c_{u1}) = 130\cdot ksi$ (1069MPa)

Concrete compressive strain $\varepsilon_c(c_{u1}) = 0.00155$

Steel tensile strain $\varepsilon_s(c_{u1}) = 0.00619$

Steel tensile stress $f_s(c_{u1}) = 60\cdot ksi$ (414MPa)

Concrete stress block factors $\beta_1(c_{u1}) = 0.73$ $\alpha_1(c_{u1}) = 0.82$

The equilibrium of the cross-section has to be checked. If the new calculated neutral axis depth is not close enough to the assumed one (a difference of less than 5 percent is advisable) revise its estimate and iterate until the equilibrium is achieved.

The new value of the neutral axis can be computed as follows:

$$c_{u2} := \frac{A_s \cdot b \cdot f_s(c_{u1}) + A_f \cdot n \cdot w_f \cdot f_{fe}(c_{u1})}{\alpha_1(c_{u1}) \cdot f'_c \cdot \beta_1(c_{u1}) \cdot b} = 0.3284 \cdot in \qquad (9.58mm)$$

The difference between the new value of the neutral axis and the value initially estimated has to be computed.

$$\frac{c_{u2} - c_{u1}}{c_{u1}} = -0.596$$

The two values, c_{u1} and c_{u2}, are not close enough, therefore a new iteration is needed.

Neutral axis depth after n iterations $c_{un} := 0.495in$ (13.8mm)

The new value of the neutral axis (relative to the n+1th iteration) can be computed as follows:

$$c_{un1} := \frac{A_s \cdot b \cdot f_s(c_{un}) + A_f \cdot n \cdot w_f \cdot f_{fe}(c_{un})}{\alpha_1(c_{un}) \cdot f'_c \cdot \beta_1(c_{un}) \cdot b} = 0.498 \cdot in \qquad (14.0mm)$$

The difference between the new value of the neutral axis and the value initially estimated has to be computed.

$$\frac{c_{un1} - c_{un}}{c_{un}} = 0.00638$$

The two values, c_{un} and c_{un1}, are close enough, therefore the following neutral axis depth is considered.

Neutral axis depth $c_u := c_{un1} = 0.498 \cdot in$ (14.0mm)

FRCM effective tensile strain $\varepsilon_{fe1}(c_u) = 0.00720$

FRCM effective tensile stress $f_{fe}(c_u) = 130 \cdot ksi$ (1069MPa)

Concrete compressive strain $\varepsilon_c(c_u) = 0.00088$

Steel tensile strain $\varepsilon_s(c_u) = 0.00632$

Steel tensile stress $f_s(c_u) = 60 \cdot ksi$ (414MPa)

Concrete stress block factors $\beta_1(c_u) = 0.70$

$\alpha_1(c_u) = 0.57$

The contribution of the steel reinforcement to the new nominal flexural strength per unit width can be calculated as follows:

$$M_{ns} := A_s \cdot f_s(c_u) \cdot \left(d - \frac{\beta_1(c_u) \cdot c_u}{2} \right) = 2137 \cdot \frac{lbf \cdot ft}{ft} \qquad \left(94.7 \cdot \frac{kN \cdot m}{m} \right)$$

The contribution of the FRCM reinforcement to the new nominal flexural strength per unit width can be calculated as follows:

$$M_{nf} := \frac{(n \cdot A_f \cdot w_f)}{b} \cdot f_{fe}(c_u) \cdot \left(d_f - \frac{\beta_1(c_u) \cdot c_u}{2} \right) = 1126 \cdot \frac{lbf \cdot ft}{ft} \qquad \left(2.99 \cdot \frac{kN \cdot m}{m} \right)$$

The new nominal flexural strength is:

$$M_{nNew} := (M_{ns} + M_{nf}) = 3263 \cdot \frac{lbf \cdot ft}{ft} \qquad \left(12.5 \cdot \frac{kN \cdot m}{m} \right)$$

Step 6 - Calculate the new design flexural strength

The flexural strength reduction factor is computed according to Eq. (11.1d):

$$\phi_m := \begin{cases} 0.90 & \text{if } \varepsilon_s(c_u) \geq 0.005 \\ 0.65 + \dfrac{0.25 \cdot (\varepsilon_s(c_u) - \varepsilon_y)}{0.005 - \varepsilon_y} & \text{if } \varepsilon_y < \varepsilon_s(c_u) < 0.005 \\ 0.65 & \text{otherwise} \end{cases}$$

$$\phi_m = 0.90$$

The new design flexural strength is:

$$\phi M_{nNew} := \phi_m \cdot (M_{ns} + M_{nf}) = 2937 \cdot \frac{lbf \cdot ft}{ft} \qquad \left(10.5 \cdot \frac{kN \cdot m}{m} \right)$$

$$\left[M_{u'} = 2260 \cdot \frac{lbf \cdot ft}{ft} \right] \qquad \left(10.1 \cdot \frac{kN \cdot m}{m} \right)$$

Check flexural strength

$$CheckFlexuralStrength := \begin{cases} \text{"OK"} & \text{if } \phi M_{nNew} \geq M_{u'} \\ \text{"Not Good!"} & \text{otherwise} \end{cases}$$

$$CheckFlexuralStrength = \text{"OK"}$$

Step 7 - Check limitation on the flexural strength provided by the FRCM reinforcement

As recommended in 11.1.1, to limit the total force per unit width transferred to the concrete, the increment in flexural strength provided by the FRCM reinforcement should not exceed 50 percent of the capacity of the structure without strengthening.

$$Check := \begin{cases} \text{"OK"} & \text{if } M_{nf} \leq 0.5 \cdot M_n \\ \text{"Limit usable flexural strength to:"} & \text{otherwise} \end{cases}$$

$[\ M_{nf} = 1126 \cdot \frac{lbf \cdot ft}{ft}]$ $(\ 4.40\ \frac{kN \cdot m}{m}\ )$

$[\ (0.5 \cdot M_n) = 995 \cdot \frac{lbf \cdot ft}{ft}\ ]$ $(\ 2.99\ \frac{kN \cdot m}{m}\ )$

Check = "Limit usable flexural strength to:" $\phi_m \cdot (1.5) \cdot M_n = 2687 \cdot \frac{lbf \cdot ft}{ft}$

Step 8 - Check service stresses

FRCM reinforcement ratio $\rho_f := \frac{n \cdot A_f \cdot w_f}{b \cdot d} = 0.00044$

The elastic depth of the cracked neutral axis can be calculated as follows:

$$c_{crNew} := d\left[\sqrt{\left(\rho_s \cdot \frac{E_s}{E_c} + \rho_f \cdot \frac{E_f}{E_c}\right)^2 + 2\left[\rho_s \cdot \frac{E_s}{E_c} + \rho_f \cdot \frac{E_f}{E_c} \cdot \left(\frac{h}{d}\right)\right]} - \left(\rho_s \cdot \frac{E_s}{E_c} + \rho_f \cdot \frac{E_f}{E_c}\right)\right]$$

$c_{crNew} = 0.751 \cdot in$ $(\ 19.2mm\ )$

The service stress in the steel reinforcement must be checked as indicated in 11.1.2. It can be calculated as follows:

$$f_{ss} := \frac{\left[M_S \cdot b + \varepsilon_{bi} \cdot n \cdot A_f \cdot w_f \cdot E_f \cdot \left(h - \frac{c_{crNew}}{3}\right)\right] \cdot (d - c_{crNew}) E_s}{A_s \cdot b \cdot E_s \cdot \left(d - \frac{c_{crNew}}{3}\right) \cdot (d - c_{crNew}) + n \cdot A_f \cdot w_f \cdot E_f \cdot \left(h - \frac{c_{crNew}}{3}\right) \cdot (h - c_{crNew})}$$

$f_{ss} = 41.2 \cdot ksi$ $(\ 282MPa)$

The service stress limit for the steel reinforcement is:

$0.8 \cdot f_y = 48.0 \cdot ksi$ $(\ 331MPa)$

$$CheckStressSteel := \begin{cases} \text{"OK"} & \text{if } f_{ss} \le 0.8 \cdot f_y \\ \text{"Not Good"} & \text{otherwise} \end{cases}$$

CheckStressSteel = "OK"

The service stress in the FRCM reinforcement must be checked as indicated in 11.1.3. It can be calculated as follows:

$$f_{fs} := f_{ss} \cdot \left(\frac{E_f}{E_s}\right) \cdot \left(\frac{h - c_{crNew}}{d - c_{crNew}}\right) - \varepsilon_{bi} \cdot E_f = 18.7 \cdot ksi \quad (\ 276MPa\ )$$

The creep rupture stress limit is computed using Table 11.1.3. For example, it is assumed that PBO fibers are used.

$k_{creep} := 0.3$

$k_{creep} \cdot f_{fd} = 39.0 \cdot ksi$ $(\ 579MPa)$

$$\text{CheckStressFRCM} := \begin{cases} \text{"OK"} & \text{if } f_{fs} \le k_{creep} \cdot f_{fd} \\ \text{"Not Good"} & \text{otherwise} \end{cases}$$

$$\text{CheckStressFRCM} = \text{"OK"}$$

Step 9 - Development length

As indicated in 14.1.2, the development length of the FRCM reinforcement should exceed the minimum length of 6 in (152 mm).

Step 10 - Shear strength

The shear strength per unit width of the slab due to the only concrete is computed as per ACI 318:

$$V_c := 2 \cdot \sqrt{f'_c \cdot \text{psi}} \cdot d = 6163 \cdot \frac{\text{lbf}}{\text{ft}} \quad \left(90 \frac{\text{kN}}{\text{m}} \right)$$

$$\text{CheckShearStrength} := \begin{cases} \text{"Shear reinforcement is required"} & \text{if } \frac{V_{u'}}{\phi} \ge V_c \\ \text{"OK. No shear reinforcement is required"} & \text{otherwise} \end{cases}$$

$$\text{CheckShearStrength} = \text{"OK. No shear reinforcement is required"}$$

16.2-Flexural strengthening of RC bridge deck (soffit)

The bottom face of a bridge deck is seriously damaged due to corrosion and has lost its 2-inch (50-mm) concrete cover and is estimated to have lost 15 percent of its reinforcement steel due to corrosion. To repair the deck, the bottom face is prepared for the FRCM reinforcement to be installed. A layer of shotcrete provides the FRCM reinforcement with the necessary substrate and replaces the preexisting cover. Information about the existing bridge deck and the FRCM reinforcement properties are listed in the following sections. The analysis of the existing bridge deck shows that the deck is still satisfactory for shear strength.

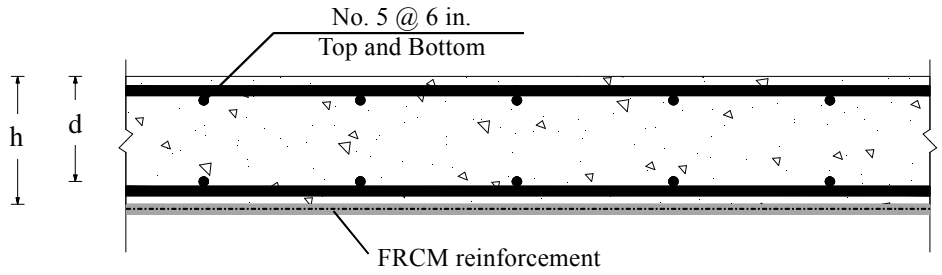

Bridge deck cross-section

Information about the existing slab

Geometrical properties

Width of the strip	$b := 12in = 305 \cdot mm$
Effective depth of steel reinforcement	$d := 7.7in = 196 \cdot mm$
Thickness of the slab	$h := 10in = 254 \cdot mm$

Concrete mechanical properties

Nominal compressive strength	$f'_c := 5000psi = 34.5 \cdot MPa$
Compressive ultimate strain	$\varepsilon_{cu} := 0.003$

Steel reinforcement geometrical and mechanical properties

Area of steel bars per unit width	$A_s := 0.62\frac{in^2}{ft} = 1.312 \cdot \frac{mm^2}{mm}$
Bar spacing	$s_{bar} := 6in = 152 \cdot mm$
Yield strength	$f_y := 60ksi = 414 \cdot MPa$
Steel modulus of elasticity	$E_s := 29000ksi = 200 \cdot GPa$

Flexural strength without FRCM

Original nominal flexural strength	$M_n := 21483\frac{lbf \cdot ft}{ft} = 95.6 \cdot \frac{kN \cdot m}{m}$
Design flexural strength after corrosion	$M_{nCorr} := 18261 \cdot \frac{lbf \cdot ft}{ft} = 81.2 \cdot \frac{kN \cdot m}{m}$
Strength-reduction factor	$\phi := 0.9$

FRCM reinforcement properties

The FRCM material system to be used should be ICC-ES approved, and its geometrical and mechanical properties should be the ones reported in the relative ICC-ES Research Report.

It must be noted that the properties reported below are valid for the sole purpose of this design example.

Area of mesh reinforcement by unit width $A_f := 0.0018 \cdot \frac{in^2}{in} = 0.046 \cdot \frac{mm^2}{mm}$

Tensile modulus of elasticity (Ave.) $E_f := 18000ksi = 124 \cdot GPa$

Ultimate tensile strength ($\varepsilon_{fd} \cdot E_f$) $f_{fd} := 130ksi = 896 \cdot MPa$

Ultimate tensile strain (ε_{fu} - 1 STD) $\varepsilon_{fd} := 0.0072$

Compute the new flexural capacity

Step 1 - Preliminary calculations

Concrete modulus of elasticity (ACI 318-11) $E_c := 57000 \cdot \sqrt{f'_c} \cdot \sqrt{psi} = 4031 \cdot ksi$ (27.8GPa)

Steel yield strain $\varepsilon_y := \frac{f_y}{E_s} = 0.00207$

A corrosion factor equal to 0.85 is considered to account for the reduction of resisting steel area.

Corrosion factor $CF := 0.85$

Area of steel reinforcement per unit width reduced due to corrosion $A_{sCorr} := A_s \cdot CF = 0.527 \cdot \frac{in^2}{ft}$ ($1.115 \frac{mm^2}{mm}$)

Steel reinforcement ratio $\rho_s := \frac{A_{sCorr} \cdot b}{d \cdot b} = 0.00570$

Effective depth of the FRCM reinforcement $d_f := h = 10.0 \cdot in$ (254mm)

Step 2 - Determine the existing state of strain of the top of the member

The existing state of strain on the bottom of the deck is considered to be negligible.

Existing tensile strain on bottom of slab $\varepsilon_{bi} := 0$

Step 3 - Calculate the FRCM design tensile strain

The FRCM design tensile strain is computed according to Eq. (11.1a):

Design ultimate strain $\varepsilon_{fe} := \min(\varepsilon_{fd}, 0.012) = 0.00720$

Step 4 - Select the number of FRCM plies and the width of the FRCM strip

The number of plies of FRCM should exceed the maximum number of plies to be used for flexural strengthening as specified in the relative ICC-ES Research Report.

Number of FRCM plies $n := 3$

The width of the FRCM strip should be in agreement with the relative ICC-ES Research Report. In this example, the FRCM reinforcement is applied continuously over the entire width of the deck.

Width of the FRCM strip $w_f := 12in = 304.8 \cdot mm$

Step 5 - Calculate the new nominal flexural strength

The effective tensile strain level in the FRCM reinforcement attained at failure can be calculated as follows as a function of the neutral axis depth:

$$\varepsilon_{fe1}(c_u) := \begin{cases} \left[0.003 \cdot \left(\frac{h - c_u}{c_u}\right) - \varepsilon_{bi}\right] & \text{if } 0.003 \cdot \left(\frac{h - c_u}{c_u}\right) - \varepsilon_{bi} \le \varepsilon_{fe} \\ \varepsilon_{fe} & \text{otherwise} \end{cases}$$

The effective stress level in the FRCM reinforcement attained at failure can be expressed as a function of the neutral axis depth and is calculated according to Eq. (11.1b):

$$f_{fe}(c_u) := E_f \cdot \varepsilon_{fe1}(c_u)$$

The concrete compressive strain level at failure can be expressed as a function of the neutral axis depth and computed as follows:

$$\varepsilon_c(c_u) := (\varepsilon_{fe} + \varepsilon_{bi}) \cdot \left(\frac{c_u}{h - c_u}\right)$$

The steel tensile strain and stress level at failure can be expressed as a function of the neutral axis depth and computed as follows:

$$\varepsilon_s(c_u) := (\varepsilon_{fd} + \varepsilon_{bi}) \cdot \left(\frac{d - c_u}{h - c_u}\right)$$

$$f_s(c_u) := \begin{cases} (\varepsilon_s(c_u) \cdot E_s) & \text{if } \varepsilon_s(c_u) \cdot E_s \le f_y \\ f_y & \text{otherwise} \end{cases}$$

The concrete stress block factors can be expressed as a function of the neutral axis depth and computed as follows according to ACI 318:

$$\varepsilon'_c := \frac{1.7 \cdot f'_c}{E_c} = 0.00211$$

$$\beta_1(c_u) := \frac{4 \cdot \varepsilon'_c - \varepsilon_c(c_u)}{6 \cdot \varepsilon'_c - 2 \cdot \varepsilon_c(c_u)}$$

$$\alpha_1(c_u) := \frac{3 \cdot \varepsilon'_c \cdot \varepsilon_c(c_u) - (\varepsilon_c(c_u))^2}{3 \cdot \beta_1(c_u) \cdot \varepsilon'^2_c}$$

A reasonable initial estimate of the neutral axis depth at failure must be considered.

Initial estimate of neutral axis depth $c_{u1} := 0.2 \cdot d = 1.540 \cdot in$ (39.1mm)

FRCM effective tensile strain $\varepsilon_{fe1}(c_{u1}) = 0.00720$

FRCM effective tensile stress $f_{fe}(c_{u1}) = 130 \cdot ksi$ (1069MPa)

Concrete compressive strain $\varepsilon_c(c_{u1}) = 0.00131$

Steel tensile strain $\varepsilon_s(c_{u1}) = 0.00524$

Steel tensile stress $f_s(c_{u1}) = 60 \cdot ksi$ (414MPa)

Concrete stress block factors $\beta_1(c_{u1}) = 0.71$

$\alpha_1(c_{u1}) = 0.69$

The equilibrium of the cross-section has to be checked. If the new calculated neutral axis depth is not close enough to the assumed one (a difference of less than 5 percent is advisable) revise its estimate and iterate until the equilibrium is achieved.

The new value of the neutral axis can be computed as follows:

$$c_{u2} := \frac{A_{sCorr} \cdot b \cdot f_s(c_{u1}) + A_f \cdot n \cdot w_f \cdot f_{fe}(c_{u1})}{\alpha_1(c_{u1}) \cdot f'_c \cdot \beta_1(c_{u1}) \cdot b} = 1.3536 \cdot in \qquad (50.3mm)$$

The difference between the new value of the neutral axis and the value initially estimated has to be compared.

$$\frac{c_{u2} - c_{u1}}{c_{u1}} = -0.121$$

The two values, c_{u1} and c_{u2}, are not close enough, therefore a new iteration is needed.

Neutral axis depth after n iterations $c_{un} := 1.42in = 36.068 \cdot mm$

The new value of the neutral axis (relative to the $n+1^{th}$ iteration) can be computed as follows:

$$c_{un1} := \frac{A_{sCorr} \cdot b \cdot f_s(c_{un}) + A_f \cdot n \cdot w_f \cdot f_{fe}(c_{un})}{\alpha_1(c_{un}) \cdot f'_c \cdot \beta_1(c_{un}) \cdot b} = 1.4543 \cdot in \qquad (44.4mm)$$

The difference between the new value of the neutral axis and the value initially estimated has to be compared.

$$\frac{c_{un1} - c_{un}}{c_{un}} = 0.02417$$

The two values, c_{un} and c_{un1}, are close enough, therefore the following neutral axis depth is considered.

Neutral axis depth $c_u := c_{un1} = 1.454 \cdot in$ (44.4mm)

FRCM effective tensile strain	$\varepsilon_{fe1}(c_u) = 0.00720$	
FRCM effective tensile stress	$f_{fe}(c_u) = 130 \cdot ksi$	(1069MPa)
Concrete compressive strain	$\varepsilon_c(c_u) = 0.00123$	
Steel tensile strain	$\varepsilon_s(c_u) = 0.00526$	
Steel tensile stress	$f_s(c_u) = 60 \cdot ksi$	(414MPa)
Concrete stress block factors	$\beta_1(c_u) = 0.71$	
	$\alpha_1(c_u) = 0.66$	

The contribution of the steel reinforcement to the new nominal flexural strength per unit width can be calculated as follows:

$$M_{ns} := A_{sCorr} \cdot f_s(c_u) \cdot \left(d - \frac{\beta_1(c_u) \cdot c_u}{2} \right) = 18935 \cdot \frac{lbf \cdot ft}{ft} \qquad \left(83.1 \cdot \frac{kN \cdot m}{m} \right)$$

The contribution of the FRCM reinforcement to the new nominal flexural strength per unit width can be calculated as follows:

$$M_{nf} := \frac{(n \cdot A_f \cdot w_f)}{b} \cdot f_{fe}(c_u) \cdot \left(d_f - \frac{\beta_1(c_u) \cdot c_u}{2} \right) = 6639 \cdot \frac{lbf \cdot ft}{ft} \qquad \left(35.1 \cdot \frac{kN \cdot m}{m} \right)$$

The new nominal flexural strength is:

$$M_{nNew} := (M_{ns} + M_{nf}) = 25574 \cdot \frac{lbf \cdot ft}{ft} \qquad \left(118 \cdot \frac{kN \cdot m}{m} \right)$$

Step 6 - Calculate the new design flexural strength

The flexural strength reduction factor is computed according to Eq. (11.1d):

$$\phi_m := \begin{cases} 0.90 & \text{if } \varepsilon_s(c_u) \geq 0.005 \\ 0.65 + \dfrac{0.25 \cdot (\varepsilon_s(c_u) - \varepsilon_y)}{0.005 - \varepsilon_y} & \text{if } \varepsilon_y < \varepsilon_s(c_u) < 0.005 \\ 0.65 & \text{otherwise} \end{cases}$$

$$\phi_m = 0.90$$

The new design flexural strength is:

$$\phi M_{nNew} := \phi_m \cdot (M_{ns} + M_{nf}) = 23017 \cdot \frac{lbf \cdot ft}{ft} \qquad \left(90.1 \cdot \frac{kN \cdot m}{m} \right)$$

$$\left[\phi \cdot M_n = 19335 \cdot \frac{lbf \cdot ft}{ft} \right] \qquad \left(86.0 \cdot \frac{kN \cdot m}{m} \right)$$

Check flexural strength

$$\text{CheckFlexuralStrength} := \begin{cases} \text{"OK"} & \text{if } \phi M_{nNew} \geq \phi \cdot M_n \\ \text{"Not Good!"} & \text{otherwise} \end{cases}$$

$\text{CheckFlexuralStrength} = \text{"OK"}$

Step 7 - Check limitation on the flexural strength provided by the FRCM reinforcement

As recommended in 11.1.1, to limit the total force per unit width transferred to the concrete, the increment in flexural strength provided by the FRCM reinforcement should not exceed 50 percent of the capacity of the structure without strengthening.

$$\text{Check} := \begin{cases} \text{"OK"} & \text{if } M_{nf} \leq 0.5 \cdot M_n \\ \text{"Not good"} & \text{otherwise} \end{cases}$$

$$\left[M_{nf} = 6639 \cdot \frac{\text{lbf} \cdot \text{ft}}{\text{ft}} \right] \qquad \left(35.1 \frac{\text{kN} \cdot \text{m}}{\text{m}} \right.$$

$$\left[\left(0.5 \cdot M_n\right) = 10742 \cdot \frac{\text{lbf} \cdot \text{ft}}{\text{ft}} \right] \qquad \left(47.8 \frac{\text{kN} \cdot \text{m}}{\text{m}} \right)$$

$\text{Check} = \text{"OK"}$

Step 8 - Check service stresses

Service-load positive bending moment $\qquad M_S := 16500 \cdot \frac{\text{lbf} \cdot \text{ft}}{\text{ft}} = 73.4 \cdot \frac{\text{kN} \cdot \text{m}}{\text{m}}$

FRCM reinforcement ratio $\qquad \rho_f := \frac{n \cdot A_f \cdot w_f}{b \cdot d} = 0.00070$

The elastic depth of the cracked neutral axis can be calculated as follows:

$$c_{crNew} := d\left[\sqrt{\left(\rho_s \cdot \frac{E_s}{E_c} + \rho_f \cdot \frac{E_f}{E_c}\right)^2 + 2\left[\rho_s \cdot \frac{E_s}{E_c} + \rho_f \cdot \frac{E_f}{E_c} \cdot \left(\frac{h}{d}\right)\right]} - \left(\rho_s \cdot \frac{E_s}{E_c} + \rho_f \cdot \frac{E_f}{E_c}\right)\right]$$

$c_{crNew} = 1.997 \cdot \text{in} \qquad (53.1\text{mm})$

The service stress in the steel reinforcement must be checked as indicated in 11.1.2. It can be calculated as follows:

$$f_{ss} := \frac{\left[M_S \cdot b + \varepsilon_{bi} \cdot n \cdot A_f \cdot w_f \cdot E_f \cdot \left(h - \frac{c_{crNew}}{3}\right)\right] \cdot \left(d - c_{crNew}\right) E_s}{A_s \cdot b \cdot E_s \cdot \left(d - \frac{c_{crNew}}{3}\right) \cdot \left(d - c_{crNew}\right) + n \cdot A_f \cdot w_f \cdot E_f \cdot \left(h - \frac{c_{crNew}}{3}\right) \cdot \left(h - c_{crNew}\right)}$$

$f_{ss} = 40.5 \cdot \text{ksi} \qquad (249\text{MPa})$

The service stress limit for the steel reinforcement is:

$0.8 \cdot f_y = 48.0 \cdot ksi \quad (331 MPa)$

$$CheckStressSteel := \begin{cases} "OK" & \text{if } f_{ss} \le 0.8 \cdot f_y \\ "Not\ Good" & \text{otherwise} \end{cases}$$

$CheckStressSteel = "OK"$

The service stress in the FRCM reinforcement must be checked as indicated in 11.1.3. It can be calculated as follows:

$$f_{fs} := f_{ss} \cdot \left(\frac{E_f}{E_s}\right) \cdot \left(\frac{h - c_{crNew}}{d - c_{crNew}}\right) - \varepsilon_{bi} \cdot E_f = 35.3 \cdot ksi \quad (472 MPa)$$

The creep rupture stress limit is computed using Table 11.1.3. For example, it is assumed that PBO fibers are used.

$k_{creep} := 0.3$

$k_{creep} \cdot f_{fd} = 39.0 \cdot ksi \quad (579 MPa)$

$$CheckStressFRCM := \begin{cases} "OK" & \text{if } f_{fs} \le k_{creep} \cdot f_{fd} \\ "Not\ Good" & \text{otherwise} \end{cases}$$

$CheckStressFRCM = "OK"$

Step 9 - Development length

As indicated in 14.1.2, the development length of the FRCM reinforcement should exceed the minimum length of 6 in (152 mm). Because of the multiple plies, a length of 12 in (304 mm) is recommended.

Step 10 - Shear strength

The shear strength per unit width of the slab due to the only concrete is computed as per ACI 318:

$$V_c := 2 \cdot \sqrt{f'_c \cdot psi} \cdot d = 1.307 \times 10^4 \cdot \frac{lbf}{ft} \quad \left(90 \frac{kN}{m}\right)$$

Assuming a factored shear force $V_{u'} := 1200 \frac{lbf}{ft} = 17.513 \cdot \frac{kN}{m}$

$$CheckShearStrength := \begin{cases} "Shear\ reinforcement\ is\ required" & \text{if } \frac{(V_{u'})}{\phi} \ge V_c \\ "OK.\ No\ shear\ reinforcement\ is\ required" & \text{otherwise} \end{cases}$$

$CheckShearStrength = "OK.\ No\ shear\ reinforcement\ is\ required"$

16.3-Shear strengthening of RC T-beam

An RC T-beam was originally designed to carry a factored ultimate shear force of 45 kips (200 kN). The design records indicate that a 4000-psi (27.6-MPa) concrete was used and that the steel shear reinforcement consisted of No. 3 (10-mm) 40-ksi (276-MPa) stirrups spaced at 4 in. (102 mm) over the first 10 feet (3 m) from the face of each of the two supports and at 12 in. over the remaining portion of the span. The beam is subjected to an increase of the original design live load. The analysis of the existing T-beam shows that the beam is still satisfactory for flexural strength but it is inadequate to support the new factored shear force of 52 kip (231 kN). Continuous FRCM U-wraps are used to strengthen the beam over a length of 10 feet (3 m) away from the face of each support.

Information about the existing beam

Geometrical properties

Width of the web	$b_w := 8in = 203 \cdot mm$
Total beam height	$h1 := 20in = 508 \cdot mm$
Thickness of the flanges	$t := 4in = 101.6 \cdot mm$
Effective depth of steel reinforcement	$d := 17.5in = 444.5 \cdot mm$

Concrete mechanical properties

Nominal compressive strength	$f'_c := 4000psi = 27.6 \cdot MPa$
Compressive ultimate strain	$\varepsilon_{cu} := 0.003$

Factored shear force

Original factored shear force	$V_u := 45kip = 200 \cdot kN$
New original factored shear force	$V_{uNew} := 52kip = 231.3 \cdot kN$

Shear strength without FRCM

Original concrete shear strength	$V_c := 20.2kip = 89.9 \cdot kN$	
Original steel shear strength	$V_s := 44.1kip = 196.2 \cdot kN$	
Original nominal shear strength	$V_n := V_c + V_s = 64.3 \cdot kip$	(644kN)
Strength-reduction factor	$\phi_v := 0.75$	
Original design shear strength	$\phi V_n := \phi_v \cdot V_n = 48.2 \cdot kip$	(483kN)

Fabric-reinforced cementitious matrix reinforcement properties

The FRCM material system to be used should be ICC-ES approved, and its geometrical and mechanical properties should be the ones reported in the relative ICC-ES Research Report.

It must be noted that the properties reported below are valid for the sole purpose of this design example.

Area of mesh reinforcement by unit width	$A_f := 0.0018 \frac{in^2}{in} = 0.046 \frac{mm^2}{mm}$
Tensile modulus of elasticity (Ave.)	$E_f := 18000ksi = 124 \cdot GPa$
Ultimate tensile strength ($\varepsilon_{fd} \cdot E_f$)	$f_{fd} := 130ksi = 896 \cdot MPa$
Ultimate tensile strain (ε_{fu} - 1 STD)	$\varepsilon_{fd} := 0.0072$

Compute the new shear capacity

Step 1 - Calculate the FRCM design tensile strain and strength

The FRCM design tensile strain is computed according to Eq. (11.2.1a):

Design tensile strain $\varepsilon_{fv} := \min\left(\varepsilon_{fd}, 0.004\right) = 0.00400$

The FRCM design tensile strength is computed according to Eq. (11.2.1b):

Design tensile strength $f_{fv} := \varepsilon_{fv} \cdot E_f = 72 \cdot ksi \quad (720MPa)$

Step 2 - Select the number of FRCM plies and the width of the FRCM strip

The number of plies of FRCM should not exceed the maximum number of plies to be used for flexural strengthening as specified in the relative ICC-ES Research Report.

Number of FRCM plies $n := 2$

Step 3 - Calculate the FRCM contribution to the nominal shear capacity

The contribution of the FRCM reinforcement to the new nominal shear strength is calculated according to Eq. (11.2.1d). The effective depth of FRCM shear reinforcement, d_f, is computed subtracting the thickness of the flanges to the effective depth of the steel reinforcement. Only PD fibers are considered in this example. A_f is multiplied by 2 to account for FRCM on both sides.

$d_f := h1 - t = 16 \cdot in \quad (406\ mm)$

$V_f := 2n \cdot A_f \cdot f_{fv} \cdot d_f = 8.3 \cdot kip \quad (67 \cdot kN)$

Step 4 - Calculate the new design shear strength

The new design shear strength is computed according to Eq. (11.2.1c):

$\phi V_{nNew} := \phi_v \cdot \left(V_c + V_s + V_f\right) = 54 \cdot kip \quad (586 \cdot kN)$

$[\ V_{uNew} = 52 \cdot kip\ ] \quad (578 \cdot kN)$

Check the new shear strength

$$CheckShearStrength := \begin{cases} \text{"OK"} & \text{if } \phi V_{nNew} \geq V_{uNew} \\ \text{"Not Good!"} & \text{otherwise} \end{cases}$$

$CheckShearStrength = \text{"OK"}$

Step 5 - Check limitation on total shear strength provided by the FRCM and the steel reinforcement

The limitation indicated in Eq. (11.2.1e) should be verified.

Total force provided by FRCM and steel reinforcement $V_s + V_f = 52.4 \cdot kip \quad (263 \cdot kN)$

$$Check\_MaximumShear := \begin{cases} \text{"OK"} & \text{if } V_s + V_f \leq 8 \cdot \sqrt{f'_c} \cdot \sqrt{psi} \cdot b_w \cdot d \\ \text{"Not Good"} & \text{otherwise} \end{cases}$$

$Check\_MaximumShear = \text{"OK"}$

Step 6 - Check limitation on the shear strength provided by the FRCM reinforcement

As recommended in 11.1.1, to limit the total force per unit width transferred to the concrete, the increment in shear strength provided by the FRCM reinforcement should also not exceed 50 percent of the capacity of the structure without strengthening.

$$\text{Check} := \begin{cases} \text{"OK"} & \text{if } V_f \le 0.5 \cdot V_n \\ \text{"Not good"} & \text{otherwise} \end{cases}$$

[$V_f = 8 \cdot \text{kip}$] (102 kN)

[$\left(0.5 \cdot V_n\right) = 32 \cdot \text{kip}$] (320kN)

Check = "OK"

16.4-Shear strengthening of RC column

An RC column was originally designed to carry a factored ultimate shear force of 72 kips (320 kN). The design records indicate that a 4000-psi (27.6-MPa) concrete was used and that the steel shear reinforcement consisted of No. 3 (10-mm) 40-ksi (276-MPa) ties spaced at 6 in. (152 mm). The building where the column is located is being renovated with an increase of the original lateral load. The analysis of the existing column shows that the column is still satisfactory for axial and flexural strength, but it is inadequate to support the new factored shear force of 82 kip (365 kN). Continuous complete FRCM wraps are used to strengthen the column.

Information about the existing column

Geometrical properties

Long side of the column $h := 24in = 610 \cdot mm$

Short side of the column $b_w := 24in = 610 \cdot mm$

Effective depth of steel reinforcement $d := 22in = 559 \cdot mm$

Concrete mechanical properties

Nominal compressive strength $f'_c := 4000psi = 27.6 \cdot MPa$

Compressive ultimate strain $\varepsilon_{cu} := 0.003$

Factored shear force

Original factored shear force $V_u := 72kip = 320 \cdot kN$

New original factored shear force $V_{uNew} := 82kip = 364.8 \cdot kN$

Shear strength without FRCM

Original concrete shear strength $V_c := 66.8kip = 297.1 \cdot kN$

Original steel shear strength $V_s := 33.3kip = 148.1 \cdot kN$

Original nominal shear strength $V_n := V_c + V_s = 100.1 \cdot kip$ ($644kN$)

Strength-reduction factor $\phi_v := 0.75$

Original design shear strength $\phi V_n := \phi_v \cdot V_n = 75.1 \cdot kip$ ($483kN$)

Fabric-reinforced cementitious matrix reinforcement properties

The FRCM material system to be used should be ICC-ES approved, and its geometrical and mechanical properties should be the ones reported in the relative ICC-ES Research Report.

It must be noted that the properties reported below are valid for the sole purpose of this design example.

Area of mesh reinforcement by unit width $A_f := 0.0018 \frac{in^2}{in} = 0.046 \frac{mm^2}{mm}$

Tensile modulus of elasticity (Ave.) $E_f := 18000ksi = 124 \cdot GPa$

Ultimate tensile strength ($\varepsilon_{fd} \cdot E_f$) $f_{fd} := 130ksi = 896 \cdot MPa$

Ultimate tensile strain (ε_{fu} - 1 STD) $\varepsilon_{fd} := 0.0072$

Compute the new shear capacity

Step 1 - Calculate the FRCM design tensile strain and strength

The FRCM design tensile strain is computed according to Eq. (11.2.1a):

Design tensile strain $\varepsilon_{fv} := \min\left(\varepsilon_{fd}, 0.004\right) = 0.00400$

The FRCM design tensile strength is computed according to Eq. (11.2.1b):

Design tensile strength $f_{fv} := \varepsilon_{fv} \cdot E_f = 72 \cdot ksi \quad (720MPa)$

Step 2 - Select the number of FRCM plies and the width of the FRCM strip

The number of plies of FRCM should not exceed the maximum number of plies to be used for shear strengthening as specified in the relative ICC-ES Research Report.

Number of FRCM plies $n := 3$

Step 3 - Calculate the FRCM contribution to the nominal shear capacity

The contribution of the FRCM reinforcement to the new nominal shear strength is calculated according to Eq. (11.2.1d). The effective depth of FRCM shear reinforcement, d_f, is taken equal to the effective depth of the steel reinforcement.

$d_f := d = 22 \cdot in \quad (559\ mm)$

$V_f := 2n \cdot A_f \cdot f_{fv} \cdot d_f = 17.1 \cdot kip \quad (67 \cdot kN)$

Step 4 - Calculate the new design shear strength

The new design shear strength is computed according to Eq. (11.2.1c):

$\phi V_{nNew} := \phi_v \cdot \left(V_c + V_s + V_f\right) = 88 \cdot kip \quad (586 \cdot kN)$

$[\ V_{uNew} = 82 \cdot kip\ ] \quad (578 \cdot kN)$

Check the new shear strength

$$CheckShearStrength := \begin{cases} \text{"OK"} & \text{if } \phi V_{nNew} \geq V_{uNew} \\ \text{"Not Good!"} & \text{otherwise} \end{cases}$$

CheckShearStrength = "OK"

Step 5 - Check limitation on total shear strength provided by FRCM and steel reinforcement

The limitation indicated in Eq. (11.2.1e) should be verified.

Total force provided by FRCM and steel reinforcement $V_s + V_f = 50.4 \cdot kip \quad (263 \cdot kN)$

$$Check\_MaximumShear := \begin{cases} \text{"OK"} & \text{if } V_s + V_f \leq 8 \cdot \sqrt{f'_c} \cdot \sqrt{psi} \cdot b_w \cdot d \\ \text{"Not Good"} & \text{otherwise} \end{cases}$$

Check_MaximumShear = "OK"

Step 6 - Check limitation on the shear strength provided by FRCM reinforcement

As recommended in 11.1.1, the increment in shear strength provided by the FRCM reinforcement should also not exceed 50 percent of the capacity of the structure without strengthening.

$$\text{Check} := \begin{cases} \text{"OK"} & \text{if } V_f \le 0.5 \cdot V_n \\ \text{"Not good"} & \text{otherwise} \end{cases}$$

$[\ V_f = 17 \cdot \text{kip}]$ (102 kN)

$[\ (0.5 \cdot V_n) = 50 \cdot \text{kip}\ ]$ (320kN)

Check = "OK"

Step 7 - Development length

As indicated in 14.1.2, the development length of the FRCM reinforcement should exceed the minimum length of 6 in (152 mm).
If the mesh is wrapped around the column continuously, a single lap is sufficient and, because of the multiple plies, a length of 12 in. (304 mm) is recommended. If the mesh wraps are applied individually, the laps should be staggered and a 6 in. (152 mm) length is sufficient.

16.5-Axial strengthening of RC column subject to pure compression

A 24 x 24 in. (610 x 610 mm) RC column of a parking garage only subject to axial load was damaged due to corrosion and has lost its 2-inch (50-mm) concrete cover and is estimated to have lost 15 percent of its reinforcing steel. The original design factored axial load is 1100 kip (4893 kN). After replacing the concrete cover, FRCM wraps are installed to make up for the loss of steel reinforcement by means of confinement

Information about the existing column

Geometrical properties

Short side of the column $b := 24in = 610 \cdot mm$

Long side of the column $h := 24in = 610 \cdot mm$

Concrete mechanical properties

Nominal compressive strength $f'_c := 4000psi = 27.6 \cdot MPa$

Compressive ultimate strain $\varepsilon_{cu} := 0.003$

Steel reinforcement geometrical and mechanical properties

Total area of longitudinal steel bars (8 No. 8 bars) $A_s := 6.28in^2 = 4052 \cdot mm^2$

Steel reinforcement ratio $\rho_s := \frac{A_s}{b^2} = 0.011$

Yield strength $f_y := 60ksi = 413.685 \cdot MPa$

Steel modulus of elasticity $E_s := 29000ksi = 200 \cdot GPa$

Axial strength without FRCM

Original design axial strength $\phi P_n := 1180kip = 5249 \cdot kN$

Strength-reduction factor $\phi := 0.65$

Damaged axial strength $\phi P_{nCorr} := \phi P_n - .15 \cdot A_s \cdot f_y = 1123 \cdot kip$

Mesh reinforcement properties

The FRCM material system to be used should be ICC-ES approved, and its geometrical and mechanical properties should be the ones reported in the relative ICC-ES Research Report.

It must be noted that the properties reported below are valid for the sole purpose of this design example.

Area of mesh reinforcement by unit width $A_f := 0.0018 \cdot \frac{in^2}{in} = 0.046 \cdot \frac{mm^2}{mm}$

Tensile modulus of elasticity (Ave.) $E_f := 18000ksi = 124 \cdot GPa$

Ultimate tensile strength ($\varepsilon_{fd} \cdot E_f$) $f_{fd} := 130ksi = 896 \cdot MPa$

Ultimate tensile strain (ε_{fu} - 1 STD) $\varepsilon_{fd} := 0.0072$

Compute the new axial capacity

Step 1 - Preliminary calculations

Corner radius $r_c := 1in$

A corrosion factor equal to 0.85 is considered to account for the reduction of resisting steel area.

Corrosion factor $CF := 0.85$

Area of steel reinforcement per unit width reduced due to corrosion $A_{sCorr} := A_s \cdot CF = 5.338 \cdot in^2 \quad (3444\ mm^2)$

New steel reinforcement ratio $\rho_{sNew} := \frac{A_{sCorr}}{b \cdot h} = 0.00927$

Step 3 - Calculate the FRCM effective tensile strain

The FRCM effective tensile strain is computed according to Eq. (11.3.1g):

Effective tensile strain $\varepsilon_{fe} := \min(\varepsilon_{fd}, 0.012) = 0.00720$

Step 4 - Select the number of FRCM plies and the width of the FRCM strip

The number of plies of FRCM should not exceed the maximum number of plies to be used for axial strengthening as specified in the relative ICC-ES Research Report.

Number of FRCM plies $n := 4$

Step 5 - Calculate the new axial strength

The efficiency factor should be calculated as given in Eq. (11.3.1.2a) when b/h=1.0:

$$\kappa_a := 1 - \frac{(b - 2 \cdot r_c)^2 + (h - 2 \cdot r_c)^2}{3 \cdot b \cdot h \cdot (1 - \rho_s)} = 0.434$$

The maximum confinement pressure provided by the FRCM wraps should be calculated according to Eq. (11.3.1f) (for rectangular cross-section):

$$f_l := \frac{2n \cdot A_f \cdot E_f \cdot \varepsilon_{fe}}{\sqrt{b^2 + h^2}} = 55 \cdot psi \quad (525kPa)$$

The maximum concrete confined compressive strength should be calculated according to Eq. (11.3.1d) (for rectangular cross-section):

$f'_{cc} := f'_c + 3.1 \cdot \kappa_a \cdot f_l = 4074 \cdot psi \quad (35.2MPa)$

The new design column axial strength is calculated according to ACI 318-11:

$$\phi P_{nNew} := \phi \cdot 0.8 \cdot \left[0.85 \cdot f'_{cc} \cdot b \cdot h \cdot (1 - \rho_{sNew}) + A_{sCorr} \cdot f_y\right] = 1194 \cdot kip$$

$$Check\_Capacity := \begin{cases} \text{"OK"} & \text{if } \phi P_{nNew} \geq \phi P_n \\ \text{"Not Good"} & \text{otherwise} \end{cases} \qquad \phi P_n = 1180 \cdot kip$$

Check_Capacity = "OK"

Step 6 - Check limitation on the shear strength provided by the FRCM reinforcement

As recommended in 12.1.4, the increment in axial strength provided by the FRCM reinforcement should also not exceed 20 percent of the capacity of the structure without strengthening.

$$Check := \begin{cases} \text{"OK"} & \text{if } \left(\phi P_{nNew} - \phi P_n\right) \le 0.2 \cdot \phi P_n \\ \text{"Not good"} & \text{otherwise} \end{cases}$$

$$\left[\ \phi P_{nNew} - \phi P_{nCorr} = 71 \cdot kip\ \right] (\ 102\ kN\ )$$

$$\left[\ 0.2 \cdot \phi P_n = 236 \cdot kip\ \right] \qquad (\ 320 kN\ )$$

$$Check = \text{"OK"}$$

Step 7 - Development length

As indicated in 14.1.2, the development length of the FRCM reinforcement should exceed the minimum length of 6 in (152 mm).
If the mesh is wrapped around the column continuously, a single lap is sufficient and, beause of the multiple plies, a length 12 in. (304 mm) is recommended. If the mesh wraps are applied individually, the laps should staggered and a 6 in. (152mm) length is sufficient.

16.6-Flexural strengthening of unreinforced masonry wall (URM) subjected to out-of-plane loads

A warehouse roof is built with steel open-joists and beams supported by steel interior columns and load bearing unreinforced ungrouted CMU walls along the building perimeter. A change in use ot he warehouse has warranted the increase of the design lateral wind load. The existing CMU is not adequate to resist the new loads. Summarized in the following sections are the information about the typical existing wall panel and the existing and new loading conditions. The schematic of the wall panel under out-of-plane condition is shown in the figure below. The wall is assumed fixed at the base and simply supported at the roof level. The existing masonry wall panel is strengthened with FRCM, whose mechanical properties are reported in the following.

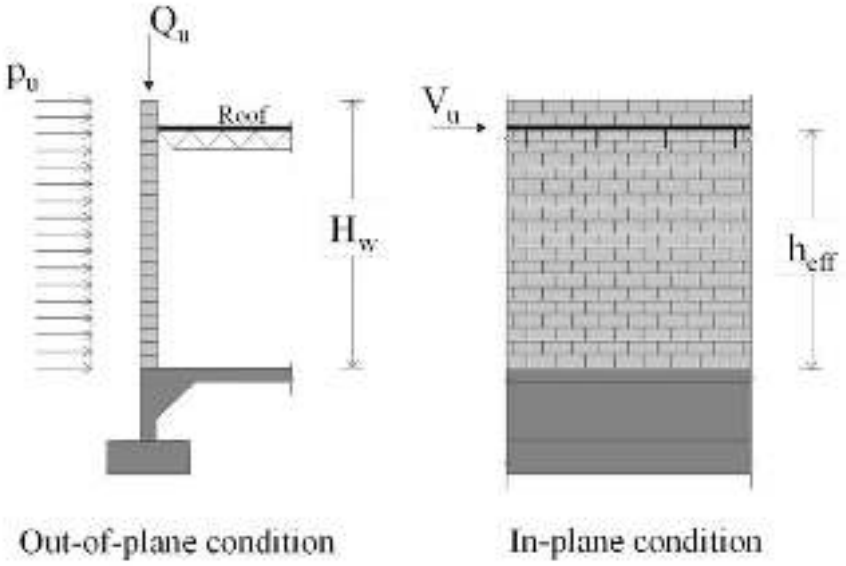

Wall panel schematic

Information about the existing wall

Geometrical properties

Height of the wall	$H_w := 18\,ft = 5\,m$
Thickness of the wall	$t_w := 11.63\,in = 295\,mm$
Length of the wall	$L_w := 17.67\,ft = 5.4\,m$
Clear height of the wall	$h_{eff} := 16\,ft = 4877\,mm$
Section area	$A_n := 36 \cdot \frac{in^2}{ft}$
Static moment of area	$S_o := 160 \cdot \frac{in^3}{ft}$

Mechanical properties of masonry (MSJC-11)

Nominal compressive strength $f'_m := 1500psi = 10 \cdot MPa$

Compressive ultimate strain $\varepsilon_{mu} := 0.0025$

Masonry elastic modulus $E_m := 900 \cdot f'_m = 1350000 \cdot psi \quad E_m = 9308 \cdot MPa$

Nominal tensile strength $f_r := 20psi = 138 \cdot kPa$

Flexural strength without FRCM

Existing nominal flexural strength $M_n := 3200 \cdot \frac{lbf \cdot in}{ft} = 1.19 \cdot \frac{kN \cdot m}{m}$

Phi-factor $\phi_m := 0.6$

Existing design flexural strength $\phi M_n := 1920 \cdot \frac{lbf \cdot in}{ft} = 0.71 \cdot \frac{kN \cdot m}{m}$

Loading Information

Existing conditions

Factored lateral pressure $p_u := 11.8psf = 0.56 \cdot \frac{kN}{m^2}$

Factored axial load $Q_u := 576 \cdot \frac{lbf}{ft} = 8.41 \cdot \frac{kN}{m}$

Factored bending moment $M_u := 4289 \cdot \frac{lbf \cdot in}{ft} = 1.59 \cdot \frac{kN \cdot m}{m}$

Anticipated conditions

New distributed factored lateral load $p_{uNew} := 15psf = 0.72 \cdot \frac{kN}{m^2}$

New maximum ultimate bending moment $M_{u'} := 5594 \cdot \frac{lbf \cdot in}{ft} = 2.07 \cdot \frac{kN \cdot m}{m}$

Mesh reinforcement properties

The FRCM material system to be used should be ICC-ES approved, and its geometrical and mechanical properties should be the one reported in the relative ICC-ES Research Report.

It must be noted that the properties reported below are valid for the sole purpose of this design example.

Area of mesh reinforcement by unit width $A_f := 0.0019 \cdot \frac{in^2}{in} = 0.0483 \cdot \frac{mm^2}{mm}$

Tensile modulus of elasticity (Ave.) $E_f := 12000ksi = 83 \cdot GPa$

Ultimate tensile strength ($\varepsilon_{fd} \cdot E_f$) $f_{fd} := 110ksi = 758 \cdot MPa$

Ultimate tensile strain (ε_{fu} - 1 STD) $\varepsilon_{fd} := 0.0092$

Compute the new flexural capacity

Step 1 - Select the number of FRCM plies and the width of the FRCM strip

The number of plies of FRCM should not exceed the maximum number of plies to be used for flexural strengthening as specified in the relative ICC-ES Research Report.

Number of FRCM plies $n_f := 1$

The width of the FRCM strip should be in agreement with the relative ICC-ES Research Report. In this example, a continuous coverage is considered.

Width of the FRCM strip $w_f := 12in = 305 \cdot mm$

Spacing of the FRCM strip $s_f := 12in = 305 \cdot mm$

Step 2 - Failure mode

It is assumed that the failure mode is governed by FRCM failure, which includes debonding of the FRCM from the concrete substrate (FRCM debonding), debonding of the fiber mesh from the cementitious matrix (mesh debonding), or tensile rupture of FRCM material. This assumption must be verified by checking that the compressive strain in the masonry does not exceed ε_{mu}. If it was assumed that the failure mode was governed by crushing of the masonry, it should have been then verified that the tensile strain in the FRCM reinforcement did not exceed the FRCM design tensile strain.

Step 3 - Calculate the FRCM design tensile strain

The FRCM effective tensile strain is computed according to Eq. (13.1.1a):

Effective tensile strain $\varepsilon_{fe} := \min\left(\varepsilon_{fd}, 0.012\right) = 0.00920$

Step 4 - Calculate the new design flexural strength

The effective stress level in the FRCM reinforcement attained at failure can be calculated according to Eq. (13.1.1b):

$f_{fe} := E_f \cdot \varepsilon_{fe} = 110 \cdot ksi \qquad (1069MPa)$

When FRCM failure is the governing failure mode, the following stress block factors can be assumed:

$\gamma := 0.7 \qquad \beta_1 := 0.7$

The equilibrium of forces can be used to calculate the neutral axis depth:

$$c_u := \frac{\left(Q_u + n_f \cdot A_f \cdot \frac{w_f}{s_f} \cdot f_{fe}\right)}{\left(\gamma \cdot f'_m \cdot \beta_1\right)} = 0.351 \cdot in \qquad (406mm)$$

The new nominal flexural strength is:

$$M_{nNew} := \gamma \cdot f'_m \cdot \beta_1 \cdot c_u \cdot \left(\frac{t_w}{2} - \beta_1 \cdot \frac{c_u}{2} \right) + n_f \cdot \frac{w_f}{s_f} \cdot A_f \cdot f_{fe} \cdot \frac{t_w}{2} = 32244 \cdot \frac{lbf \cdot in}{ft} \quad \left(6.64 \cdot \frac{kN \cdot m}{m} \right)$$

The new design flexural strength is:

$$\phi M_{nNew} := \phi_m \cdot M_{nNew} = 19346 \cdot \frac{lbf \cdot in}{ft} \qquad \left(2.89 \cdot \frac{kN \cdot m}{m} \right)$$

$$\left[M_{u'} = 5594 \cdot \frac{lbf \cdot in}{ft} \right] \qquad \left(2.07 \cdot \frac{kN \cdot m}{m} \right)$$

Check flexural strength

$$CheckFlexuralStrength := \begin{cases} \text{"OK"} & \text{if } \phi M_{nNew} \geq M_{u'} \\ \text{"Not Good!"} & \text{otherwise} \end{cases}$$

$$CheckFlexuralStrength = \text{"OK"}$$

Step 5 - Verify failure mode

Verify the assumption made in Step 2. If it was assumed that the failure mode was governed by FRCM failure, it should be now verified that the compressive strain in the masonry does not exceed ε_{mu}. If it was assumed that the failure mode was governed by crushing of the masonry, it should be now verified that the tensile strain in the FRCM reinforcement does not exceed ε_{fd}.

$$Check\_Strain := \begin{cases} \text{"OK"} & \text{if } \varepsilon_{fd} \cdot \left(\frac{c_u}{t_w - c_u} \right) \leq \varepsilon_{mu} \\ \text{"Not Good"} & \text{otherwise} \end{cases}$$

$$Check\_Strain = \text{"OK"}$$

In Step 2, it was assumed that the failure mode was governed by fiber rupture or delamination. It is now verified that the compressive strain in the masonry, ε_m, does not exceed ε_{mu}.

$$\varepsilon_m := \varepsilon_{fd} \cdot \left(\frac{c_u}{t_w - c_u} \right) = 0.00029$$

$$\varepsilon_m < \varepsilon_{mu} \qquad \text{where} \qquad \varepsilon_{mu} = 0.0025$$

Step 6 - Verify failure mode

The cracking moment does not have to exceed the design flexural strength.

$$M_{cr} := \left(f_r + \frac{Q_u}{A_n} \right) S_o = 480 \cdot \frac{ft \cdot lbf}{ft} \qquad \left(2.14 \cdot \frac{kN \cdot m}{m} \right)$$

$$Check\_Mcr := \begin{cases} \text{"OK"} & \text{if } \phi_m \cdot M_{nNew} \geq 1.3 M_{cr} \qquad (MSJC - 11) \\ \text{"Not Good"} & \text{otherwise} \end{cases}$$

$$Check\_Mcr = \text{"OK"}$$

Step 7 - Maximum force in the FRCM reinforcement

The maximum force in the FRCM reinforcement can be computed as follows:

$$\text{Check\_MaximumForce} := \begin{cases} \text{"OK"} & \text{if } A_f \cdot \varepsilon_{fd} \cdot E_f \cdot \frac{w_f}{s_f} < 6000 \frac{\text{lbf}}{\text{ft}} \quad \left(86.7 \cdot \frac{\text{kN}}{\text{m}} \right) \\ \text{"Not Good"} & \text{otherwise} \end{cases}$$

$$A_f \cdot \varepsilon_{fd} \cdot E_f \cdot \frac{w_f}{s_f} = 2517 \cdot \frac{\text{lbf}}{\text{ft}} \quad \left(10 \cdot \frac{\text{kN}}{\text{m}} \right)$$

$$\text{Check\_MaximumForce} = \text{"OK"}$$

Step 8 - Out-of-plane shear strength

The out-of-plane design shear strength is calculated according to MSJC-11.

$$V_n := \min\left[\frac{\left(3.8 \cdot A_n \cdot \frac{\text{ft}}{\text{in}^2} \cdot \sqrt{f'_m} \right)}{\sqrt{\text{psi}}}, \frac{\left(300 \cdot A_n \right)}{\frac{\text{in}^2}{\text{ft}}}, \frac{\left(56 \frac{\text{lbf}}{\text{ft}^2} \cdot A_n \right)}{\frac{\text{lbf}}{\text{ft}}} + \frac{\left(0.45 \cdot Q_u \right)}{\frac{\text{lbf}}{\text{ft}}} \right] \frac{\text{lbf}}{\text{ft}}$$

$\phi_{vf} := 0.8$ is the shear strength reduction factor for out-of-plane masonry (MSJC-11)

$$\phi_{vf} \cdot V_n = 219 \cdot \frac{\text{lbf}}{\text{ft}} \quad \left(3.2 \cdot \frac{\text{kN}}{\text{m}} \right)$$

The factored shear force acting on the wall can be computed as follows:

$$V_u := p_{uNew} \cdot \frac{H_w}{2} = 135 \cdot \frac{\text{lbf}}{\text{ft}} \quad \left(1.9 \cdot \frac{\text{kN}}{\text{m}} \right)$$

$$\text{Check\_ShearStrength} := \begin{cases} \text{"OK"} & \text{if } \phi_{vf} \cdot V_n > V_u \\ \text{"Not Good"} & \text{otherwise} \end{cases}$$

$$\text{Check\_ShearStrength} = \text{"OK"}$$

Step 9 - Development length

As indicated in Section 14.1.2, the development length of the FRCM reinforcement should exceed the minimum length of 6 in (152 mm).

16.7-Shear strengthening of URM wall subjected to in-plane loads

The warehouse analyzed in the previous example is subjected to a factored lateral in-plane force equal to 8 kip (35.6 kN) acting at the level of the roof. Summarized in the following sections are the information about the typical existing wall panel, and the existing and new loading conditions. The existing masonry wall panel is strengthened with FRCM, whose mechanical properties are reported below.

Information about the existing wall

Geometrical properties

Height of the wall $H_w := 18ft = 5m$

Thickness of the wall $t_w := 11.63in = 295mm$

Length of the wall $L_w := 17.67ft = 5.4m$

Clear height of the wall $h_{eff} := 16ft = 4877mm$

Section area $A_n := 36 \cdot \frac{in^2}{ft}$

Static moment of area $S_o := 160 \cdot \frac{in^3}{ft}$

Mechanical properties of masonry (MSJC-11)

Nominal compressive strength $f'_m := 1500psi = 10MPa$

Compressive ultimate strain $\varepsilon_{mu} := 0.0025$

Masonry elastic modulus $E_m := 900 \cdot f'_m = 1350000psi$ $E_m = 9308MPa$

Lower-bound shear strength $\nu_{tL} := 15psi = 103kPa$

Loading information

Anticipated conditions

New ultimate shear force $V_u := 5.5kip = 24.47kN$

Superimposed dead load $P_D := 280 \cdot \frac{lbf}{ft} = 4.09 \cdot \frac{kN}{m}$

Lower-bound axial compressive force due to gravity load $Q_G := 400 \cdot \frac{lbf}{ft} = 5.84 \cdot \frac{kN}{m}$

Ultimate axial load $Q_u := 10kip = 44kN$

Fabric-reinforced cementitious matrix reinforcement properties

The FRCM material system to be used should be ICC-ES approved, and its geometrical and mechanical properties should be the one reported in the relative ICC-ES Research Report.

It must be noted that the properties reported below are valid for the sole purpose of this design example.

Area of mesh reinforcement by unit width $A_f := 0.0019 \cdot \frac{in^2}{in} = 0.0483 \cdot \frac{mm^2}{mm}$

Tensile modulus of elasticity (Ave.) $E_f := 12000ksi = 83 \cdot GPa$

Ultimate tensile strength ($\varepsilon_{fd} \cdot E_f$) $f_{fd} := 110ksi = 758 \cdot MPa$

Ultimate tensile strain (ε_{fu} - 1 STD) $\varepsilon_{fd} := 0.0092$

Compute the nominal shear capacity of the CMU wall panel

Step 1 - Compute the lower-bound masonry shear strength

The lower-bound masonry shear strength is found according to the provisions of ASCE 41 (Section 7.2.2.6) as follows:

$$\nu_{mL} := 0.75 \cdot \frac{0.75 \cdot \nu_{tL} + \frac{P_D}{A_n}}{1.5} = 10 \cdot psi$$

Step 2 - Compute the desired lateral capacity of the wall

The desired shear capacity of the unreinforced masonry wall is found according to the provisions of ASCE 41 (Section 7.3.2.2.1) as follows:

$\alpha := 1.0$ is a factor accounting for the boundary conditions.

$$V_{mE} := 0.9\alpha \cdot P_D \cdot L_w \cdot \frac{L_w}{h_{eff}} = 4918 \cdot lbf$$

where L_w is the length of wall in direction of the shear force, and h_{eff} is the height to resultant of lateral force.

The ratio L_w/h_{eff} cannot be taken less than 0.67. $\frac{L_w}{h_{eff}} = 1.10$

Step 3 - Compute the lower-bound lateral capacity of the wall

The lower-bound lateral capacity, V_{mL}, is taken as the lesser of the lateral capacity values based on lower-bound shear strength or toe compressive stress calculated according to the provisions of ASCE 41, Section 7.3.2.2.2.

The lower bound shear capacity is computed as follows:

$V_{mL} := \nu_{mL} \cdot A_n \cdot L_w = 6052 \cdot lbf$

The shear capacity due to toe crushing is computed as follows:

$f_a := \frac{Q_G}{A_n} = 11 \cdot psi$ is the axial compressive stress due to gravity loads

$$V_{tc} := \alpha \cdot Q_G \cdot \left(\frac{L_w}{h_{eff}}\right) \cdot \left(1 - \frac{f_a}{0.7f'_m}\right) L_w = 7723 \cdot lbf$$

The lower-bound lateral capacity, V_{mLB}, is calculated as follows:

$V_{mLB} := \min(V_{mL}, V_{tc}) = 6052 \cdot lbf$

Compute the shear capacity of the FRCM strengthened wall

Step 1 - Select the number of FRCM plies and the width of the FRCM strip

The number of plies of FRCM should exceed the maximum number of plies to be used for flexural strengthening as specified in the relative ICC-ES Research Report.

Number of FRCM plies $n_f := 1$

The width of the FRCM strip should be in agreement with the relative ICC-ES Research Report. In this example, a width of 12 in. (304 mm) is considered.

Width of the FRCM strip $w_f := L_w = 17.67 \cdot ft$

A continuous layer of FRCM reinforcement is applied on both sides of the wall.

Step 2 - Calculate the FRCM design tensile strain and strength

The FRCM design tensile strength is computed according to Eq. (13.2.1a):

Design tensile strain $\varepsilon_{fv} := \min\left(\varepsilon_{fd}, 0.004\right) = 0.00400$

The FRCM redesign tensile stress is computed according to Eq. (13.2.1a):

Design tensile strength

$f_{fv} := \varepsilon_{fv} \cdot E_f = 48 \cdot ksi$

Step 3 - Calculate the FRCM design tensile strain and strength

The total force per unit width that the FRCM system can transfer to the masonry substrate is computed according to Eq. (13.2.1d):

$V_f := 2 \cdot \left(A_f \cdot f_{fv}\right) \cdot L_w = 38676 \cdot lbf$

Step 4 - Compute the nominal shear capacity of the strengthened wall

The nominal shear capacity of the unstrengthened masonry wall is the minimum between the expected lateral shear capacity (V_{mE}) and the lower-bound lateral capacity (V_{mLB}):

$V_m := \min\left(V_{mE}, V_{mLB}\right) = 4918 \cdot lbf$

The nominal shear strength of the strengthened unreinforced masonry wall is computed according to Eq. (13.2.1d) (no Φ_V) cannot exceed $0.5\,V_m$:

$V_{fd} := \min\left(V_f, 1.5 \cdot V_m\right) = 7376 \cdot lbf$

$V_{ns1} := V_m + V_{fd} = 12294 \cdot lbf$

Additionally, V_{ns1} cannot be larger than V_{tc} (shear capacity due to toe crushing)

$$V_{ns} := \begin{cases} V_{ns1} & \text{if } V_{ns1} \le V_{tc} \\ V_{tc} & \text{otherwise} \end{cases}$$

$V_{ns} = 7723 \cdot lbf$

Step 5 - Compute the nominal flexural strength of the FRCM strengthened wall

As the design lateral strength determined in the previous step is larger than the lateral strength due to toe crushing of the unreinforced masonry wall, a check needs to be performed to ensure that the FRCM reinforcement selected in the previous example will prevent the rupture of the wall due to toe crushing.

The nominal flexural strength of the unreinforced masonry wall under in-plane loads is computed as follows:

The mechanical properties of the FRCM material to resist out-of-plane loads are taken as indicated in the previous example.

$\varepsilon_{fd'} := \min\left(\varepsilon_{fd}, 0.012\right) = 0.00920$ $\quad f_{fd'} := E_f \cdot \varepsilon_{fd'} = 110 \cdot ksi$

Continuous FRCM reinforcement is considered.

$w_{f'} := 12in$ $\quad s_{f'} := 12in$

The FRCM reinforcement is assumed to be uniformly distributed over the entire length and on both sides of the wall, and an equivalent area of FRCM reinforcement per unit width is considered.

$$A_{f\_Eq} := A_f \cdot \frac{w_{f'}}{s_{f'}} = 0.0228 \cdot \frac{in^2}{ft}$$

The effective tensile strain of the FRCM reinforcement can be expressed as a function of the neutral axis depth.

$$\varepsilon_m\left(c_{IP}\right) := \varepsilon_{fd'} \cdot \frac{c_{IP}}{L_w - c_{IP}}$$

When FRCM failure is the governing failure mode, the following stress block factors can be assumed:

$\gamma := 0.7$ $\quad \beta_1 := 0.7$

The neutral axis depth is computed by establishing the equilibrium of the forces acting on the cross-section of the wall. By trials and errors, the following value of neutral axis depth is computed.

$c_{IP} := 45in$

The sum of the forces is computed as follows.

The thickness of the shell of the masonry blocks is: $t_{shell} := 1in$

$$\Sigma F := Q_u - \frac{1}{2} \cdot 2 \cdot E_f \cdot \varepsilon_m\left(c_{IP}\right) \cdot A_{f\_Eq} \cdot \left(L_w - c_{IP}\right) = 561 \cdot lbf$$

It must be noted that the FRCM reinforcement to resist out-of-plane loading is applied on both sides (see previous example), therefore following value is assumed:

The maximum compressive strain of the masonry at failure is: $\varepsilon_m\left(c_{IP}\right) = 0.00248$

This value is smaller than ε_{mu} and, therefore, the failure mode assumption is verified.

The nominal flexural strength can be computed as follows:

$$M_n := Q_u \cdot \left(\frac{L_w}{2} - \frac{\beta_1 \cdot c_{IP}}{2}\right) + \frac{1}{3} \cdot 2 \cdot E_f \cdot \varepsilon_{fd'} \cdot A_{f\_Eq} \cdot \left(L_w - c_{IP}\right)^2$$

$M_n = 4805 \cdot kip \cdot in$

$\phi_m := 0.6$

$\phi_m \cdot M_n = 2883 \cdot kip \cdot in$

The maximum lateral force, V_{nf} that the wall can sustain before flexural failure is computed as follows:

$k_b := 0.5$ is a constant depending on the boundary conditions

k_b is equal to 0.5 and 1.0 for a fixed-fixed and fixed-free wall, respectively.

$$V_{nf} := \frac{\phi_m \cdot M_n}{k_b \cdot h_{eff}} = 30029 \cdot lbf$$

Step 6 - Compute the design shear strength of the strengthened wall

The nominal shear strength, V_n, is obtained as the minimum of the nominal shear strength as determined in Step 4, and the nominal lateral strength corresponding to flexural failure of the strengthened wall as determined in Step 5:

$V_n := \min\left(V_{ns}, V_{nf}\right) = 7.72 \cdot kip$

$\phi_v := 0.75$

$V_u = 5.5 \cdot kip$

$\phi_v \cdot V_n = 5.8 \cdot kip$

$$Check\_Shear := \begin{cases} \text{"OK"} & \text{if } \phi_v \cdot V_n \geq V_u \\ \text{"Not Good"} & \text{otherwise} \end{cases}$$

$Check\_Shear = \text{"OK"}$

Step 7 - Development length

As indicated in 14.1.2, the development length of the FRCM reinforcement should exceed the minimum length of 6 in (152 mm). An anchorage length of the FRCM reinforcement at the base of the wall not smaller than 6 in. (152mm) is necessary to prevent rocking of the panel and, therefore, a toe crushing type of failure.

CHAPTER 17—REFERENCES

Committee documents are listed first by document number and year of publication followed by authored documents listed alphabetically.

American Concrete Institute

ACI 318-11—Building Code Requirements for Structural Concrete and Commentary

ACI 440.2R-08–Guide for the Design and Construction of Externally Bonded FRP Systems for Strengthening Concrete Structures

ACI 440.7R-10–Guide for the Design and Construction of Externally Bonded Fiber-Reinforced Polymer Systems for Strengthening Unreinforced Masonry Structures

ACI 440R-07—Report on Fiber-Reinforced Polymer (FRP) Reinforcement for Concrete Structures

ACI 544.1R-96—Report on Fiber Reinforced Concrete (Reapproved 2009)

ACI 544.5R-10–Report on the Physical Properties and Durability of Fiber-Reinforced Concrete

ACI 562-13—Code Requirements for Evaluation, Repair, and Rehabilitation of Concrete Buildings and Commentary

American Society of Civil Engineers

ASCE 7-10—Minimum Design Loads for Buildings and Other Structures

ASCE 41-06—Seismic Rehabilitation of Existing Buildings

ASTM International

ASTM C109/109M— Standard Test Method for Compressive Strength of Hydraulic Cement Mortars (Using 2-in. or [50-mm] Cube Specimens)

ASTM C138/C138M-10—Standard Test Method for Density (Unit Weight), Yield, and Air (Gravimetric) of Concrete

ASTM C157/C157M-08—Standard Test Method for Length Change of Hardened Hydraulic-Cement Mortar and Concrete

ASTM C387/C387M-11—Standard Specification for Packaged, Dry, Combined Materials for Concrete and High Strength Mortar

ASTM C1583/C1583M-13—Standard Test Method for Tensile Strength of Concrete Surfaces and the Bond Strength or Tensile Strength of Concrete Repair and Overlay Materials by Direct Tension (Pull-off Method)

ASTM D2344/D2344M-00(2006)—Standard Test Method for Short-Beam Strength of Polymer Matrix Composite Materials and Their Laminates

ICC Evaluation Service, Inc.

AC434-2013—Acceptance Criteria for Masonry and Concrete Strengthening Using Fabric-reinforced Cementitious Matrix (FRCM) Composite Systems

International Code Council

IBC 2012—International Building Code

Prestressed/Precast Concrete Institute

MNL128-01—Recommended Practice for Glass Fiber-Reinforced Concrete Panels

The Masonry Society

MSJC-11—Building Code Requirements and Specification for Masonry Structures and Related Commentaries

Cited references

Abegaz, A.; Suaris, W.; De Luca, A.; and Nanni, A., 2012, "Fiber Reinforced Cementitious Matrix (FRCM) Composites as Confining Systems for Reinforced Concrete Columns," *X International Symposium on Ferrocement and Thin Reinforced Cement Composites (FERRO 10)*, Havana, Cuba.

Aindow, A. J.; Oakley, D. R.; and Proctor, B. A., 1984, "Comparison of the Weathering Behavior of GRC with Predictions made from Accelerated Aging Tests," *Cement and Concrete Research*, V. 14, pp. 271-274.

Al-Salloum, Y. A.; Elsanadedy, H. M.; Alsayed, S. H.; and Iqbal, R. A., 2012, "Experimental and Numerical Study for the Shear Strengthening of Reinforced Concrete Beams Using Textile-Reinforced Mortar," *Journal of Composites for Construction*, V. 16, No. 1, pp. 74-90.

Al-Salloum, Y. A.; Siddiqui, N.; Elsanadedy, H. M.; Abadel, A. A.; and Aqel, M. A., 2011, "Textile-Reinforced Mortar versus FRP as Strengthening Material for Seismically Deficient RC Beam-Column Joints," *Journal of Composites for Construction*, V. 15, No. 6, pp. 920-933.

Aldea, C.-M., ed., 2007, *Thin Fiber and Textile Reinforced Cementitious Systems*, SP-244, American Concrete Institute, Farmington Hills, MI. (CD-ROM)

Aldea, C.-M., ed., 2008, *Design and Applications of Textile-Reinforced Concrete*, SP-251, American Concrete Institute, Farmington Hills, MI. (CD-ROM)

Aldea, C.-M.; Mobasher, B.; and Jain, N., 2007, "Cement Based Matrix-Fabric System for Masonry Rehabilitation," *Thin Fiber and Textile Reinforced Cementitious Systems*, SP-244, C.-M. Aldea, ed., American Concrete Institute, Farmington Hills, MI, pp. 141-156. (CD-ROM)

Antons, U.; Raupach, M.; Kulas, C.; and Hegger, J., 2012, "High-Temperature Tests on Concrete Specimens Reinforced with Alkali-Resistant Glass Rovings under Bending Loads," *Proceedings of the CICE 2012 – The 6th International Conference on FRP Composites in Civil Engineering*, G. Monti, ed., Sapienza University of Rome, Italy, 8 pp.

Arboleda, D.; Loreto, G.; De Luca, A.; and Nanni, A., 2012, "Material Characterization of Fiber- Reinforced Cementitious Matrix (FRCM) Composite Laminates," X International Symposium on Ferrocement and Thin Reinforced Cement Composites (FERRO 10), Havana, Cuba.

Augenti, N.; Parisi, F.; Prota, A.; and Manfredi, G., 2011, "In-Plane Lateral Response of a Full-Scale Masonry Sub-Assemblage with and without an Inorganic Matrix-Grid Strengthening System," *Journal of Composites for Construction*, V. 15, No. 4, pp. 578-590.

Balsamo, A.; Iovinella, I.; Di Ludovico, M.; and Prota, A., 2010, "Experimental Behaviour of Tuff Masonry Strengthened with Lime Matrix-Grid Composites," *Proceedings of*

the Third International Workshop on Civil Structural Health Monitoring—Conservation of Heritage Structures Using FRM and SHM (CSHM-3), N. Banthia and A. Mufti, eds., Shield Ottawa-Gatrineau, Canada.

Banholzer, B., 2004, "Bond Behavior of a Multi-filament Yarn Embedded in a Cementitious Matrix," PhD dissertation, Department of Civil engineering, RWTH Aachen University.

Banholzer, B.; Brockmann, T.; and Brameshuber, W., 2006, "Material and Bonding Characteristics for Dimensioning and Modeling of Textile Reinforced Concrete (TRC) Elements," *Materials and Structures*, V. 39, pp. 749-763.

Banthia, N., and Gupta, R., 2006, "Influence of Polypropylene Fiber Geometry on Plastic Shrinkage Cracking in Concrete," *Cement and Concrete Research*, V. 36, No. 7, pp. 1263-1267.

Bentur, A.; Cohen. Z.; Peled, A.; Larianovsky, P.; Tirosh, R.; Puterman, M.; and Yardimci M., 2008, "Controlled Telescopic Reinforced System for High Performance Fiber-Cement Composites" *Seventh RILEM Symposium on Fiber-Reinforced Concretes (FRC)*, BEFIB, Chennai, India, pp. 243-251.

Bentur, A.; Peled, A.; and Yankelevsky, D., 1997, "Enhanced Bonding of Low Modulus Polymer Fibers-Cement Matrix by Means of Crimped Geometry," *Cement and Concrete Research Journal*, V. 27, No. 7, pp. 1099-1111.

Berardi, F.; Focacci, F.; Mantegazza, G.; and Miceli, G., 2011, "Rinforzo di un Viadotto Ferroviario con PBO-FRCM," *Proceedings, 1° Convegno Nazionale Assocompositi*, Milan, Italy, May 25-26. (in Italian)

Bisby, L. A.; Roy, E. C.; Ward, M.; and Stratford, T. J., 2009, "Fiber-Reinforced Cementitious Matrix Systems for Fire-Safe Flexural Strengthening of Concrete: Pilot Testing at Ambient Temperature," *Fourth International Conference on Advanced Composites in Construction (ACI C09)*, University of Edinburgh, UK.

Bisby, L. A.; Stratford, T. J.; Smith, J.; and Halpin, S., 2011, "FRP versus Fiber-Reinforced Cementitious Mortar Systems at Elevated Temperature," *Proceedings of the Tenth International Symposium on Fiber Reinforced Polymer Reinforcement for Concrete Structures (FRPRCS-10)*, SP-275, V. 2, R. Sen., R. Seracino, C. Shield, and W. Gold, eds., American Concrete Institute, Farmington Hills, MI, pp. 863-881.

Blanksvärd, T.; Täljsten, B.; and Carolin, A., 2009, "Shear Strengthening of Concrete Structures with the use of Mineral-Based Composites," *Journal of Composites for Construction*, V. 13, No. 1, pp. 25-34.

Bournas, D. A.; Lontou, P.; Papanicolaou, C. G.; and Triantafillou, T. C., 2007, "Textile-Reinforced Mortar (TRM) versus FRP Confinement in Reinforced Concrete Columns," *ACI Structural Journal*, V. 104, No. 6, pp. 740-748.

Bournas, D. A., and Triantafillou, T. C., 2011, "Bar Buckling in RC Columns Confined with Composite Materials," *Journal of Composites for Construction*, V. 15, No. 3, pp. 393-403.

Bournas, D. A.; Triantafillou, T. C.; Zygouris, K.; and Stavropoulos, F., 2009, "Textile-Reinforced Mortar (TRM) versus FRP Jacketing in RC Columns with Deformed Continuous or Lap-Spliced Bars," *Journal of Composites for Construction*, V. 13, No. 5, pp. 360-371.

Bournas, D. A.; Triantafillou, T. C.; Zygouris, K.; and Stavropoulos, F., 2011, "Bond Strength of Lap Spliced Bars in Concrete Confined with Composite Jackets," *Journal of Composites for Construction*, ASCE, V. 15, No. 2, pp. 156-16 7.

Brückner, A.; Ortlepp, R.; and Curbach, M., 2006, "Textile Reinforced Concrete for Strengthening in Bending and Shear," *Materials and Structures*, V. 39, pp. 741-748.

Butnariu, E.; Peled, A.; and Mobasher, B., 2006, "Impact Behavior of Fabric-Cement Based Composites," *Proceedings of the 8th International Symposium on Brittle Matrix Composites (BMC8)*, pp. 293-302.

Chin, J. W.; Nguyen, T.; and Aouadi, K., 1997, "Effects of Environmental Exposure on Fiber-Reinforced Plastic (FRP) Materials Used in Construction," *Journal of Composites Technology and Research*, V. 19, No. 4, pp. 205-213.

Cohen, Z., and Peled, A., 2010, "Controlled Telescopic Reinforcement System of Fabric-Cement Composites—Durability Concerns," *Cement and Concrete Research Journal*, V. 40, pp. 1495-1506.

Cohen, Z., and Peled, A., 2012, "Effect of Nanofillers and Production Methods to Control the Interfacial Characteristics of Glass Bundles in Textile Fabric Cement-Based Composites," *Composites: Part A*, V. 43, pp. 962-972.

Colombo, I.; Colombo, M.; Magri, A.; Zani, G.; and di Prisco, M., 2011, "Textile Reinforced Mortar at High Temperatures," *Applied Mechanics and Materials*, V. 82, pp. 202-207.

Contamine, R.; Si Larbi, A.; and Hamelin, P., 2011, "Contribution to Direct Tensile Testing of Textile Reinforced Concrete (TRC) Composites," *Materials Science and Engineering A*, V. 528, pp. 8589-8598.

D'Ambrisi, A. D.; Feo, L.; and Focacci, F., 2012, "Bond-slip Relations for PBO-FRCM Externally Bonded to Concrete," *Composites. Part B, Engineering*, V. 43, No. 8, pp. 2938-2949.

D'Ambrisi, A. D.; Feo, L.; and Focacci, F., 2013, "Experimental Analysis on Bond Between PBO-FRCM Strengthening Materials and Concrete," *Composites. Part B, Engineering*, V. 44, No. 1, pp. 524-532.

D'Ambrisi, A. D., and Focacci, F., 2011, "Flexural Strengthening of RC Beams with Cement Based Composites," *Journal of Composites for Construction*, V. 15, No. 5, pp. 707-720.

De Caso y Basalo, F.; Matta, F.; and Nanni, A., 2009, "Fiber Reinforced Cementitious Matrix Composites for Infrastructure Rehabilitation," *Ninth International Symposium on Fiber Reinforced Polymer Reinforcement for Concrete Structures (FRPRCS-9)*, D. Oehlers, D.; M. Griffith, and R. Seracino, eds., Sydney, Australia. (CD-ROM)

De Caso y Basalo, F.; Matta, F.; and Nanni, A., 2012, "Fiber Reinforced Cement-Based Composite System for Concrete Confinement," *Construction & Building Materials*, V. 32, pp. 55-65.

Di Ludovico, M.; Prota, A.; and Manfredi, G., 2010, "Structural Upgrade Using Basalt Fibers for Concrete Confinement," *Journal of Composites for Construction*, V. 14, No. 5, pp. 541-552.

Dubey, A., ed., 2008, *Textile-Reinforced Concrete*, SP-250, American Concrete Institute, Farmington Hills, MI. (CD-ROM)

Faella, C.; Martinelli, E.; Nigro, E.; and Paciello, S., 2004, "Experimental Tests on Masonry Walls Strengthened with an Innovative C-FRP Sheet," *Proceedings of the First International Conference on Innovative Materials and Technologies for Construction and Restoration*, Lecce, V. 2, pp. 458-474.

Fallis, G. J., 2009, "Innovation for Renovation: Cementitious Matrix is Used to Bond High-strength Polymeric Mesh to Concrete and Masonry," *Concrete International*, V. 31, No. 4, Apr., pp. 62-64.

Gencoglu, M., and Mobasher, B., 2007, "Monotonic and Cyclic Flexural Behavior of Plain Concrete Beams Strengthened by Fabric-Cement Based Composites," *Third International Conference on Structural Engineering, Mechanics and Computation (SEMC 2007)*, A. Zingoni, ed., pp. 1961-1966.

Grimes, H. R., 2009, "The Longitudinal Shear Behavior of Carbon Fiber Grid Reinforced Concrete Toppings," MSc thesis, North Carolina State University, Raleigh, NC, 159 pp.

Haim, E., and Peled, A., 2011, "Impact Behavior of Fabric-Cement Hybrid Composites," *ACI Materials Journal*, V. 108, V. 3, May - June, pp. 235-243

Hartig, J.; Häubler-Combe, U.; and Schicktanz, K., 2008, "Influence of Bond Properties on the Tensile Behavior of Textile Reinforced Concrete," *Cement and Concrete Composites*, V. 30, pp. 898-906.

Jones, J.; Driver, M.; and Harmon, T., 2008, "An Evaluation of the use of Finely Ground E-glass Fiber as a Pozzolan in GFRC Composites," GFRCA 15th International Congress, Prague, Czech Republic.

Katz, A.; Tsesarsky, M.; Peled, A.; and Anteby, I., 2011, "Textiles Reinforced Cementitious Composites for Retrofit and Strengthening of Concrete Structures under Impact Loading," *Workshop on High Performance Fiber Reinforced Cement Composites (RILEM) HPFRCC 6*, Ann Arbor, MI.

Kulas, C.; Hegger, J.; Raupach, M.; and Antons, U., 2011, "High-Temperature Behavior of Textile Reinforced Concrete" *Advances in Construction Materials Through Science and Engineering*, Proceedings of the International RILEM Conference, C. Leung, and K. T. Wan, eds., RILEM Publications S.A.R.L., Bagneux, France. (CD-ROM)

Kumar, A., and Roy, D. M., 1986, "Microstructure of Glass Fiber/Cement Paste Interface in Admixture Blended Portland Cement Samples," *Proceedings of the Durability of Glass Fiber Reinforced Concrete Symposium*, S. Diamon, ed., pp. 147-156.

Langone, I.; Venuti, F.; Eusebio, M.; Bergamo, G.; and Manfredi, G., 2006, "Behavior of Masonry Buildings Strengthened with G-FRP Grid Bonded with Cementitious Matrix," *Proceedings of First European Conference on Earthquake Engineering and Seismology*, Geneva, Switzerland.

Leonard, S., and Bentur, A., 1984, "Improvement of the Durability of Glass Fiber Reinforced Cement Using Blended Cement Matrix," *Cement and Concrete Research*, V. 14, pp. 717-728.

Litherland, K. L., 1986, "Test Methods for Evaluating the Long Term Behavior of GFRC," *Proceedings of the Durability of Glass Fiber Reinforced Concrete Symposium,* S. Diamond, ed., pp. 210-221.

Litherland, K. L., and Proctor, B. A., 1986, "The Effect of Matrix Formulation, Fibre Content and Fibre Composition on the Durability of Glassfibre Reinforced Cement," *Proceedings of the Durability of Glass Fiber Reinforced Concrete Symposium*, S. Diamond, ed., pp. 124-135.

Marshall, O., 2002, "Test Report on CMU Wall Strengthening Technology," *Internal Report*, U.S. Army Construction Engineering Research Laboratory (CERL), Urbana, IL.

Mechtcherine, V., 2012, "Towards a Durability Framework for Structural Elements and Structures Made of or Strengthened with High-Performance Fibre-Reinforced Composites," *Construction & Building Materials*, V. 31, pp. 94-104.

Mechtcherine, V., and Lieboldt, M., 2011, "Permeation of Water and Gases through Cracked Textile Reinforced Concrete," *Cement & Concrete Composites*, V. 33, No. 1, pp. 725-734.

Mobasher, B., 2012, *Mechanics of Fiber and Textile Reinforced Cement Composites*, CRC Press, 473 pp.

Mobasher, B.; Jain, N.; Aldea, C.-M.; and Soranakom, C., 2007, "Development of Fabric Reinforced Cement Composites for Repair and Retrofit Applications," *Textile Reinforced Concrete (TRC)—German/International Experience Symposium Sponsored by ACI Committee 549*, SP-244, American Concrete Institute, Farmington Hills, MI, pp. 125-139.

Mobasher, B.; Peled, A.; and Pahilajani, J., 2004, "Pultrusion of Fabric Reinforced High Flyash Blended Cement Composites," *Proceedings, RILEM Technical Meeting*, BEFIB, pp. 1473-1482.

Mobasher, B.; Peled, A.; and Pahilajani, J., 2006, "Distributed Cracking and Stiffness Degradation in Fabric-cement Composites," *Materials and Structures*, V. 39, pp. 317-331.

Nanni, A., 2012, "A New Tool in the Concrete and Masonry Repair," *Concrete International*, V. 34, No. 4, Apr., pp. 43-49.

Ortlepp, R.; Hampel, U.; and Curbach, M., 2006, "A New Approach for Evaluating Bond Capacity of TRC Strengthening," *Cement and Concrete Composites*, V. 28, pp. 589-597.

Ortlepp, R.; Ortlepp, S.; and Curbach, M., 2004, "Stress Transfer in the Bond Joint of Subsequently Applied Textile Reinforced Concrete Strengthening," *Proceedings Fiber-Reinforced Concretes (FRC),* RILEM, PRO 39, Varenna, Italy.

Papanicolaou, C. G.; Triantafillou, T. C.; Karlos, K.; and Papathanasiou, M., 2007, "Textile Reinforced Mortar (TRM) Versus FRP as Strengthening Material of URM Walls: In-Plane Cyclic Loading," *Materials and Structures*, V. 40, No. 10, pp. 1081-1097.

Papanicolaou, C. G.; Triantafillou, T. C.; and Lekka, M., 2011, "Externally Bonded Grids as Strengthening and Seismic Retrofitting Materials of Masonry Panels," *Construction & Building Materials*, V. 25, No. 2, pp. 504-514.

Papanicolaou, C. G.; Triantafillou, T. C.; Papantoniou, I.; and Balioukos, C., 2009, "Strengthening of Two-Way Slabs with Textile-Reinforced Mortars (TRM)," *11th International fib Symposium*, London, UK.

Papanicolaou, C. G.; Triantafillou, T. C.; Papathanasiou, M.; and Karlos, K., 2008, "Textile Reinforced Mortar (TRM) Versus FRP as Strengthening Material of URM Walls: Out-of-Plane Cyclic Loading," *Materials and Structures*, V. 41, No. 1, pp. 143-157.

Parisi, F.; Lignola, G. P.; Augenti, N.; Prota, A.; and Manfredi, G., 2011, "Nonlinear Behavior of a Masonry Sub-Assemblage Before and After Strengthening with Inorganic Matrix-Grid Composites," *Journal of Composites for Construction*, V. 15, No. 5, pp. 821-832.

Peled, A., 2007a, "Pre-Tensioning of Fabrics in Cement-Based Composites," *Cement and Concrete Research Journal*, V. 37, No. 5, pp. 805-813.

Peled, A., 2007b, "Textiles as Reinforcements for Cement Composites Under Impact Loading," *Workshop on High Performance Fiber Reinforced Cement Composites (RILEM) HPFRCC-5*, H. W. Reinhardt and A. E. Naaman, eds., Mainz, Germany, pp. 455-462.

Peled, A., 2007c, "Confinement of Damaged and Non-Damaged Structural Concrete with FRP and TRC Sleeves," *Journal of Composites for Construction*, V. 11, No. 5, pp. 514-523.

Peled, A., and Bentur, A., 1998, "Reinforcement of Cementitious Matrices by Warp Knitted Fabrics," *Materials and Structures Journal*, V. 31, Oct, pp. 543-550.

Peled, A.; Bentur A.; and Yankelevsky, D., 1999, "Flexural Performance of Cementitious Composites Reinforced with Woven Fabrics," *Journal of Materials in Civil Engineering*, V. 11, No. 4, pp. 325-330.

Peled, A., and Bentur, A., 2000, "Geometrical Characteristics and Efficiency of Textile Fabrics for Reinforcing Composites," *Cement and Concrete Research*, V. 30, pp. 781-790.

Peled, A., and Bentur, A., 2003, "Fabric Structure and Its Reinforcing Efficiency in Textile Reinforced Cement Composites," *Composites: Part A*, V. 34, pp. 107-118.

Peled, A.; Bentur, A.; and Yankelevsky, D., 1994, "Woven Fabric Reinforcement of Cement Matrix," *Advanced Cement Based Materials*, National Research Institute, Technion, Israel Institute of Technology, Haifa, Israel, V. 1, No. 5, July, pp. 216-223.

Peled, A.; Bentur, A.; and Yankelevsky, D., 1998a, "Effect of Woven Fabrics Geometry on The Bonding Performance of Cementitious Composites: Mechanical Performance," *Advanced Cement Based Materials*, V. 7, No. 1, pp. 20-27.

Peled, A.; Bentur, A.; and Yankelevsky, D., 1998b, "The Nature of Bonding Between Monofilament Polyethylene Yarns and Cement Matrices," *Cement and Concrete Composites*, V. 20, No. 4, pp. 319-328.

Peled, A.; Cohen, Z.; Janetzko, S.; and Gries, T., 2011a, "Hybrid Fabrics as Cement Matrix Reinforcement," *Sixth Colloquium on Textile Reinforced Structures (CTRS6)*, M. Curbach and R. Ortlepp, eds., Berlin, Germany, Sept., pp. 1-14.

Peled, A.; Cohen, Z.; Pasder, Y.; Roye, A.; and Gries, T., 2008a, "Influences of Textile Characteristics on the Tensile Properties of Warp Knitted Cement Based Composites," *Cement and Concrete Composites*, V. 30, No. 3, pp. 174-183.

Peled, A., and Mobasher, B., 2006, "Properties of Fabric-Cement Composites Made by Pultrusion," *Materials and Structures*, V. 39, No. 8, Oct., pp. 787-797.

Peled, A., and Mobasher, B., 2007, "Tensile Behavior of Fabric Cement-Based Composites: Pultruded and Cast," *Journal of Materials in Civil Engineering*, V. 19, No. 4, pp. 340-348.

Peled, A.; Mobasher, B.; and Cohen, Z., 2009, "Mechanical Properties of Hybrid Fabrics in Pultruded Cement Composites," *Cement and Concrete Composites*, V. 31, No. 9, pp. 647-657.

Peled, A.; Sueki, S.; and Mobasher, B., 2006, "Bonding in Fabric-Cement Systems: Effects of Fabrication Methods," *Journal of Cement and Concrete Research*, V. 36, No. 9, pp. 1661-1671.

Peled, A.; Yankelevsky, D.; and Bentur, A., 1997, "Microstructural Characteristic of Cementitious Composites Reinforced With Woven Fabrics," *Advances in Cement Research Journal*, V. 9, No. 36, pp. 149-155.

Peled, A.; Zaguri, E.; and Marom, G., 2008b, "Bonding Characteristics of Multifilament Polymer Yarns and Cement Matrices," *Composites: Part A*, V. 39, No. 6, pp. 930-939.

Peled, A.; Zhu, D.; and Mobasher, B., 2011b, "Impact Behavior of 2D and 3D Fabric Reinforced Cementitious Composites" RILEM HPFRCC-4 Workshop, Ann Arbor MI, June.

Poursaee, A.; Peled, A.; and Weiss, W. J., 2010, "Cracking and Fluid Transport in Coated and Non-Coated Carbon Fabrics in Fabric Reinforced Cement-Based Composites," *Proceedings RILEM International Conference on Textile Reinforced Concrete*, W. Brameshuber, ed., RILEM Publications SARL, Sept., pp. 257-269.

Poursaee, A.; Peled, A.; and Weiss, W. J., 2011, "Fluid Transport in Cracked Fabric Reinforced Cement-Based Composites," *Journal of Materials in Civil Engineering*, V. 23, No. 8, pp. 1227-1238.

Proctor, B. A.; Oakley, D. R.; and Litherland, K. L., 1982, "Developments in the Assessment and Performance of GRC Over 10 Years," *Composites*, V. 13, pp. 173-179.

Prota, A.; Marcari, G.; Fabbrocino, G.; Manfredi, G.; and Aldea, C.-M., 2006, "Experimental In-Plane Behavior of Masonry Strengthened with Cementitious Matrix-Grid System," *Journal of Composites for Construction*, V. 10, No. 3, pp. 223-233.

Qi, C., and Weiss, J., 2003, "Characterization of Plastic Shrinkage Cracking in Fiber Reinforced Concrete Using Image Analysis and a Modified Weibull Function," *Materials and Structures*, V. 35, No. 6, pp. 386-395.

RILEM Technical Committee (TC) 201, 2006, "Textile Reinforced Concrete, State-of-the-Art Report, W. Brameshuber, ed., 292 pp.

Seidel, A.; Lepenies, I.; Engler, T.; Cherif, C.; and Zastrau, B., 2009, "Aspects of Creep Behavior of Textile Reinforcements for Composite Materials," *Open Materials Science Journal*, V. 3, pp. 67-79.

Soranakom, C., and Mobasher, B., 2009, "Geometrical and Mechanical Aspects of Fabric Bonding and Pullout in Cement Composites," *Materials and Structures*, V. 42, pp. 765-777.

Soranakom, C., and Mobasher, B., 2010a, "Modeling of Tension Stiffening in Reinforced Cement Composites: Part I -Theoretical Modeling," *Materials and Structures*, V. 43, pp. 1217-1230.

Soranakom, C., and Mobasher, B., 2010b, "Modeling of Tension Stiffening in Reinforced Cement Composites: Part II—Simulations vs. Experimental Results," *Materials and Structures*, V. 43, pp. 1231-1243.

Sueki, S.; Soranakom, C.; Peled, A.; and Mobasher, B., 2007, "Pullout-Slip Response of Fabrics Embedded in a Cement Paste Matrix," *Journal of Materials Engineering*, ASCE, V. 19, No. 9.

Triantafillou, T. C., 2007, "Textile-Reinforced Mortars (TRM) versus Fibre-Reinforced Polymers (FRP) as Strengthening and Seismic Retrofitting Materials for Reinforced Concrete and Masonry Structures," *International Conference on Advanced Composites in Construction (ACIC07),* University of Bath.

Triantafillou, T. C., and Papanicolaou, C. G., 2006, "Shear Strengthening of Reinforced Concrete Members with Textile Reinforced Mortar (TRM)," *Materials and Structures*, V. 39, No. 1, pp. 93-103.

Triantafillou, T. C.; Papanicolaou, C. G.; Zissinopoulos, P.; and Laourdekis, T., 2006, "Concrete Confinement with Textile-Reinforced Mortar Jackets," *ACI Structural Journal*, V. 103, No. 1, pp. 28-37.

Wiberg, A., 2003, "Strengthening of Concrete Beams Using Cementitious Carbon Fiber Composites," PhD dissertation, Royal Institute of Technology, Stockholm, Sweden.

Wu, H. C., and Sun, P., 2005, "Fiber Reinforced Cement Based Composite Sheets for Structural Retrofit," *Proceedings of the International Symposium on Bond Behavior of FRCM in Structures*, BBFS 2005, Hong Kong, China.

Zastrau, B.; Lepenies, I.; and Richter, M., 2008, "On the Multi Scale Modeling of Textile Reinforced Concrete," *Technische Mechanik*, V. 28, pp. 53-63.

Zhu, D.; Peled, A.; and Mobasher, B., 2011, "Dynamic Tensile Testing of Fabric-Cement Composites," *Construction and Building Materials Journal*, V. 25, No. 1, pp. 385-395.

Zhu, D.; Rajan, S. D.; Mobasher, B.; Peled, A.; and Mignolet, M., 2010a, "Modal Analysis of a Servo-hydraulic High Speed Machine and Its Application to Dynamic Tensile Testing at an Intermediate Strain Rate," *Experimental Mechanics Journal*, V. 51, No. 8, pp. 1347-1363.

Zhu, D.; Silva, F.; Mobasher, B.; and Peled, A., 2010b, "High Speed Tensile Behavior of Fabric-Cement Composites" *Proceeding of the International RILEM Conference on Materials Science (MatSci) V*, 2nd ICTRC, Textile Reinforced Concrete, W. Brameshuber, ed., Aachen, Germany, pp. 205-213.

APPENDIX A—CONSTITUENT MATERIALS PROPERTIES OF COMMERCIALLY AVAILABLE FRCM SYSTEMS

Constituent Characteristics	US Cust.	SI	US Cust.	SI	US Cust.	SI	US Cust.	SI	US Cust.	SI	US Cust.	SI	US Cust.	SI
FIBER FILAMENT PROPERTIES			**AR-GLASS**		**BASALT**		**BASALT**		**CARBON**		**CARBON**		**PBO**	
Density	lb/cu.ft	(g/cm³)	156	2.50	169	2.70	172	2.75	109	1.74	113	1.81	97	1.56
Tensile strength	ksi	(GPa)	188	1.29	382	2.60	705	4.80	557	3.79	720	4.90	852	5.80
Modulus of elasticity	ksi	(GPa)	10,581	72	11,462	85	13,079	88	33,801	230	37,475	255	39,679	270
Ultimate deformation	-	-	0.018	0.018	0.031	0.031	0.030	0.030	0.016	0.016	0.019	0.019	0.025	0.025
Breakdown temperature	°F	(°C)			1,462	1350	2,372	1,300	4,532	2500	1,202	650	1,202	650
Coefficient of thermal dilation	10^{-6}·°F^{-1}	(10^{-6}·°C^{-1})			0.31	0.55			0.01	-0.01	0.28	0.50	-1.33	-6.00
MESH PROPERTIES														
Weight of the mesh	oz/sq.ft.	(g/m²)	0.74	225	0.72	220	0.82	250	0.88	270	0.66	202	0.36	111
Weight of fibers in the mesh	oz/sq.ft.	(g/m²)	0.57	175	0.56	170	0.70	214	0.72	220	0.56	172	0.23	70
Equivalent dry fabric thickness in the direction of the we	in	(mm)	0.0014	0.035	0.0012	0.032	0.0035	0.089	0.0025	0.063	0.0019	0.048	0.0038	0.096
Equivalent dry fabric thickness in the direction of the wa	in	(mm)	0.0014	0.035	0.0012	0.032	0.0035	0.089	0.0025	0.063	0.0019	0.048	0.0005	0.012
Ultimate tensile strength of the warp by width unit	kip/ft	(kN/m)	3.1	45	5.6	82	4.1	60	16.4	240	17.2	252	18.9	276
Ultimate tensile strength of the weft by width unit	kip/ft	(kN/m)	3.1	45	5.6	82	4.1	60	16.4	240	17.2	252	5.1	75
Ultimate tensile strain of the warp by width unit	-	-	0.018	0.018	0.031	0.031	0.018	0.018	0.016	0.016	0.019	0.019	0.081	0.081
Ultimate tensile strain of the weft by width unit			0.018	0.018	0.031	0.031	0.018	0.018	0.016	0.016	0.019	0.019	0.081	0.081
Axial Stiffness of the warp by width unit	kip/ft	(kN/m)	178	2,539	183	2,678	228	3,333	906	14,536	898	13,100	234	1,421
Axial Stiffness of the weft by width unit	kip/ft	(kN/m)	174	2,539	183	2,678	228	3,333	906	14,536	898	13,100	64	932
Area of the warp by width unit	sq in/in	(mm^2/m)	0.0014	35.27	0.0012	31.50	0.0035	88.91	0.0025	63.20	0.0020	51.37	0.0009	47.52
Area of the weft by width unit	sq in/in	(mm^2/m)	0.0014	35.27	0.0012	31.50	0.0035	88.91	0.0025	63.20	0.0020	51.37	0.0005	12.95
MORTAR PROPERTIES			**Powder & liquid**		**Single component**		**Single component**		**Single component**		**Single component**		**Single component**	
Consistency (single component)	in	(mm)									6.5	165	6.9	175
Specific weight (component A)	lb/cu.ft	(g/cm³)	68	1.10			87	1.40						
Specific weight (component B)	lb/cu.ft	(g/cm³)	64	1.02										
Specific weight (grown mortar)	lb/cu.ft	(g/cm³)	112	1.8	100 ± 2	1.60 ± 0.04	124	2.0	94±2	1.54 ± 0.04	94±3	1.50 ± 0.05	112 ± 3	1.80 ± 0.05
Dry solids content (component A)	%	%	100	100			100	100						
Dry solids content (component B)	%	%	23	23			-	-						
Mixing ratio (comp. A to comp. B)	-	-	3 to 7	3 to 7			-	-						
Water/Mortar mix ratio by weight	%	(%)			14 - 16.6	14 - 16.6	16	16	14.8 - 18	14.8 - 18	25 - 27	25 - 27	25 - 27	25 - 27
Tensile strength (at 28 days)	psi	(MPa)	882	6.0			294	2.0						
Compressive strength (at 28 days)	psi	(MPa)	2,645	18.0	3,674	25.0*	2,206	>15	3,674	25.0	2,903	>20.0	4,354	>30.0
Bending strength (28 days)	psi	(MPa)	1,176	8.0	882	6.0	882	6.0	1,029	7.0	508	>4.5	581	>4.0
Secant modulus of elasticity (28 days)	ksi	(MPa)	1,161	8,000			1,451	10,000			1,016	7,000	1,016	7,000
Adhesion to concrete substrate (at 28 days)	psi	(MPa)	>367	>2.5			>103	>0.7						
Adhesion to masonry substrate (at 28 days)	psi	(MPa)	>294	>2			>103	>0.7						

Legend and notes

Manufacturer A

Manufacturer B

Manufacturer C

Blank cell means value not available

APPENDIX B—DESIGN LIMITATIONS

	Concrete			Masonry	
Parameter	Flexure	Shear	Axial	Out-of-plane	In-plane
ε_{fe} or ε_{fd}	Less than 0.012	Less than 0.004	Less than 0.012 and ε_{ccu} less than 0.01	Less than 0.012	Less than 0.004
ϕ	0.9 to 0.65 based on ε_t	0.75	0.9 to 0.65 based on ε_t	0.6 for flexure 0.8 for shear	0.75
f_{fs}/f_{fd}	0.2 to 0.55 based on fiber	NA	NA	NA	NA
Allowable maximum enhancement*	50 percent	50 percent	20 percent	URM: 6000 lbf./ft (87.6 kN/m); Reinforced masonry: 50 percent	50 percent

*Allowable maximum enhancement is above existing capacity. ACI 562-13 supersedes when limits are lower than as listed in this table.

American Concrete Institute®
Advancing concrete knowledge

As ACI begins its second century of advancing concrete knowledge, its original chartered purpose remains “to provide a comradeship in finding the best ways to do concrete work of all kinds and in spreading knowledge.” In keeping with this purpose, ACI supports the following activities:

- Technical committees that produce consensus reports, guides, specifications, and codes.
- Spring and fall conventions to facilitate the work of its committees.
- Educational seminars that disseminate reliable information on concrete.
- Certification programs for personnel employed within the concrete industry.
- Student programs such as scholarships, internships, and competitions.
- Sponsoring and co-sponsoring international conferences and symposia.
- Formal coordination with several international concrete related societies.
- Periodicals: the ACI Structural Journal and the ACI Materials Journal, and Concrete International.

Benefits of membership include a subscription to Concrete International and to an ACI Journal. ACI members receive discounts of up to 40% on all ACI products and services, including documents, seminars and convention registration fees.

As a member of ACI, you join thousands of practitioners and professionals worldwide who share a commitment to maintain the highest industry standards for concrete technology, construction, and practices. In addition, ACI chapters provide opportunities for interaction of professionals and practitioners at a local level.

American Concrete Institute
38800 Country Club Drive
Farmington Hills, MI 48331
U.S.A.
Phone: **248-848-3700**
Fax: **248-848-3701**

www.concrete.org

Externally Bonded FRCM Systems for Repair and Strengthening Concrete and Masonry Structures

The AMERICAN CONCRETE INSTITUTE

was founded in 1904 as a nonprofit membership organization dedicated to public service and representing the user interest in the field of concrete. ACI gathers and distributes information on the improvement of design, construction and maintenance of concrete products and structures. The work of ACI is conducted by individual ACI members and through volunteer committees composed of both members and non-members.

The committees, as well as ACI as a whole, operate under a consensus format, which assures all participants the right to have their views considered. Committee activities include the development of building codes and specifications; analysis of research and development results; presentation of construction and repair techniques; and education.

Individuals interested in the activities of ACI are encouraged to become a member. There are no educational or employment requirements. ACI's membership is composed of engineers, architects, scientists, contractors, educators, and representatives from a variety of companies and organizations.

Members are encouraged to participate in committee activities that relate to their specific areas of interest. For more information, contact ACI.

www.concrete.org

American Concrete Institute®
Advancing concrete knowledge